Assessing the mechanism of Reovirus oncolysis

Jay D. Majithia

Thesis submitted to

The Faculty of Graduate and Postdoctoral Studies of

The University of Ottawa

in partial fulfillment of the requirements for the degree of

Masters of Science

Department of Biochemistry, Microbiology and Immunology
Faculty of Medicine

© Jay D. Majithia, Ottawa, Ontario.
Canada, 2011

॥ ॐ ॥

या देवी सर्वभूतेषु विद्या रुपेण संस्थिता ।
नमस्तस्यै नमस्तस्यै नमस्तस्यै नमो नमः ॥

yaa devi sarvabhooteshu vidya rupena samsthitaa |
namastasyai namastasyai namastasyai namo namaha | |

To that primordial Goddess, who resides in all beings as Knowledge,
Salutations and prostrations to you, Oh Mother Divine!

I dedicate all my years of education to

my Mum and Dad,

without whom, this entire journey would be meaningless.

I love and respect you both…

...and to my brother Deip – the light of my life.

ACKNOWLEDGEMENTS

I stand where I stand today because of the two most important people in my life, who have sacrificed more than what they had, to put me through school – thank you Mum and Dad, for your tireless efforts, encouragement and support throughout the course of my education. No amount of gratitude can convey how much both of you have done for Deip and me throughout our lives. I owe this to both of you.

I would like to thank my supervisor, Dr. Earl Brown, for allowing me to be part of the lab, who with his wisdom, advice and encouragement has enhanced my ability to look at things through a different perspective. I am very grateful to Dr. Brown for all the assistance he had provided me throughout my time in graduate school, and also for giving me the time off to volunteer in India during the course of my graduate degree.

I would also like to thank my advisory committee, Dr. Ken Dimock and Dr. John Bell, for their input, advice and suggestions on my projects.

If I were to list each and everyone who have in some way or the other played a role in the work I submit today, I would probably fill a volume with just names. Instead, let me say thank you to all those friends and colleagues. Of course, some names cannot go unmentioned and so I would like to thank my lab-mates and lab-neighbors (in no order of preference) – Trevor Beaudoin, Jasminka Bozic, Jeremy Brammer, Nicole Forbes, Dr. Sujeeve Jeganathan, Dr. Jihui Ping, Will Stecho, Samra Uzicanin, Dr. Shuai Wang, and

James Yi. A special mention to Dr. Yu-Wen Hu and Dr. John Basso for their faith and support.

I would like to specially thank two of my favorite lab-mates and friends – Dr. Liya Keleta and (soon to be Dr.) Samar Dankar. I cannot explain how much of a help both of you have been in the final version of this thesis. Samar – thanks to your constant whining that today I can proudly say that you helped me drive this to the end. I am sure Queen Liya agrees, nodding in sarcasm. As time passes, I am sure I will look back on the long coffee breaks, dinners, sarcastic comments, gossip sessions, the Chinese accents and all the 'goooood' times we've had in and outside of the lab – and it will all definitely bring a smile back to my face.

I specially thank my Kaka and Kaki for their constant love and support. I consider myself to be truly blessed to find a family in a place so far away from home. Thanks to both of you, today I stand a proud Indian in a foreign land, with my language, roots and culture intact.

I would like to thank Dilini – my friend, my sister, my guide – you have been a great source of constant moral support in ways you don't even know. We have come a long way over the last eight years, and I hope this continues till the end.

And lastly, I would like to thank my special someone, without whom this journey through these past eleven months would not have been the same. Thanks Krupa, for being 'just the way you are.' ☺

The Earth is round, the Earth moves – not seen, but true
The sky is blue, the sunset is golden – seen, but false
Energy in the atom, vitality in the sun, gravitational force – not seen, but true
Double moon, mirage waters, dreams and hallucinations – seen, but false

The world we see, but not true
Truth we see not, but true

– Swami Chinmayananda

ABSTRACT

Cancer remains to be one of the leading causes of death worldwide. Current treatment methods are not effective, and so newer therapies are needed, particularly in applied virology, where aspects of viral growth and replication are targeted to tumour lysis (termed viral oncolysis). Reoviruses are naturally occurring oncolytic viruses. Since most cancers are epithelial in origin, but also include fibroblastic properties due to the epithelial-mesenchymal transitions within tumours, my investigations mainly focused on the biology of Reoviruses in both fibroblast and epithelial cells. We studied the genetic basis for Protein Kinase R sensitivity and its role in lung tropism, as well as the study of tumour oncolysis by Reoviruses and their reassortants. We also investigated the growth and protein production of Reovirus and four oncolytic reassortants and their interferon susceptibilities in L929 fibroblast cells, CT26 mouse colon tumour cells, interferon-deficient Vero cells and interferon producing CV-1 cells.

We found that PKR protected the bronchiolar epithelium from infection from Reovirus. In PKR knockout mice lungs, the ability to infect the bronchial epithelium was attributed to the T3D σ1s non-structural protein, encoded by the S1 gene segment. T1L infection of PKR+/+ Balb-c mice enhanced disease, whereas T3D growth and replication was limited by PKR.

Studies in viral oncolysis showed that treatments of CT26 tumour-bearing mice with high viral doses of Reovirus or oncolytic reassortants resulted in death from enhanced virus toxicity. However, treatments at lower and multiple doses significantly increased survival rates of mice.

Growth of parental Reoviruses in mouse colon tumour CT26 cells showed that there is an enhanced effect of the virus infection leading to the 18 hour time point, where the virus induced the breakdown of host factors. There was also a major increase in T3D viral proteins at this time point, where we also observed the decrease in host proteins such as actin, eIF2α, interferon

regulatory factors and PKR. We proposed that the Reovirus μ2 protein may be involved in this process, which induces the degradation of host inhibitors to result in enhanced viral gene and protein expression.

Our results also showed that parental and oncolytic reassortant viruses behaved differently with respect to growth and IFN response in different cell lines. We demonstrated a complicated interplay between Reovirus gene products, resulting in a unique interaction involving other viral and cell proteins to achieve a certain trait, in the context of the cell type.

TABLE OF CONTENTS

CHAPTER ONE – INTRODUCTION pg. 12

1.1 Classification of Reovirus pg. 13
1.2 Pathogenesis pg. 13
1.3 Reoviruses: Genome and Morphology pg. 15
1.4 Reovirus Genome Reassortment pg. 19
1.5 The Reovirus Replication Cycle pg. 19
1.6 The Interferon Pathway pg. 23
1.7 Reovirus and the Interferon System pg. 26
1.8 Reovirus and the PKR pathway pg. 27
1.9 The Epithelial-Mesenchymal Transition and Cancer pg. 31
1.10 Ras and Oncolysis pg. 32

CHAPTER TWO – RATIONALE AND OVERALL OBJECTIVES pg. 35

CHAPTER THREE – MATERIALS AND METHODS pg. 37

3.1 Cells and Viruses pg. 37
3.2 Infection of cells, collection of protein samples and virus titration pg. 37
3.3 Immunoblotting pg. 38
3.4 Antibodies pg. 39
3.5 Infection of Balb-c mice and tumour implantation pg. 39
3.6 Immunochemistry and Immunofluorescence pg. 40
3.7 Interferon-β ELISA Assay pg. 41
3.8 Interferon Sensitivity Assay pg. 41

CHAPTER FOUR – STUDYING THE GENETIC BASIS FOR PKR SENSITIVITY AND ASPECTS OF REOVIRUS LUNG TROPISM pg. 42

4.1 Background and prior studies pg. 42
4.2 Specific objectives pg. 49
4.3 Results pg. 49

4.3.1 PKR protects the mouse lung bronchiolar epithelium from Reovirus T3D infection pg. 49
4.3.2 Differential staining of alveoli and bronchial epithelium observed after infection of PKR -/- lungs with a panel of Reovirus reassortants pg. 52
4.3.3 Single S1 genome reassortment determined infection of the Primary lung bronchial epithelium in PKR -/- mice pg. 56
4.3.4 Infection of the mouse bronchial epithelium is σ1s dependant pg. 59
4.3.5 The effects of PKR on the Reovirus parental strains with respect to Reovirus-induced disease pg. 62

4.3.6 Growth of Reoviruses and Reassortants in Balb-c and PKR -/- mice lungs and PKR sensitivity with respect to the S1 gene segment pg. 65

4.4 Discussion pg. 66

4.4.1 Lung PKR inhibits T3D and also prevents infection of bronchioles pg. 66
4.4.2 Lung PKR enhances T1L replication pg. 69
4.4.3 Differential Reovirus parental growth patterns in wild type and PKR -/- Balb-c lungs are attributed to the S1 gene segment pg. 70

4.5 Summary of Conclusions pg. 73

CHAPTER FIVE – STUDY OF TUMOUR ONCOLYSIS BY PARENTAL REOVIRUSES T1L & T3D AND ONCOLYTIC REASSORTANTS pg. 74

5.1 Background and prior studies pg. 74
5.2 Specific objectives pg. 79
5.3 Results pg. 79

5.3.1 Treatments with Reoviruses at 10^9 pfu are fatal to CT26 tumour-bearing mice pg. 79
5.3.2 Treatments with 10^8 pfu of Reoviruses and reassortants in CT26 tumour-bearing mice pg. 80
5.3.3 Treatments with multiple doses of Reoviruses at 10^7 does not enhance mouse survival, but does show early signs of viral oncolysis pg. 83
5.3.4 Treatments with multiple doses of Reoviruses at 10^6 enhances mouse survival and evidence of viral oncolysis pg. 86
5.3.5 Treatments with transgenic VSV expressing Reovirus T3D M1 gene enhanced survival pg. 89

5.4 Discussion pg. 96

CHAPTER SIX – COMPARISON OF REOVIRUS PROTEIN PRODUCTION IN L929 FIBROBLAST AND CT26 EPITHELIAL CELLS pg. 100

6.1 Background and prior studies pg. 100
6.2 Specific objectives pg. 103

6.3 Results pg. 106

6.3.1 Effect of Reovirus infection on total viral protein production and the inner capsid protein μ2 in CT26 epithelial cells pg. 106
6.3.2 Effect of Reovirus infection on total and phosphorylated PKR in CT26 epithelial cells pg. 109
6.3.3 Effect of Reovirus infection on the total and phosphorylated eukaryotic initiation 2-alpha in CT26 cells pg. 113
6.3.4 Effect of Reovirus infection on Interferon regulatory factors-3 and -7 in CT26 epithelial cells pg. 116

6.4 Discussion pg. 117

CHAPTER SEVEN – ASSESSING THE INTERFERON SENSITIVITIES AND EMERGENT PROPERTIES OF ONCOLYTIC REOVIRUS AND REASSORTANTS IN FIBROBLAST AND EPITHELIAL CELLS pg. 120

7.1 Background pg. 120
7.2 Specific objectives pg. 124
7.3 Results pg. 125

7.3.1 T3D induces IFN-β to a greater level than T1L in L929 cells, while the oncolytic Reassortants have varying levels of IFN-β induction pg. 125
7.3.2 EB88 induces 4-fold more IFN-β than parental serotype T3D, while T1L and oncolytic Reassortants have low or undetectable levels of IFN-β induction in CT26 cells pg. 128
7.3.3 Reovirus reassortants display different yield and interferon sensitivity properties compared to their parental strains in L929 cells pg. 131
7.3.4 Reovirus reassortants display interferon dependent protein synthesis patterns in L929 cells pg. 137
7.3.5 Reovirus reassortants display emergent properties of yield and interferon sensitivity compared to the growth of the parental strains in CT26 cells pg. 140
7.3.6 IFN either enhances or inhibits viral protein production of different Reoviruses in CT26 lung epithelial cells pg. 146
7.3.7 Reovirus and Reassortant yield and IFN sensitivity in Vero cells map to the M2 and the S4 gene segments, respectively pg. 152
7.3.8 Parental Reoviruses and reassortants display interferon dependent protein synthesis patterns in Vero cells that map to the M2 gene segment pg. 155
7.3.9 Reovirus and Reassortant yields in CV-1 cells were similar to Vero cells pg. 161

7.3.10 Reovirus and Reassortants display differences in interferon dependent protein synthesis in CV-1 cells pg. 164
7.4 Discussion pg. 167
7.4.1 Ability to induce IFN-β in L929 fibroblast and CT26 epithelial cells pg. 168
7.4.2 Reovirus replication and protein synthesis between fibroblasts and epithelium cell lines pg. 170
7.4.3 IFN sensitivity amongst the Parental T1L and T3D and the oncolytic reassortants in the four cells types – protein synthesis and replication pg. 171
7.4.4 Mapping Reovirus biological properties to individual gene segments pg. 172
7.5 Summary of Conclusions pg. 175

REFERENCES pg. 176

LIST OF FIGURES and TABLES

Figure 1.	Reovirus structure	pg. 18
Figure 2.	The Reovirus Replication Cycle	pg. 22
Figure 3.	The Interferon Pathway	pg. 25
Figure 4.	Activation and effect of Protein Kinase R	pg. 30
Figure 5.	Reovirus replication and protein production in PKR+/+ and PKR-/- mouse embryo fibroblast cells	pg. 44
Figure 6.	The yield of T1L and T3D in wild type and PKR knock-out Balb-c mice lungs	pg. 47
Figure 7.	Immunofluorescent staining of wt Balb-c mice lungs (PKR +/+) and TIK mice lungs (PKR -/-)	pg. 51
Figure 8.	Genetic basis for infection of the mouse bronchiolar epithelium by T3D S1	pgs. 53-54
Figure 9.	Infection of single segment reassortant in PKR -/- mice lungs	pg. 58
Figure 10.	Viral staining by Reoviruses that differ in their expression of σ1s	pg. 61
Figure 11.	Average body weight loss in Balb-c (PKR+/+) and PKR-/- mice after infection with parental Reoviruses T1L or T3D	pg. 64
Figure 12.	Growth of Reovirus and Reassortants in Balb-c (PKR+/+) and Balb-c (PKR -/-) mice	pg. 68
Figure 13.	Survival curve of Balb-c mice bearing CT26 lung tumours following a single intranasal dose of Reovirus (1 x 10^7pfu/ml)	pg. 77
Figure 14.	Survival curve of Balb-c mice bearing CT26 lung tumours, infected with a single dose of 1 x 10^9 pfu Reovirus or Reassortants	pg. 82
Figure 15.	Survival curve of Balb-c mice bearing CT26 lung tumours, infected with a single dose of 1 x 10^8 pfu Reovirus or Reassortants	pg. 85
Figure 16.	Survival curve of Balb-c mice bearing CT26 lung tumours, infected with three doses of 1 x 10^7 pfu Reovirus or Reassortants	pg. 88
Figure 17.	Survival curve of Balb-c mice bearing CT26 lung tumours, infected with three doses of 1 x 10^6 pfu of Reovirus reassortants	pg. 91

Figure 18.	Balb-c tumour bearing lungs of mice treated with PBS (top left) and with 10^7 pfu/mouse of reassortant treatment groups (EB88, EB97 and EB123), 8 days post treatment	pg. 93
Figure 19.	Survival curve of Balb-c mice bearing CT26 lung tumours, infected with 1 x 10^7 pfu/mouse of transgenic VSV expressing the Reovirus M1 gene from either parental strain	pg 95
Figure 20.	Reovirus growth and protein synthesis in L929 mouse fibroblasts	pg. 102
Figure 21.	Protein synthesis of parental Reovirus and reassortant in CT26 cells	pg. 105
Figure 22.	Protein synthesis of parental Reovirus T1L and T3D in CT26 cells	pg. 108
Figure 23.	Protein synthesis of host proteins PKR and phosphorylated-PKR over 24 hours post infection with Reovirus T1L and T3D in CT26 cells	pg. 111
Figure 24.	Protein synthesis of host proteins showing total eIF2α, phosphorylated-eIF2α, Interferon Regulatory Factors (IRF) -3 and -7 over 24 hours post infection with Reovirus T1L and T3D in CT26 cells	pg. 115
Figure 25.	Schematic summary of the IFN system	pg. 122
Figure 26.	IFN-β induction by Parental Reovirus (T1L and T3D) and Reassortants (EB88, EB96, EB97 and EB123) 24 hours post infection in L929 cells	pg. 127
Figure 27.	IFN-β induction by Parental Reovirus (T1L and T3D) and Reassortants (EB88, EB96, EB97 and EB123) 24 hours post infection in CT26 cells	pg. 130
Figure 28.	Reovirus titers at 72 hpi in L929 cells that were pretreated and untreated with IFN	pg. 133
Figure 29.	Relative IFN-sensitivity of Reovirus and reassortants in L929 cells	pg. 136
Figure 30.	Reovirus and reassortant protein production at 16, 24, 48 and 72 hours post infection in IFN pretreated and untreated L929 cells	pg. 139
Figure 31.	Reovirus titers at 72 hpi in CT26 cells that were pretreated and untreated with IFN	pg. 143
Figure 32.	Relative IFN-sensitivity of Reovirus and reassortants in CT26 cells	pg. 145
Figure 33.	Reovirus and reassortant protein production at 16, 24, 48 and 72 hours post infection in IFN pretreated and untreated CT26 cells	pg. 148

Figure 34. Reovirus titers at 72 hpi in Vero cells that were pretreated and untreated with IFN pg. 151
Figure 35. Relative IFN-sensitivity of Reovirus and reassortants in Vero cells pg. 154
Figure 36. Reovirus and reassortant protein production at 16, 24, 48 and 72 hours post infection in IFN pretreated and untreated Vero cells pg. 157
Figure 37. Reovirus titers at 72 hpi in CV-1cells that were pretreated and untreated with IFN pg. 160
Figure 38. Relative IFN-sensitivity of Reovirus and reassortants in CV-1 cells pg. 163
Figure 39. Reovirus and reassortant protein production at 16, 24, 48 and 72 hours post infection in IFN pretreated and untreated CV-1 cells pg. 166

Table 1. Genome Segments and Proteins in Reovirus pg. 16
Table 2. Genome map of the 18 Reovirus Reassortants pg. 55
Table 3. Genetic Map of Reovirus parental and four reassortants pg. 78

LIST OF ABBREVIATIONS

ATP	Adenosine triphosphate
BCIP/NBT	5-bromo-4-chloro-3-indolyl phosphate/nitro blue tetrazolium
CNS	Central Nervous System
dpi	days post infection
dsRNA	double stranded Ribonucleic Acid
eIF2α	eukaryotic Initiation Factor 2α
ELISA	Enzyme Linked Immunosorbent Assay
FB	Fibroblast
FBS	Fetal Bovine Serum
GDP	Guanosine Diphosphate
GFP	Green Fluorescent Protein
GTP	Guanosine Triphosphate
hpi	hours post infection
HRP	Horseradish Peroxidase
IFN	Interferon
IgG	Immunoglobulin G
IRF	Interferon Regulatory Factor
ISVP	Infectious (or intermediate) Subvirion Particle
JAM	Junction Adhesion Molecule
kDa	Kilo Dalton
MEF	Mouse Embryo Fibroblast
MEM	Minimum Essential Medium

MOI	Multiplicity of Infection
mRNA	messenger RNA
nt	nucleotide
p	probability
PBS	Phosphate Buffer Saline
PFU	Plaque Forming Units
PKR	Protein Kinase R
PKR -/-	PKR knockout
p-PKR	phosphorylated Protein Kinase R
PVDF	Polyvinylidene Fluoride
SDS-PAGE	Sodium Dodecyl Sulfate-Polyacrylamide Gel Electrophoresis
ssRNA	single stranded RNA
T1L	Type 1 Lang
T3D	Type 3 Dearing
U	Units
UT	Untreated
V	Volts
VSV	Vesicular Stomatitis Virus
wt	wild type

CHAPTER ONE
INTRODUCTION

Cancer is one of the leading causes of death in developed countries. Current treatment methods (chemotherapy and radiation) are not effective and thus newer therapies are needed. There is potential in treating cancer by infecting with viruses, termed viral oncolysis, where aspects of viral replication are targeted to cancer cells. This follows the observation that many tumours are more susceptible to viral infections than normal cells (5). The working hypothesis for oncolytic therapy is that cancer cells have acquired defects in their interferon (IFN) responses in the processes of becoming tumorogenic. This is because IFN is involved in the regulation of growth control and apoptosis (both of which are compromised in cancer) as well as the antiviral and the immune response.

The parental Reovirus serotype T3D has shown to be a promising candidate in the field of applied cancer therapeutics. Being able to target and lyse a good proportion of Ras-mediated cancers, such as breast, pancreatic, ovarian, colorectal, lung, glioblastomas and leukemia, there still remains a subset of tumour types that are resistant to viral oncolysis (42, 44). There is therefore a growing need to improve the oncolytic ability of Reovirus.

Due to the nature of the Reovirus genome, exchange of the segments between the parental serotypes can be achieved to generate reassortant strains. These reassortants can have unique biology compared to the parental wild types, due to the specific combination of the genome segments acquired from either parental serotypes. The Reovirus reassortants therefore provide an opportunity for more study of the basic virus biology of oncolysis that may identify specific gene segments that give rise to the virus' increased oncolytic abilities.

In addition to oncolysis, we studied the basic biology of Reovirus growth in cells and lungs. Since most cancers are epithelial in origin, but also include fibroblastic properties due to

epithelial-mesenchymal transition within tumours, we sought to study the biology of Reoviruses in both fibroblasts and epithelium.

1.1 Classification of Reovirus

The family *Reoviridae* is one of the largest and the most diverse in terms of its host range, infecting invertebrates, vertebrates and plants. Mammalian Reoviruses are ubiquitous in nature and have been isolated from various mammalian species, as well as from different environmental sources, such as untreated sewage, river and stagnant waters (42, 86). Their most unique feature is the composition of their double stranded RNA (dsRNA) genomes. The mammalian Reovirus is a member of the *Orthoreovirus* genus. The name r*eo*virus is an acronym for Respiratory Enteric Orphan virus, indicating that the virus is isolated from respiratory and intestinal tracts of its host, but is not associated with any known disease symptoms (21, 41). There are three Reovirus serotypes that are represented by prototype strains Type 1 Lang (T1L), Type 2 Jones (T2J), and Type 3 Dearing (T3D). Both prototypes T1L, T3D, as well as T1L x T3D reassortants have been used in the experiments carried out and presented in this thesis.

1.2 Pathogenesis

Reoviruses have been isolated from a wide variety of mammals, including humans. The majority of human *Orthoreovirus* infections are in the gastrointestinal and respiratory tracts, but are generally asymptomatic. The few reported cases of experimental infections in humans have suffered mild respiratory/enteric symptoms, including diarrhea and fever (41, 42). Almost everyone has been exposed to Reovirus by the age of five years, and a significant proportion of the human population is seropositive for Reovirus antibodies (46, 77). Although the virus does

not cause any disease in humans, infections in mice have been used as an experimental model system to study Reovirus pathogenesis. Reovirus infection in mice is systemic, and is able to spread from the gastrointestinal tract to extra-intestinal organs, as well as to the central nervous system (21, 22). A well characterized model for Reovirus pathogenesis is the infection of the murine central nervous system, where both parental serotypes T1 and T3 have distinct patterns of disease (22).

Oral inoculation of mice with Reovirus Type 1 causes the infection of the epithelial cells of the small intestine (ileum). T1L also infects the spleen via the bloodstream. In newborn mice, Reovirus Type 3 spreads from the intestinal tract through neurons, causing infection in the central nervous system. Intramuscular inoculation of Reovirus T3D spreads to the spinal cord, resulting in the development of lethal encephalitis. Intracerebral inoculation by Reovirus Type 3 infects neurons and produces lethal meningoencephalitis (21, 22).

Reovirus infection is systemic and affects many organs and tissues, including the hepatic system, the myocardium, lungs and endocrine tissues, and thus is not limited to the infection of the central nervous system. Both parental strains, T1L and T3D, have varied pathogenesis and differ in their tropism for different organs owing to their distinct genome segments. Myocarditis, resulting from myocarditic strains of Reovirus cause damage to myocytes, involves differential effects of the interferon and apoptosis pathways (62). Many aspects of parental Reovirus pathogenesis have been mapped to properties of their genome segments. The various different Reovirus gene products involved in RNA synthesis, transcription and genome replication play distinct roles in determining the extent of infection, route of spread and pathogenicity (21, 22).

1.3 Reoviruses: Genome and Morphology

Reoviruses are non-enveloped, icosahedral viruses (Triangulation number = 13), composed of a double protein shell – the outer capsid of 80nm in diameter and an inner core of 60nm in diameter (21, 78). The concentric capsids surround a double stranded RNA genome, comprised of 10 gene segments (Fig.1a, Table 1). Reovirus can exist as three distinct forms: the virion, the infectious subvirion particle (ISVP) and the core, the latter two being the result of progressive proteolysis of the virion. The virion is released after a complete replication cycle in cell culture or *in vivo*. (Fig. 1b) (9, 21, 78).

The Reovirus genome has 10 gene segments categorized into three size classes: three large (L), three medium (M) and four small (S) segments. The large, medium and small gene segments encode proteins designated λ, μ and σ, respectively. The genome segments range in size from ~3.9kbp (L), to ~1kbp (S). The total genome size is ~23.5 kbp. (9, 21, 78)

The virus is composed of 8 structural proteins: 4 proteins in the outer capsid (λ2, μ1, σ1 and σ3), and 4 proteins in the inner capsid (λ1, λ3, μ2 and σ2). The gene segments are transcribed into full-length mRNAs, and the plus strands of the gene segments have a 5'cap. Most Reovirus gene segments encode one protein, except M2 and S1, which are dicistronic, producing two proteins due to the presence of an alternative downstream initiation site (9, 21, 78). Table 1 outlines the genome segments and the proteins in the Reovirus particles.

Table 1. Genome Segments and Proteins in Reovirus

Gene Segment	Protein Encoded	Amino Acids	Protein Mass (kDa)	Number per virion	Location	Role/Function
L1	λ3	1267	142	12	Inner capsid	dsRNA-dependent RNA polymerase
L2	λ2	1288	145	60	Outer capsid, core spike	Capsid assembly, Guanyltransferase (capping), Methyltransferase, mRNA capping
L3	λ1	1275	143	120	Inner capsid	RNA binding, RNA helicase, NTPase
M1	μ2	736	83	20	Inner capsid	RNA binding (subunit/co-factor for RNA polymerase), RNA tri-phosphatase, role in transcription/ translation, viral growth, tropism and disease
M2	μ1	708	76	600	Outer capsid	virus penetration, forms bulk of virion outer capsid, transcriptase activation
M3	μNS	721	80	0	Non-structural	secondary transcription, RNA assortment/replication, associates with cytoskeleton, anchor
	μNSC	711	75	0	Non-structural	Unknown
S1	σ1	~470	49	36	Outer capsid	cell attachment protein, receptor binding, primary serotype determinant, virus tropism, viral hemagluttinin, type-specific antigen, responsible for virus-induced apoptosis
	σ1s	125	14	0	Non-structural	Highly variable between Reovirus isolates, responsible for some differences in biological properties of S1
S2	σ2	418	47	150	Inner capsid	Anchoring/bind to base of outer capsid protein μ1, binds dsRNA
S3	σNS	366	41	0	Non-structural	binds ssRNA, role in RNA assortment and packaging
S4	σ3	365	41	600	Outer capsid	formation of outer capsid, binds dsRNA, translation

Figure 1. Reovirus structure. (A) Reovirus and its structural proteins. (B) Structural differences between the Virion, ISVP and the Core Reovirus particles.

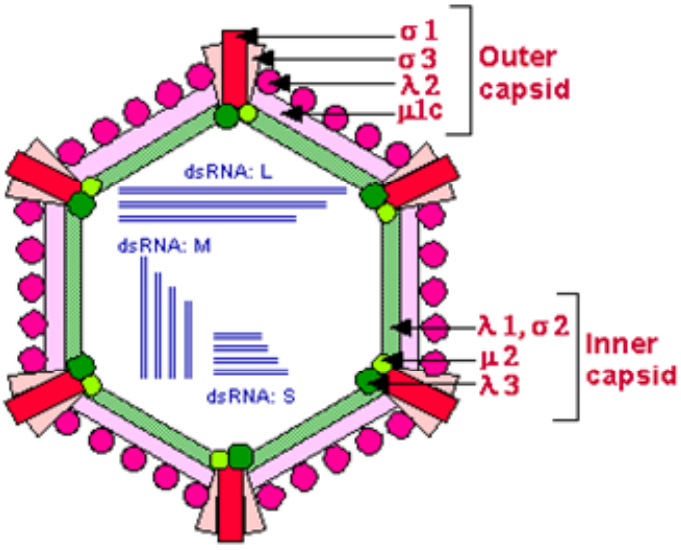
σ 1
σ 3
λ 2
μ1c
Outer capsid
dsRNA: L
dsRNA: M
dsRNA: S
λ 1, σ 2
μ 2
λ 3
Inner capsid

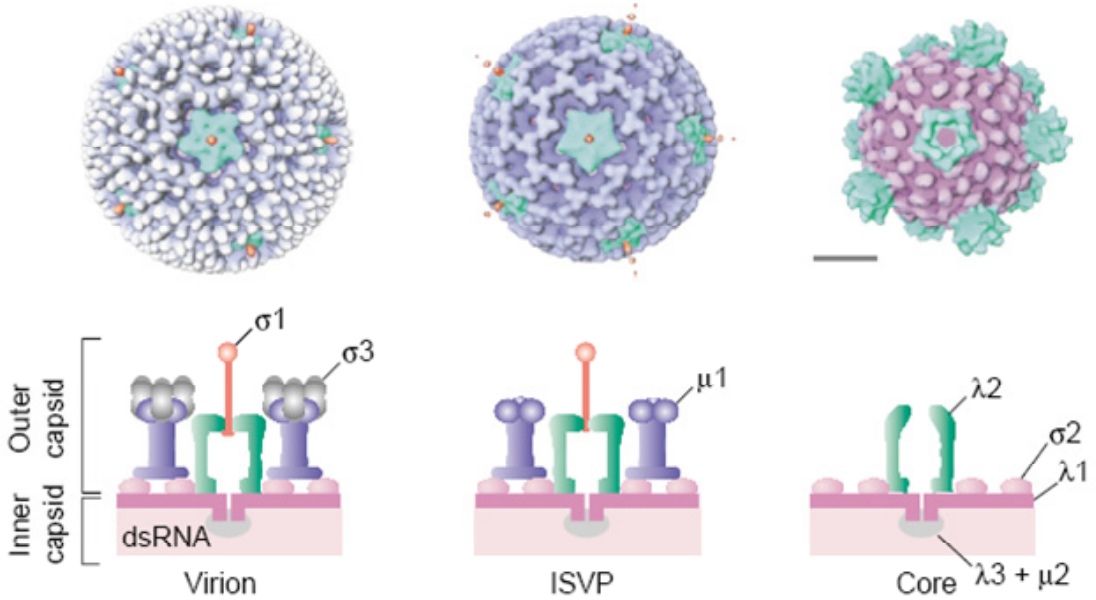
σ1
σ3
Outer capsid
Inner capsid
dsRNA
Virion
μ1
ISVP
λ2
σ2
λ1
λ3 + μ2
Core

1.4 Reovirus Genome Reassortment

Reovirus genome segments can reassort in nature, which therefore allows the manipulation of the mammalian Reovirus gene segments among the various serotypes to generate reassortants. This has been done in many genetic studies. It is due to this ability to reassort their genome segments that the Reovirus genome has been mapped, as well as the functions of the various gene segments have been defined in viral pathogenesis (78, 82). The genome of Reoviruses is comprised of 10 dsRNA genome segments.

Genome segment reassortment occurs when cells (*in vitro*) or humans and animals (*in vivo*) are simultaneously infected with two distinct Reovirus serotypes, generating, in theory, a potential of 1024 (2^{10}) possible progeny reassortants. These reassortants contain mixed gene segments acquired from both parental serotypes, as demonstrated by Wenske et al, 1985 where non-random gene segment reassortment was observed between serotypes T1L and T3D, in a stable manner, and through a specific reassortment mechanism (48, 78, 82).

1.5 The Reovirus Replication Cycle

The Reovirus life cycle begins with binding of the viral attachment protein σ1 to cell surface receptors, sialic acid and junction adhesion molecule-1. Reovirus particles are internalized via receptor mediated endocytosis, with the uptake of the virus particle into an endosome. Within these acidic endo-lysosomes, the virions are proteolytically processed and disassembled to uncoat the outer shell. Post-infection processing thus generates the infectious sub-viral particles (ISVPs), which lack the outer capsid protein σ3, but possesses a conformationally altered form of σ1, as well as a cleaved outer μ1 protein. The ISVPs are able to be transported through the endosomal membrane, which allows the penetration and consequent delivery of the ISVP

intermediate into the cytoplasm as an exposed Reovirus core. Once the core is in the cytoplasm, the viral RNA-dependent RNA polymerase is activated to initiate primary transcription and replication. (21, 51, 68, 69, 86) (Fig. 2)

Reovirus transcription occurs at two stages, an early primary step and a late secondary step. Following primary transcription, capped viral mRNAs are released into the cytoplasm, and early translation occurs using the host translational machinery. The primary protein products assemble to form RNA assortment complexes, serving as templates for secondary transcription as well as the process of replication that involves the synthesis of the minus strand. These late transcripts are templates for viral protein synthesis later in infection, resulting in the formation of complete progeny virion particles (21, 51, 68, 69, 86). These are gathered within viral factories or inclusion bodies. The core is recruited to viral inclusion bodies by the non-structural protein μNS and the structural μ2 protein. The morphology of the inclusion bodies is specific to the Reovirus parental serotype (52). The final assembly of the progeny virus leads to the lysis of the infected cell, followed by the release of the progeny virus, allowing virus spread and a consequent round of the viral life cycle to initiate (21, 51, 68, 69, 86).

Figure 2. The Reovirus Replication Cycle. (A) Simplified overview of the Reovirus life cycle. (B) Detailed viral life cycle, from Field's Virology, Chapter 52.

A

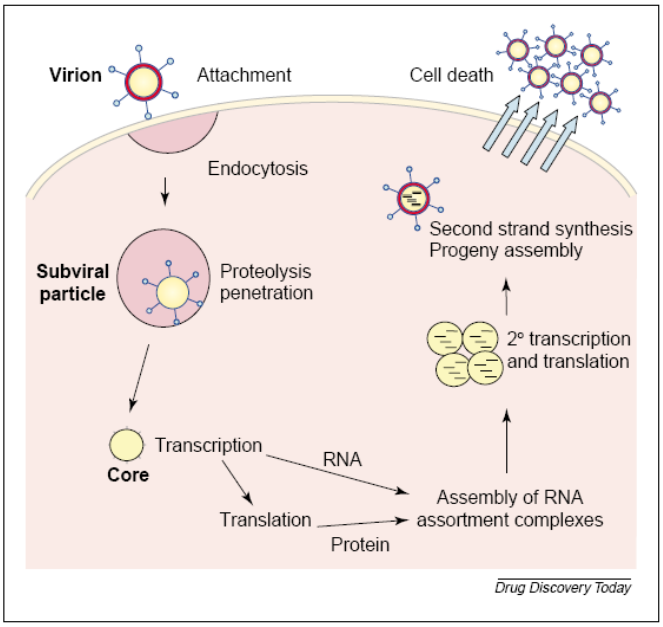
Virion
Attachment
Cell death
Endocytosis
Second strand synthesis
Progeny assembly
Subviral particle
Proteolysis penetration
2° transcription and translation
Transcription
Core
RNA
Translation
Protein
Assembly of RNA assortment complexes
Drug Discovery Today

B

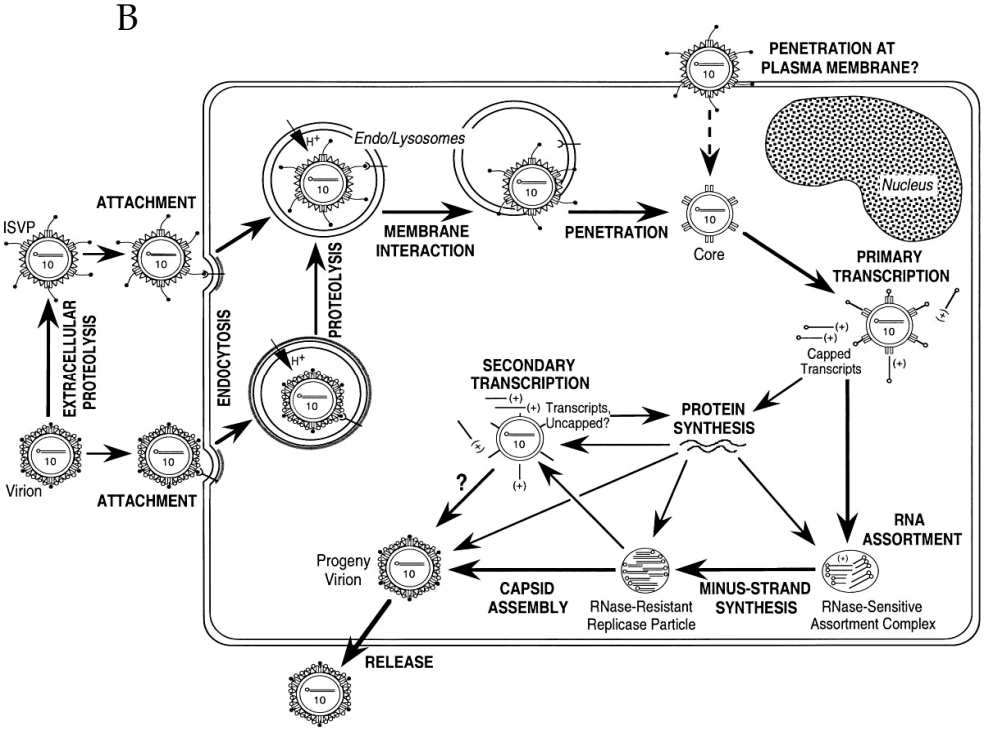
PENETRATION AT PLASMA MEMBRANE?
Endo/Lysosomes
Nucleus
ATTACHMENT
ISVP
MEMBRANE INTERACTION
PENETRATION
Core
PRIMARY TRANSCRIPTION
Capped Transcripts
EXTRACELLULAR PROTEOLYSIS
ENDOCYTOSIS
PROTEOLYSIS
SECONDARY TRANSCRIPTION
Transcripts, Uncapped?
PROTEIN SYNTHESIS
Virion
ATTACHMENT
?
RNA ASSORTMENT
Progeny Virion
CAPSID ASSEMBLY
RNase-Resistant Replicase Particle
MINUS-STRAND SYNTHESIS
RNase-Sensitive Assortment Complex
RELEASE

1.6 The Interferon Pathway

Interferons (IFN) are members of a multi-gene cytokine family of proteins and have many functions, with antiviral action being one of their characteristic activities. The IFN system includes all nucleated cells which are able to produce IFN upon some external stimulus, such as infection by a virus. Binding of IFN to its receptor can allow the cell to respond to IFN by inducing and establishing an antiviral state. Many viruses such as influenza and Reoviruses are both inducers of interferon and are also sensitive to its effect (25, 58).

Interferons are categorized into two types: type I and type II. Type I IFNs include four subtypes: IFN-α, IFN-β, IFN-ω and IFN-τ. These are also known as viral IFNs, as they are induced by virus infection and are inhibitors of viral infection. Type II IFN is induced by an antigenic stimulus, including virus infections, and is also known as IFN-γ, or immune IFN (25). Double-stranded RNA or 5' triphosphated RNA synthesized by viruses during viral infection cycles can be recognized by Toll-like receptors in endosomes or by RIG-1 or MDA-5 within the cytoplasm (34). This detection leads to a signaling cascade, which results in the phosphorylation of interferon regulatory factors (IRFs), which are transcription factors. One of the first IRFs involved in this cascade is IRF-3. Upon phosphorylation, IRF-3 is translocated to the nucleus and IFN β (34, 62). IFN β is produced and secreted, which "primes" neighboring cells for viral infection. The secreted IFN is recognized by IFN receptors and cause a signaling cascade leading to the phosphorylation of a downstream transcription factor IRF-7. This activated transcription factor is translocated in the nucleus, causing the induction of over 300 interferon stimulated genes that are cytokines, chemokines and apoptosis-related genes (2, 58) (Fig. 3).

Figure 3. The Interferon Pathway. Simplified schematic of the IFN-pathway, involving interferon regulatory factors-3 and -7, and the induction and secretion of IFN-β that induces an antiviral state in an autocrine and a paracrine manner.

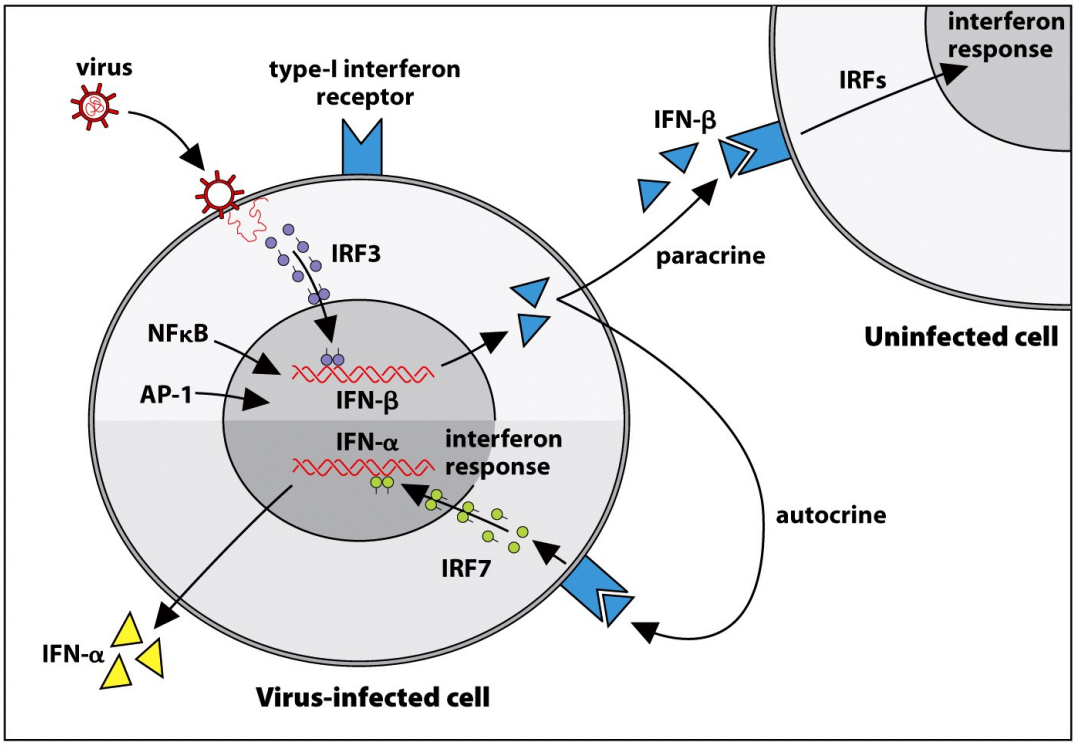

Figure 2.44 The Immune System, 3ed. (© Garland Science 2009)

1.7 Reovirus and the Interferon System

Infection of an animal cell by Reovirus results in the induction of IFN. However, the extent of induction and the virus sensitivity to IFN varies between the two parental serotypes, T1L and T3D (38). As shown by Jacobs & Ferguson, 1991, replication of the Dearing strain was reduced by 17- to 100- fold, and that of the Lang strain was reduced by 2- to 3- fold in IFN pre-treated mouse L cells, indicating that T3D is more sensitive to IFN than T1L (38). T3D also induces IFN to a greater extent that T1L (27). Moreover, IFN pretreatment has shown to differently inhibit Reovirus growth and protein synthesis in different cell lines (16, 78).

There are three well-known mechanisms of IFN action that may be involved in inhibiting Reovirus growth and protein production: (i) a 2' 5'oligoadenylate (2'-5'- oligoA) synthetase pathway, which activates RNAse L that cleaves both viral and cellular RNAs; (ii) PKR activation, which phosphorylates the α subunit of the eukaryotic initiation factor, consequently resulting in the shutdown of protein synthesis; and (iii) RNA editing by ADAR adenosine deaminase, (16, 57). Reovirus, however, has found ways to block the effects of these antiviral proteins (31). Bergeron et al, 1998, found that a mutant of the Reovirus σ3 protein lacked its association with capsid protein μ1 and increased its binding to dsRNA. This suggested a role of the σ3 in the interferon resistance by preventing the binding and activation of PKR (6, 63).

An important reovirus protein, μ2 has been recently found to inhibit IFN signaling. The Reovirus M1 gene determines strain-specific differences in IFN sensitivity/resistance between the parental serotypes. The μ2 protein of T1L (encoded by the M1 gene segment) can repress the IFN induction of a subset of interferon stimulated genes. Zurney et al, 2009, proposed a novel mechanism that involves the nuclear accumulation of IRF-9 by the T1L μ2, which most likely disrupts its function, thereby preventing the induction of interferon stimulated genes (63, 89).

Other genetic approaches have identified Reovirus λ2 and σ2 proteins in strain-specific modulation of the IFN response, though the mechanisms remain to be elucidated (63).

1.8 Reovirus and the PKR Pathway

Upon the stimulation of the IFN pathway by viral infection, one of the over 300 genes that are induced encodes for protein kinase R (PKR). PKR is a 68kDa protein, with its N-terminus containing a dsRNA binding domain, and its C-terminus containing a serine/threonine phosphorylation domain. Binding of dsRNA by PKR results the exposure of the ATP binding site, and induces dimerization of the protein (40). This in turn stimulates autophosphorylation, which converts the kinase to a catalytically active form that can bind and interact with one of its substrates, the eukaryotic initiation factor 2α. (eIF2α) (26, 40, 88).

PKR phosphorylation of eIF2α results in the increased affinity of eIF2 for GDP. This prevents the exchange of GDP for GTP, therefore preventing the initiation of another round of translation (40). The phosphorylation of eIF2α by PKR activation therefore results in a protein synthesis shutdown and, since the virus uses the host translational machinery, consequently halts the production of viral proteins. (Fig 3 and 4). However, many viruses have dedicated specific proteins to counter PKR and its effects. Some of these mechanisms include (i) the production of RNAs or proteins that act as dsRNA antagonists; (ii) production of proteins that bind dsRNA and sequester it; (iii) synthesis of proteins that prevent PKR activation; (iv) proteins that interfere with PKR/ eIF2α interaction; (v) proteins that dephosphorylate eIF2α; (vi) degradation of PKR. Combinations of one of more of these mechanisms have been employed by viruses that have become evolved to become resistant to IFN (26, 40, 88).

Reovirus is no exception when it comes to interacting with PKR. Its σ3 protein has been found to bind dsRNA (36) and this was further confirmed by Yue et al, 1997 that Reovirus mutants with defects in σ3 had a direct correlation with dsRNA binding and the reversal of translation by PKR, as well as the Reovirus μ1 protein that blocks the binding of σ3 to dsRNA, thereby allowing protein translation to continue (87). It has also been found that avian Reoviruses express the σA protein, which has a higher affinity for dsRNA and also effects PKR activation and function (26, 28). Not only does it have an inhibiting effect on PKR, Reovirus also interacts with PKR in both fibroblasts and epithelial cell lines in an interesting manner, where it is degraded followed by an increase in viral protein production (Brown et al, unpublished).

PKR is expressed in the cells of many vertebrates, as well as plants. In addition to its induction via the IFN pathway and the control of protein synthesis, PKR plays a role in the anti-proliferative pathway (cell cycle), induction of apoptosis, cell differentiation, cytokine signaling, tumour suppressor activity and the innate immune response (26, 40, 80).

Figure 4: Activation and effect of Protein Kinase R. PKR activation by dsRNA results in dimerisation and autophosphorylation, which causes the subsequent phosphorylation of its effector eIF2α, leading to the inhibition of protein synthesis.

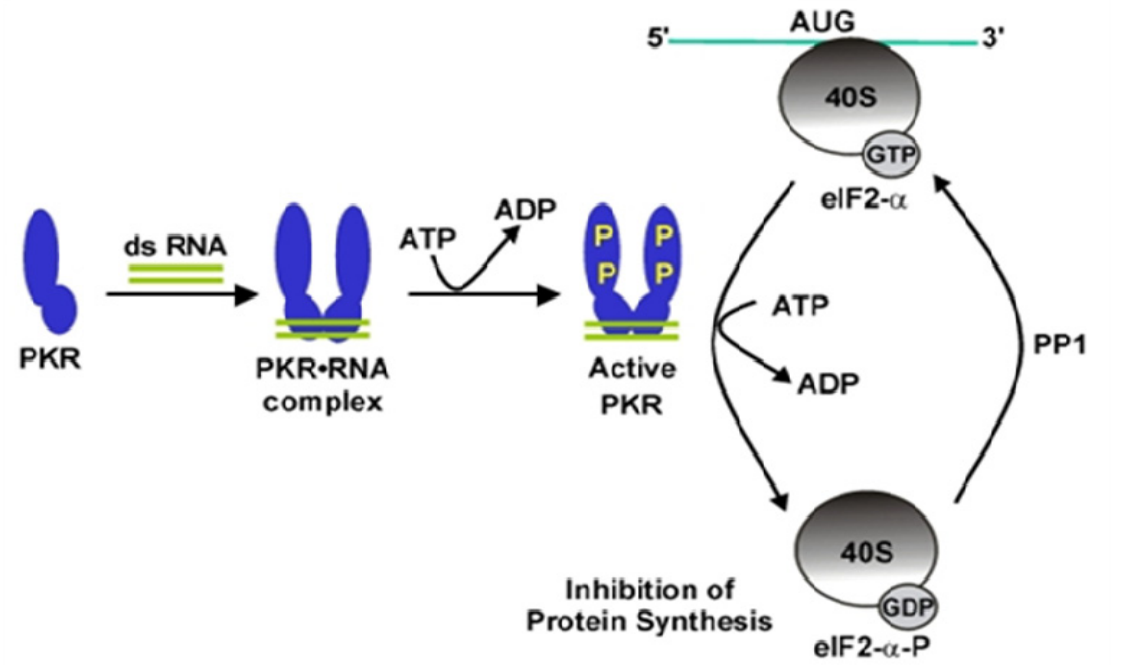
AUG
5'
3'
40S
GTP
eIF2-α
ds RNA
ATP
ADP
P
P
P
P
PKR
PKR•RNA
complex
Active
PKR
ATP
ADP
PP1
40S
GDP
Inhibition of
Protein Synthesis
eIF2-α-P

1.9 The Epithelial-Mesenchymal Transition and Cancer

Cancer research has mostly focused on the biology and dynamics within a cultured tumour cell. However, over the recent years, research and development has shed light onto the micro-environment in which the cancer cell exists. Tumour progression and metastasis is a multifaceted process, involving the epithelial-mesenchymal transition, a term we normally come across in embryogenesis. This biological progression results in a modification of a polarized epithelial cell, by undergoing multiple morphological and biochemical changes that allow it to behave as a mesenchymal (migratory) cell, therefore possessing enhanced motility, invasiveness, and elevated resistance to apoptosis (37, 39, 43).

During the past few decades, an increasing number of studies have shown that the epithelial-mesenchymal transition is associated with cancer progression, tumour metastases and drug resistance. The epithelial-mesenchymal transition in cancer research is important as it applies to epithelial-derived cancers, which account for 90% of human tumours (43). For tumour cells to invade the basal membrane, and enter the blood vessels, they must 'give-up' their epithelial properties. Therefore beginning with an initial loss of epithelial cell markers such as E-cadherin and a gain in mesenchymal markers such as vimentin, cell-cell adhesion is reduced, followed by the loss of the basal-apical polarization, as well as cytoskeletal remodeling and changes in the adhesion of the cell matrix (37, 39, 43). Therefore, through an applied cancer therapeutics point of view, there is greater complexity involved in the eradication of cancer cells that includes both epithelial and mesenchymal type cells.

1.10 Ras and Oncolysis

The oncolytic ability of Reovirus was first indicated in early studies, where it was shown that Reovirus induces cytotoxicity to certain tumor cells and spontaneously transformed cell lines, whereas normal cells were resistant to infection (19, 30). Reovirus has shown promise in the field of novel emerging cancer therapeutics as an oncolytic virus, due to its preferential replication in transformed cell lines. Several recent studies have shown the preference of replication in a variety of tumour types that have an activated *Ras* pathway, such as Strong et al, 1998 who showed that when cells were transformed with oncogenes such as *Ras*, *Sos* and *v-erbB* and *c-myc*, they become susceptible to infection by Reovirus (42, 75, 76). Reovirus can exploit the *Ras* pathway, and this is probably the underlying molecular basis for its preferential replication in transformed versus untransformed cells (74).

When tumour cells are transformed, many cell cycle regulatory pathways involved in the control of growth and apoptosis are altered. Strong et al, 1991 & 1993, showed that cells that are not permissive to Reovirus can be made so by overexpression of the epidermal growth factor receptor (EGFR), which when bound, results in a signaling cascade that induces transformation (75, 76). *Ras* is an oncogene that is activated in many types of cancers, such as pancreatic, breast, ovarian, colorectal, lung, and leukemia. *Ras* proteins are versatile in their effects. They are involved in extracellular communication signals that induce cell differentiation, proliferation and movement. Activated *Ras* induces transformation of cells, inducing over 18 effectors such as *Raf* kinases, PI3-kinase, and guanosine exchange factors for *Ral*. Due to this, *Ras* is a key player in tumour initiation, progression, promoting metastasis, angiogenesis and loss of growth control. Over 30% of cancers have activating mutations in *Ras* genes that cause it to be constitutively active (44, 50).

Reovirus infection of untransformed cells, results in PKR activation and the phosphorylation of its eIF2α subunit, to result in a shutdown of protein synthesis. In cells that have an activated Ras pathway, PKR phosphorylation is inhibited due to a release of a block in the downstream signaling of the *Ras* pathway, allowing viral protein synthesis to continue. The tumour cells therefore lack the activity of PKR and are susceptible to reovirus replication, allowing the virus to replicate. This causes the lysis of the tumour cells at the end of the viral life cycle (66). While an increase in Reovirus protein translation was inferred to increase oncolysis, Marcato et al, 2010 show that *Ras* transformation mediates Reovirus oncolysis by enhancing three major steps in the Reovirus life cycle: (i) increase viral uncoating/proteloytic disassembly, which is three-fold more efficient in Ras-transformed cells; (ii) increased particle infectivity, where virions purified from Ras-transformed cells are four-fold more infectious than those purified from non-transformed cells; and (iii) apoptosis-dependent release, which is mediated by caspases, is nine-fold more efficient in Ras-transformed cells. Over one round of replication, the combined effects of the three steps result in over 100-fold differences in viral yield between *Ras*-transformed and non-transformed cells (44). Shmulevitz et al, 2010 have recently shown that activated oncogenic *Ras* signaling significantly enhances reovirus replication and promotes reovirus spread by suppressing IFN-β (65, 67).

In addition to its control in host translation, PKR also plays a role in transcriptional regulation, cell differentiation, signal transduction, and tumor suppression (26, 40, 80). Many cancers have PKR either missing or inactivated (5), and the fact that many viruses have proteins that target PKR suggests that it is an important pathway to allow viral protein synthesis to continue. Defects in PKR and IFN pathways are characteristics of many tumours and

transformed cells. This enables replication of viruses that are sensitive to interferon to infect and be able to replicate within these cells, VSV and Reovirues being prime examples.

Reovirus oncolysis has been applied *in vivo*, and Coffey et al, 1998, showed that a single intratumoral injection of virus resulted in tumour regression of 65% to 80% of mice in pre-clinical studies (12, 29). Treatment by Reovirus was also effective in tumour regression and survival of SCID/immuno-compromised mice implanted with human colon, ovarian, breast, lymphoma, brain and spinal cancer cells (1, 32, 49, 84, 85). Oncolytics Biotech® is currently conducting clinical trials in the United States and United Kingdom, using Reolysin® as a cancer therapeutic. The current clinical program includes eight Phase I/II or Phase II human trials examining Reolysin® alone or in combination with radiation and chemotherapy. Reovirus acts as a systemic cancer therapeutic to treat a variety of *Ras*-mediated cancers, and this makes it a promising candidate, bringing us a step closer to the cure for cancer.

CHAPTER TWO
RATIONALE AND OVERALL OBJECTIVES

2.1 Objectives and Approach

The overall objectives of my studies addressed basic virology and biological process of gene expression in various cell types to further understand and assess the underlying mechanism for Reovirus oncolysis. This study has also employed Reovirus reassortants, which have novel combinations of gene segments, resulting in different biological properties that were applied to the development of improved oncolytic viruses.

The scope of my work spans across four sub-projects: Reovirus biology, interaction with host factors and the interferon system and viral oncolysis. The overall objectives of my project were:

I. **To study the genetics basis for PKR sensitivity and its role in tropism:** Growth and replication of Reovirus were studied in wild-type (PKR+/+) and PKR -/- Balb-c mice; aspects of lung tropism and infection patterns of Reovirus and reassortants were also investigated.

II. **To study tumour oncolysis by Reoviruses and their reassortants:** A tumour-bearing mouse model was used to study the survival after treatment with parental Reoviruses T1L and T3D, four reassortant strains, as well as the use of Vesicular Stomatitis Virus (VSV) that express Reovirus genes.

III. **To compare Reovirus growth and protein production in fibroblast and epithelial cells:** The growth and protein production were compared between the two parental serotypes T1L and T3D in the fibroblastic cell line, L929 cells versus the CT26 epithelial cell line.

IV. **To compare interferon sensitivities of parental and oncolytic reassortant Reoviruses in fibroblast and epithelium cells:** The growth and protein production of parental Reovirus strains T1L and T3D, and four reassortants were studied in interferon pre-treated and untreated fibroblasts L929 cells, and epithelial cell lines: Vero, CV-1 and CT26 cells.

CHAPTER THREE
MATERIALS AND METHODS

3.1 Cells and Viruses

Mouse connective tissue L929 fibroblasts, mouse colon tumour CT26 epithelial cells, adult African green monkey kidney cells Vero and CV-1 cells were cultured in Minimum Essential Medium (MEM) (Gibco, Grand Island, New York, USA) supplemented with 10% Fetal Bovine Serum (FBS) (Wisent Inc., Canada), 100U/ml penicillin, 100µg/ml streptomycin and 0.225% $NaHCO_3$ and propagated at 37^{o}C in 4% CO_2. Reovirus strains used in this study were the parental strains Type 1 Lang (T1L) and Type 3 Dearing (T3D) initially obtained from B. N. Fields (Harvard University, Cambridge, MA). The T1L x T3D reassortant strains were previously produced by Earl G. Brown (Brown *et al*., 1983). The single segment reassortants T1HA3 (T1L with S1 segment of T3D) and T3HA1 (T3D with S1 segment of T1L), as well as the σ1s expressing T3C84 strain and the σ1s-null strain T3C 84 MA were provided by Dr. Terry Dermody (Vanderbilt University, Nashville, TN).

3.2 Infection of cells, collection of protein samples and virus titration

To grow viruses, a confluent monolayer of the desired cell line was infected with parental Reovirus and reassortant strains, at an MOI of 10. At 3 days post infection infected cells were subjected to three freeze-thaw cycles, centrifugation (1000 rpm, 3 minutes) for subsequent viral titration by plaque assay as previously described (Zou & Brown, 1996). To collect samples for protein production in various cell lines, monolayers of the studied cell line were infected in 6-well plates at an MOI of 10, overlaid with 3ml of complete MEM before incubation at 37^{o}C for defined times (hours post viral infection) until collection of supernatant (for viral titration) or infected cells in SDS PAGE sample buffer (for western blot analysis).

For virus titration, virus samples were serially diluted in PBS. Six well plates of confluent monolayers of L929 cells were infected with 100µl of the different virus dilutions in duplicates for each dilution. The plates were incubated at 37°C for 30 min to allow virus adsorption. Following adsorption, the cells were overlaid with 3ml of 1% agar (Becton, Dickinson and Company, MD, USA), in complete MEM. The plates were incubated at 37°C. Overlay medium was added every 3 days. On day 6, the third and final overlay was supplemented with 1.5% neutral red (Fisher Scientific, USA), and plaques were counted the following day to determine virus titers.

3.3 Immunoblotting

Infected cell monolayers were lysed in 1 x SDS sample buffer (62.5mM Tris-HCl, pH 6.8, 10% glycerol, 2% SDS, 0.05% bromophenol blue and 5% 2-mercaptoethanol). The proteins were separated by SDS-PAGE on 10 % gels and then transferred to PVDF membranes (Immobilon-P, Millipore Corp. Mississauga, Canada) by semi-dry transfer at 15 V for 45 minutes. The membrane was blocked with 5% skim milk in PBS for 1 hour at room temperature, followed by the addition of the primary antibody (refer to section 3.4 in materials and methods for a complete list of antibodies used and working dilutions) in fresh 5% skim milk in PBS and incubated for 2 hours at room temperature. The membrane was washed three times for 10 minutes in PBS, followed by incubation in secondary antibody in 5% milk in PBS for 1 hour at room temperature. The membrane was washed four times in PBS before reaction with the SuperSignal WestPico Chemiluminescent Substrate kit (Thermo Scientific, Rockford, IL) and exposed to Kodak scientific imaging films.

3.4 Antibodies

The following is a list of the antibodies used in all the experiments in this research.

Antibody	Working Dilution	Source	Primary / Secondary	Used for
Rabbit anti-T1L	1:500	Dr. E. Brown, University of Ottawa	Primary	IB, IF
Rabbit anti-T3D	1:1000	Dr. E. Brown, University of Ottawa	Primary	IB, IF
Rabbit anti-μ2	1:1000	Dr. E. Brown, University of Ottawa	Primary	IB
Rabbit anti-mouse PKR	1:1000	Dr. J. Bell, University of Ottawa	Primary	IB
Anti-phospho-PKR ($pThr^{451}$)	1:1000	Sigma-Aldrich	Primary	IB
Rabbit anti-eIF2α	1:500	Stressgen Bioreagents Corp, Victoria, BC	Primary	IB
Rabbit anti phospho-p51 eIF2α	1:1000	Santa Cruz Biotechnology, Inc.	Primary	IB
Rabbit anti-IRF-3	1:500	Santa Cruz Biotechnology, Inc.	Primary	IB
Rabbit anti-IRF-7	1:1000	Santa Cruz Biotechnology, Inc.	Primary	IB
Rabbit anti-actin	1:1000	Sigma, St. Louis, MO	Primary	IB
Goat anti-rabbit IgG-HRP conjugated	1:10,000	Sigma, St. Louis, MO	Secondary	IB
Donkey anti-rabbit IgG-Cy3 conjugated	1:800	Jackson Immunoresearch Lab, Inc.	Secondary	IF
Donkey anti-rabbit IgG-FITC conjugated	1:800	Jackson Immunoresearch Lab, Inc.	Secondary	IF

IB – immunoblotting; IF – immunofluorescence.

3.5 Infection of Balb-c Mice and Tumour implantation

All protocols in this study were approved by the University of Ottawa Animal Care and Veterinary Services (ACVS) and conformed to the Canadian Council on Animal Care guidelines. Wild type Balb-c (Charles River Laboratories, Quebec) and PKR knockout Balb-c mice (generously provided by Dr. John Bell, Ottawa Regional Cancer Center) were intranasally infected with the parental T1L and T3D or reassortant reovirus strains (at desired doses, specified in results and figure legends). Body weights were measured on a daily basis. For

studies on viral growth in mice lungs, the mice were euthanized and the lungs were harvested at determined days post-infection for titration of infectious yield of the virus after sonication, with values indicated as pfu/g.

To establish the *in vivo* tumor model, 4-6 week old adult female Balb-c mice (Charles River Laboratories, St. Hyacinthe, PQ) were administered 3 x 10^5 CT26 cells intravenously. Seven days post tail-vein injections, the mice were anaesthetized with isofurane (3% in oxygen) for 3 minutes, and given the required dose for Reovirus treatment, depending on the study, 1 or 3 treatments at days 1, 4 and 7 were administered (doses specified in results and figure legends). The mice were placed into different groups and were administered either parental Reovirus T1L or T3D, one of the four reassortant strains EB88, EB96, EB97 or EB123, or a mock PBS treatment. For further studies, VSV strains expressing both T1L and T3D M1 genes (VSV-T1M1 and VSV-T3M1, respectively), along with a VSV-control virus expressing GFP (VSV-GFP) were also used to treat tumour bearing Balb-c mice, at a single dose of 10^7 pfu/mouse. Mice were monitored daily to assess post-treatment survival.

3.6 Immunochemistry and Immunofluorescence

Infected lungs were harvested and fixed in 3.7% formaldehyde for 24 hours, followed by storage at 20% sucrose at 4^{o}C. Cryostat lung sections were cut to 12 μm thickness, fixed in acetone and stained with a primary antibody cocktail of 1:1000 dilution of anti-T1L and 1:1000 dilution of anti-T3D rabbit serum. 1:800 of Donkey anti-rabbit (Jackson ImmunoResearch Laboratories, Pennsylvania, USA) Cy3-conjugated was used as the secondary antibody. Lung sections were washed three times with 10mM PBS (154mM NaCl, 2.5mM NaH_2PO_4, 15mM NaH_2PO_4) after primary and secondary antibody staining and once after Hoescht staining. Lungs were mounted with anti-fade mounting medium (90% glycerol, 10% PBS, 1 mg/ml p-

phenylenediamine). Stained lung sections were visualized using an inverted fluorescent microscope (BMAX Series Microscopes, Olympus America Inc.) using the 20x and 40x objective lenses, and processed in a parallel manner using Adobe Photoshop 7.0

3.7 Interferon-β ELISA Assay

Monolayers of L929 or CT26 cells were infected with each of the parental Reovirus strains T1L and T3D and the four reassortant strains EB88, EB96, EB97 and EB123 at an MOI of 2. Twenty-four hours post infection, the cell supernatant was collected and was measured for IFN-β production. Mouse IFN-β was titrated relative to mouse IFN-β standards by commercial ELISA as described by the manufacturer, PBL Biomedical Laboratories (New Jersey, USA).

3.8 Interferon Sensitivity Assay

Confluent monolayers of L929, CT26, CV-1 and Vero cells were seeded onto 6-well plates. Cells were either pre-treated with complete MEM containing mouse or human interferon (200U/ml, 2ml per well; Sigma, St. Louis, USA) for 24 hours. Complete MEM was added to untreated cells. Following 24 hours with or without interferon pretreatment, the monolayers were infected at an MOI of 10 with parental Reovirus strains T1L or T3D or the four reassortant strains EB88, EB96, EB97 or EB123. Cells were incubated for 30 minutes, to allow for virus adsorption, before 3ml of fresh MEM was added to each well and the cells incubated at 37°C until sample collection. Protein samples for interferon treated and untreated monolayers were collected at 16, 24, 48 and 72 hours post infection in 1 x SDS sample buffer, followed by SDS-PAGE and immunoblotting for actin and viral proteins. The supernatants from all interferon treated and untreated monolayers of each line were collected at 72 hours post infection to determine viral titers (previously described). All experiments were done in triplicate for each virus and cell line.

CHAPTER FOUR
STUDYING THE GENETIC BASIS FOR PKR SENSITIVITY AND ASPECTS OF REOVIRUS LUNG TROPISM

4.1 Background and prior studies

The molecular genetic basis for Reovirus PKR sensitivity has been previously studied in our lab. It was shown that when PKR +/+ and PKR -/- mouse embryo fibroblast (MEF) cells were infected with parental T1L and T3D serotypes, that both serotypes grew well in the absence of PKR; in addition T1L replicated better than T3D in both the absence and presence of PKR. The parental serotypes were sensitive to growth and replication in wild type (PKR+/+) MEFs, as shown by the yield in Figure 5, where we saw that PKR inhibited the yield of T1L and T3D. It was reasoned that the sensitivities to PKR differed between the two serotypes due to differences in their biological properties controlled by their gene segments.

To further elucidate the genetic basis for increased PKR dependent and PKR independent growth of T1L in fibroblasts, the yield of 19 Reovirus reassortant strains in wild type and PKR -/- MEFs was analyzed, and it was shown that the M1 gene segment from T3D controlled PKR sensitivity and both the L3 and M1 gene segment from T1L controlled the virus yield in the absence of PKR.

Figure 5. Reovirus replication and protein production in PKR+/+ and PKR-/- mouse embryo fibroblast cells. Infectious yield was measured in PKR+/+ and PKR-/- MEF cells after infection with T1L or T3D at an MOI of 10, and harvested at 3dpi. Viral yields were obtained by plaque assay. The yield of both parental serotypes, T1L and T3D, was inhibited by PKR in mouse embryo fibroblast (MEF) cells.

YIELD IN PKR-/- VS PKR+/+ MEF

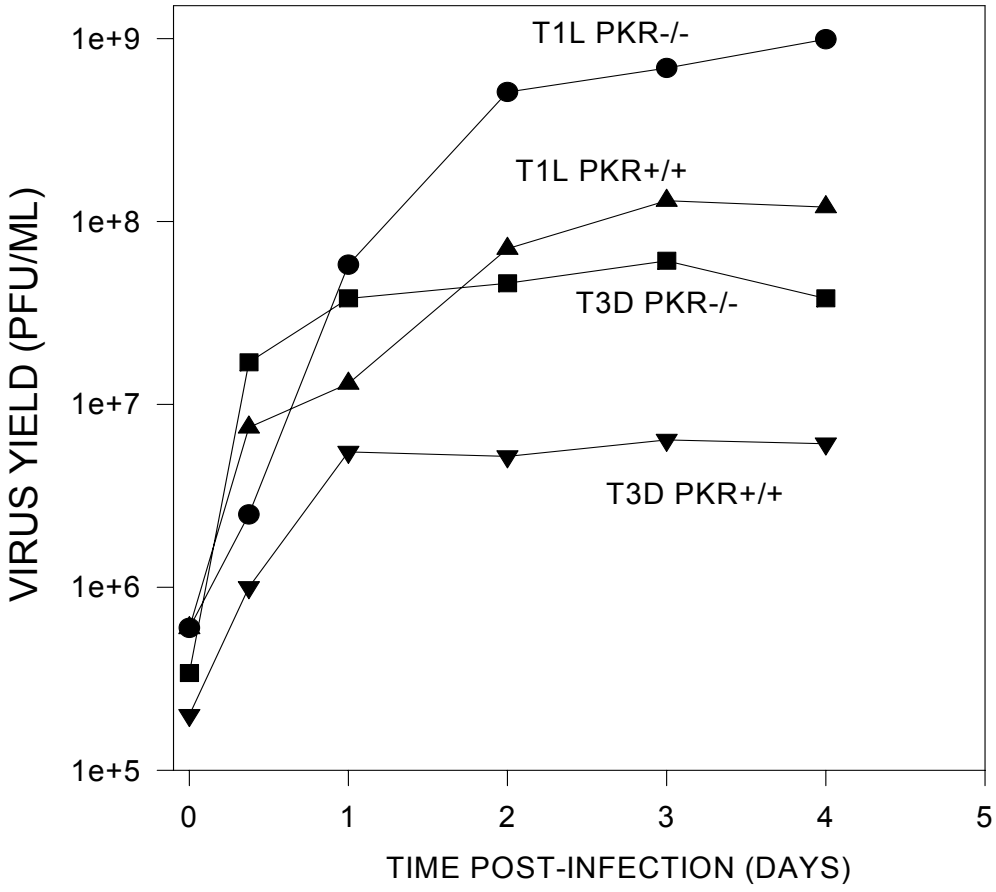

However, when the role of PKR on T1L viral growth and replication was assessed in the adult mouse lung model, it replicated less well in the PKR -/- lung, but better in the wild type PKR+/+ lung. In contrast, T3D had a higher yield than T1L in the PKR-/- lung, as shown in Figure 6. This suggested that the biology of Reovirus growth and replication differed between the fibroblasts and the lung epithelium.

While the analysis of fibroblasts revealed that the M1 genome segment controlled PKR sensitivity, it was found that the S1 gene segment determined the primary control of PKR-dependent replication in the bronchial epithelium. My project extended these observations to further elucidate the biology of the S1 gene segment.

Figure 6. The yield of T1L and T3D in wild type and PKR knock-out Balb-c mice lungs. Mice were infected with 10^5 pfu of T1L or T3D, and lungs were harvested at various days post infection to observe viral yield by plaque titration. Values are show as averages titers/gram for two animals, with standard errors.

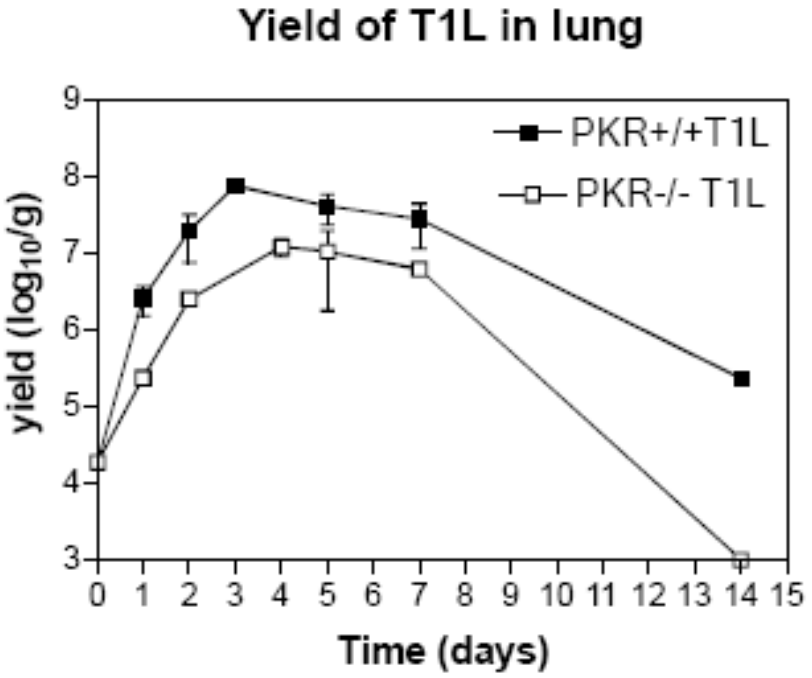
Yield of T1L in lung
PKR+/+T1L
PKR-/- T1L
yield (log10/g)
Time (days)

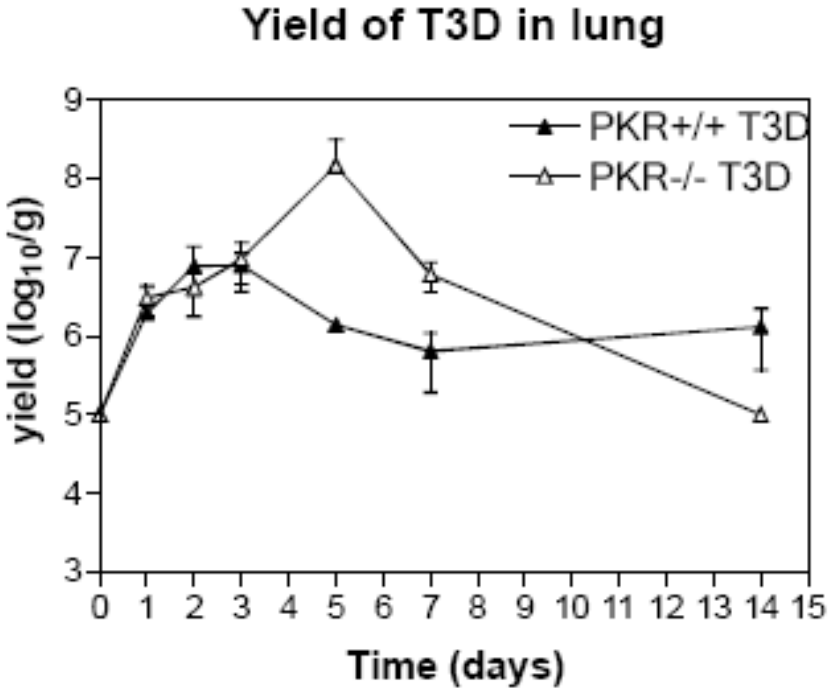
Yield of T3D in lung
PKR+/+ T3D
PKR-/- T3D
yield (log10/g)
Time (days)

The Reovirus S1 gene segment is bicistronic, encoding σ1, a 49kDa viral receptor protein and the 14kDa σ1s non-structural protein, encoded by an overlapping alternate reading frame (60). The σ1 protein is a structural protein located on the outer capsid of the virus, that functions as the cell attachment protein, and therefore specifies tissue tropism for target cells within the host. It also determines the primary serotype, the pattern of reovirus spread and is responsible for viral hemagglutination (23, 55, 72). The differences in pathogenesis of the parental T1L and T3D Reovirus strains in causing myocarditis and encephalitis is due, at least in part, to the specific tropism and spread that is controlled by the σ1 protein, encoded by the S1 genes (22, 23, 55).

Each mammalian Reovirus serotype (T1L, T2J and T3D) has its own unique S1 gene segment that defines classification in each serotype, and thus this genome segment shows the greatest difference relative to the rest of the viral proteins. T1L and T3D share approximately 25% amino acid identity in their σ1 protein (18). Joklik et al, 1980 has also shown that neutralizing antibodies against T1L cross-react with T3D proteins only if they are specific to viral proteins other than σ1 (24). Antibodies to σ1 mediate virus neutralization and serve as the basis for classifying Reoviruses into serotypes.

The other protein encoded by the Reovirus S1 gene segment, σ1s, is a non-structural protein, which is located 55 nucleotides downstream and has an alternate initiation site (60). σ1s is a key determinant of the ability of Reovirus to induce cell cycle arrest (53, 54) and influence the kinetics of apoptosis induction in the heart and the central nervous system (35). A recent study by Boehme et al, 2009, has shown that σ1s is required for the establishment of viremia and systemic dissemination (7), although the protein is expressed at low levels and at early stages post-infection in cell culture (55).

4.2 Specific Objectives

The S1 gene segment plays a key role in Reovirus biology, pathogenesis and cell tropism in the lung (J. Major and E. Brown, unpublished), therefore, we intended to understand the S1 gene biology in the context of viral growth, replication and yield in PKR +/+ and PKR -/- mice lungs.

The specific objectives for this portion of my project were:

i. To compare parental Reovirus growth and lung infection patterns in wild type Balb-c (PKR +/+) and TIK knock-out Balb-c lungs (PKR -/-)
ii. To further confirm that the S1 gene segment plays a role in the observed pattern of lung infections
iii. To use single segment S1 Reovirus reassortants to verify if S1 hypothesis holds
iv. To assess the role of the σ1s protein in controlling infection of mouse lung epithelium

4.3 Results

4.3.1 PKR Protects the Mouse Lung Bronchial Epithelium from Reovirus T3D Infection

To compare the growth and infection patterns of parental Reovirus in PKR +/+ and PKR -/- mice lungs, wild type Balb-c and PKR -/- mice were intranasally infected with 10^7 pfu/mouse of T1L, T3D or PBS. Three days post infection, mice lungs were harvested and were stained for viral antigens using anti-Reovirus antibodies (Figure 7).

In wild type Balb-c mice lungs, Reovirus infection by both parental serotypes T1L and T3D was limited to scattered foci of infection in the alveolar regions, without infection in the bronchiolar epithelium. However, in the PKR knock-out mice lungs, infection by T1L was again restricted to the alveoli, whereas T3D was able to infect both the alveoli and the bronchiolar

Figure 7. Immunofluorescent staining of wt Balb-c mice lungs (PKR +/+) and TIK mice lungs (PKR -/-). Mice infected with 10^7 pfu of T1L or T3D and lungs were harvested at 3 dpi. Viral antigens were detected by staining frozen lung sections with anti-T1L or anti-T3D primary antibody, followed by Cy3-conjugated (red) secondary antibody. Nuclei were stained with Hoechst (blue). Infection of the alveolar region was observed in wt Balb-c PKR+/+ lungs for both T1L and T3D, where as infection of the bronchioles was observed in TIK mice infected with T3D. Figure shown is a representation of other stained regions.200x magnification, arrows point to bronchioles (B).

Balb-c Mice lungs (PKR+/+)

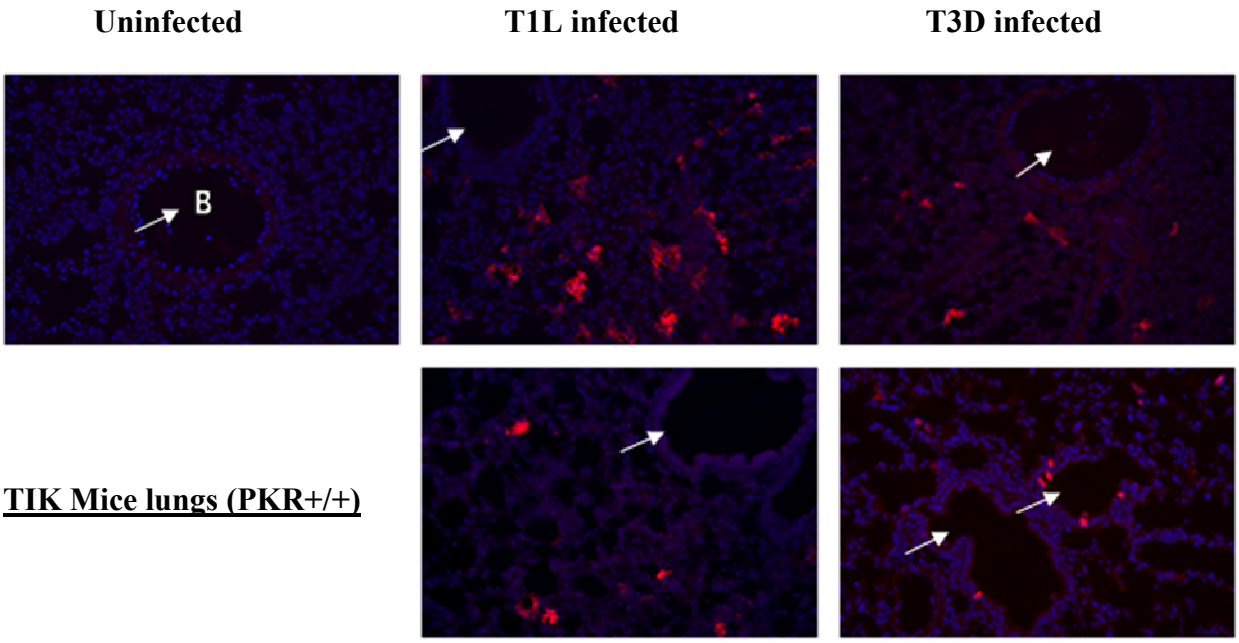

epithelium, as seen by viral staining of the cuboidal shaped cells lining the airway. PKR therefore was able to protect the wild-type lung bronchial epithelium from infection from Reovirus T3D.

Increased infection by T3D, but not T1L to the bronchiolar epithelium in PKR-/- Balb-c mouse lung indicated that the parental Reoviruses differed due to the genetic determinants for replication in bronchiolar epithelium of PKR-/- mice. Moreover, since Reovirus tropism of the bronchial epithelium was controlled by the S1 segment, we further investigated the role of the T3D S1 in the infection of the lung epithelium.

4.3.2 Differential staining of alveoli and bronchial epithelium observed after infection of PKR -/- lungs with a panel of Reovirus reassortants.

To further confirm the genetic basis for tropism of the bronchiolar epithelium, PKR -/- mice were infected with a panel of 18 Reovirus reassortant strains, at a dose of 10^6 pfu/mouse. Mice lungs were harvested 3 days post infection, and stained using anti-Reovirus antibodies. Figure 8 shows the viral staining of mice lungs infected with each of the Reovirus reassortants.

The reassortant viruses that had the T3D S1 genome segment were observed to infect both the alveolar and the bronchiolar epithelium whereas those containing the T1L S1 genome segment were limited to alveolar regions only. This clearly mapped the increased bronchiolar tropism to the T3D S1 genome segment (Figure 8, Table 2), with the only exception being EB96, which possessed the S1 from T1L, and this will be discussed later. Thus bronchiolar tropism in PKR-/- mice was primarily mapped to the T3D S1 genome segment.

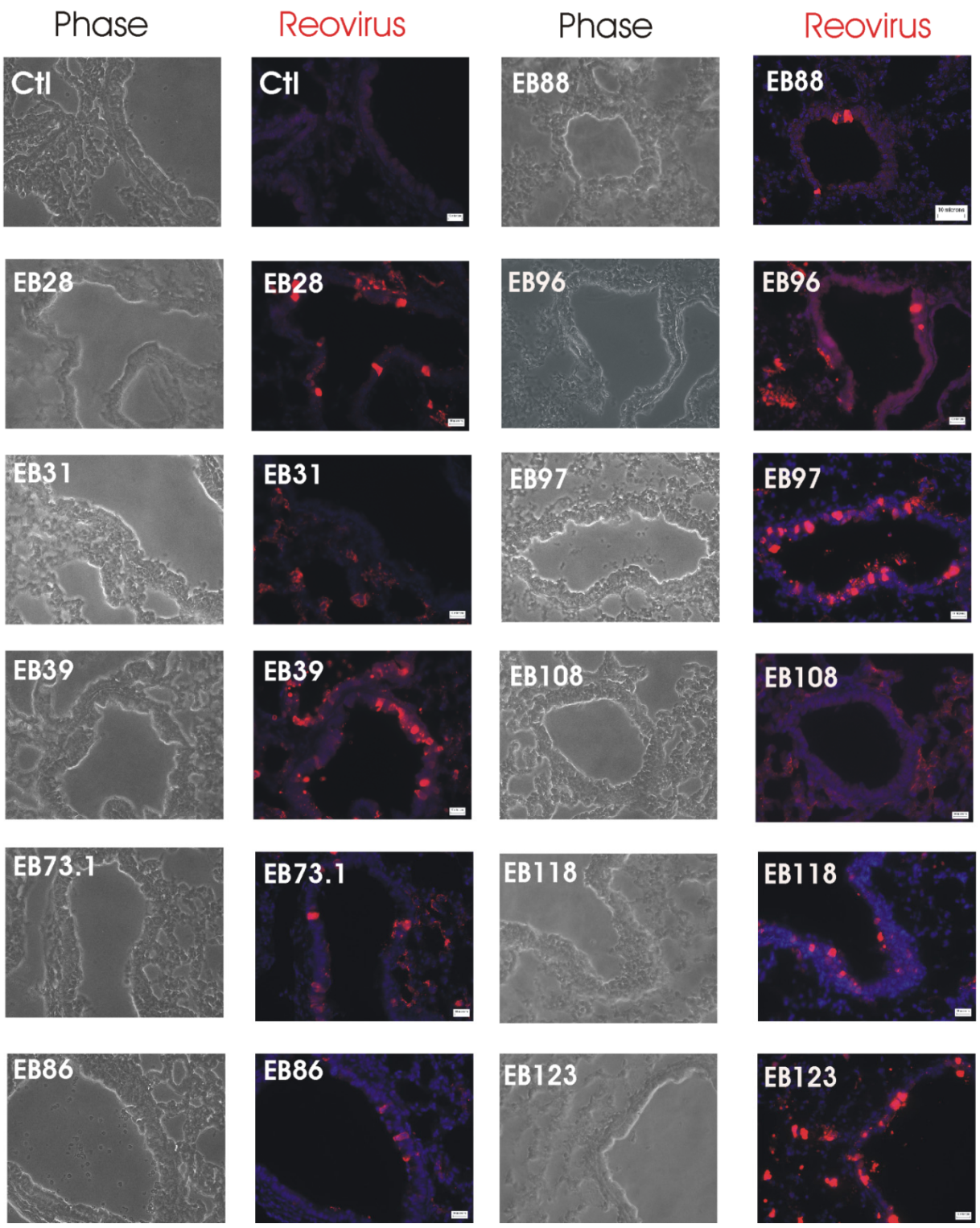
Phase
Reovirus
Phase
Reovirus
Ctl
Ctl
EB88
EB88
EB28
EB28
EB96
EB96
EB31
EB31
EB97
EB97
EB39
EB39
EB108
EB108
EB73.1
EB73.1
EB118
EB118
EB86
EB86
EB123
EB123

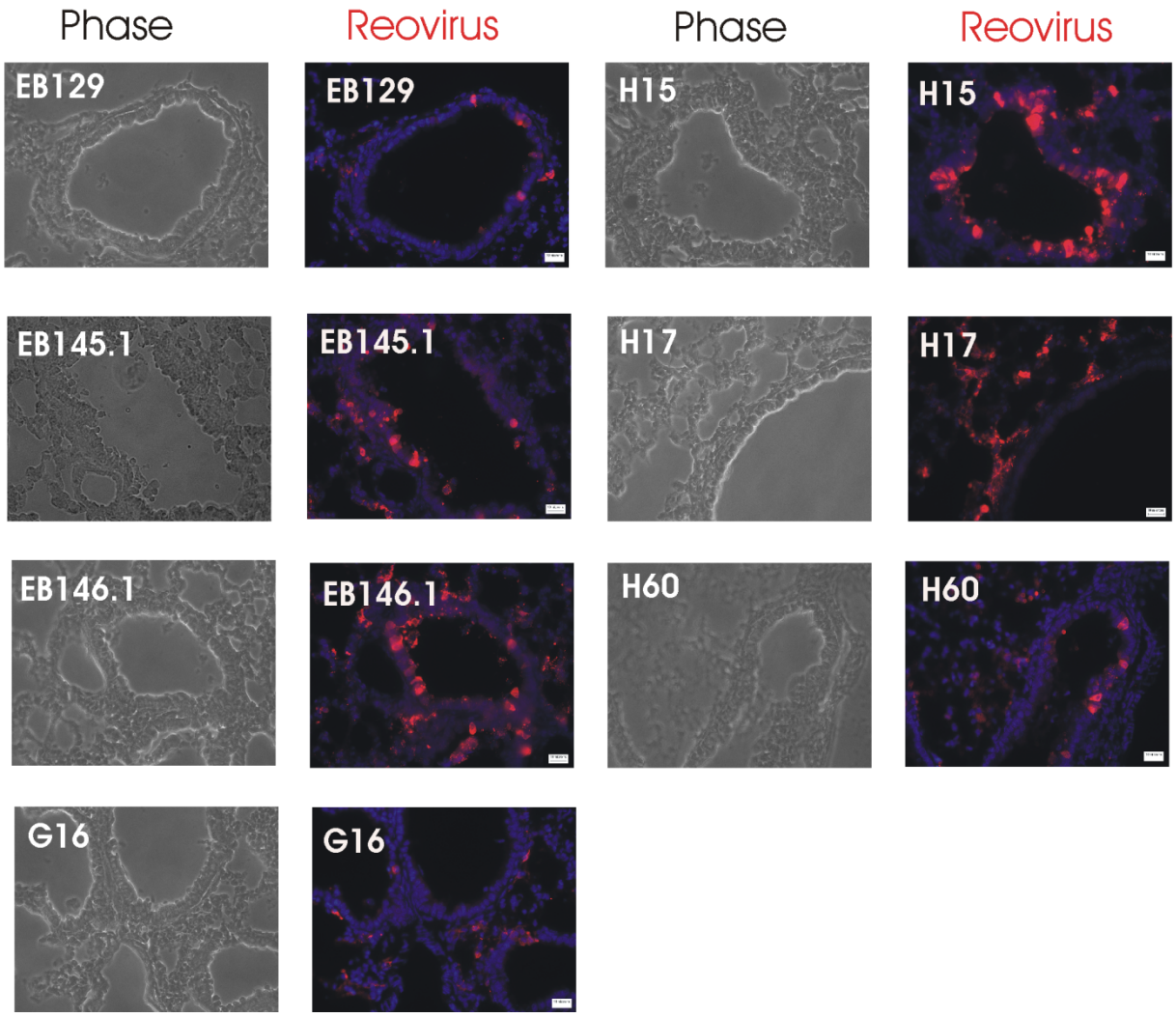

Figure 8. Genetic basis for infection of the mouse bronchiolar epithelium by T3D S1. A panel of 18 T1L x T3D reassortants (see Table 2) was used to intranasally infect PKR -/- mice at 10^6 pfu or mock infected with PBS (ctl) before lungs were harvested at 3 dpi and cryostat sectioning and staining with a cocktail of anti-T1L and anti-T3D primary antibody, followed by Cy3-conjugated (red) secondary antibody. Nuclei were stained with Hoechst (blue); All reassortants viruses that possessed the T3D S1 genome segment were able to infect the bronchial epithelium, whereas those reassortants that possessed the T1L S1 genome segment were only able to infect the alveolar region. Images were obtained at 40x magnification. B, bronchioles. Scale bars: 10μm.

Table 2. Genome map of the 18 T1L x T3D Reovirus Reassortants

Reassortant	L1	L2	L3	M1	M2	M3	S1	S2	S3	S4	Bronchiolar tropism
EB31	L	L	L	D	L	L	L	D	D	L	–
EB96	L	D	L	D	L	L	L	L	D	L	+
EB108	L	D	L	D	L	L	L	L	D	D	–
G16	L	L	L	D	L	L	L	D	L	L	–
H17	D	D	L	L	D	D	L	D	D	L	–
EB28	D	D	L	D	D	D	D	L	D	D	+
EB39	L	D	D	L	D	D	D	D	D	D	+
EB73.1	L	D	L	L	D	D	D	D	D	D	+
EB86	L	D	D	D	D	L	D	D	D	L	+
EB88	D	D	D	D	L	D	D	D	D	D	+
EB97	D	D	L	D	D	D	D	D	D	L	+
EB118	D	D	L	L	D	D	D	D	L	L	+
EB123	D	D	L	D	D	D	D	D	L	D	+
EB129	D	D	D	D	D	L	D	L	L	D	+
EB145.1	D	D	D	D	D	D	D	D	D	L	+
EB146.1	L	D	L	L	D	D	D	D	D	D	+
H15	L	D	D	L	D	D	D	D	D	L	+
H60	D	D	L	L	D	D	D	D	D	L	+

4.3.3 Single S1 genome reassortment determined infection of the primary lung bronchial epithelium in PKR -/- mice

To further confirm the role of the T3D S1 gene in bronchiolar tropism, we used single segment reassortants that had interchanged S1 gene segments from T1L and T3D on the genetic backbone of the alternate serotype, i.e. reassortant T1HA3 had a T1L genome with the exception of its S1 gene segment, which was from T3D, and vice versa for T3HA1, which possessed a T1L S1 genome segment on the T3D genetic background.

After infection of PKR -/- mice with 10^6 pfu/mouse of the single segment reassortants, T1HA3 infection was observed in both the alveoli as well as the bronchiolar epithelium. However, infection by reassortant strain T3HA1 resulted in the detection of viral antigens to be limited to the alveoli, with no bronchiolar staining observed in any section. Results from this experiment further confirmed that the difference between T1L and T3D infection of the primary lung epithelium was controlled by the S1 genome segment from T3D (Figure 9).

Figure 9. Infection of single segment reassortant in PKR -/- mice lungs. PKR-/- mice were infected with 10^5 pfu of T1HA3 (T1L with S1 from T3D) and T3HA1 (T3D with S1 from T1L). Lungs were harvested 5 days post infection for immunofluorescence staining of frozen lung tissue using a cocktail of anti-T1L plus anti-T3D primary antibody, followed by Cy3-conjugated (red) secondary antibody. Nuclei were stained with Hoechst (blue). Images obtained at 400x magnification; Figure shown is a representation of other stained regions; arrows point to bronchioles (B); scale bars: 10μm.

PKR -/- Mice Lungs

PBS

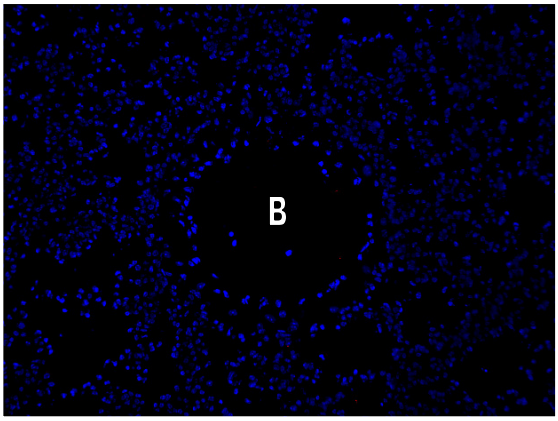

T1HA3

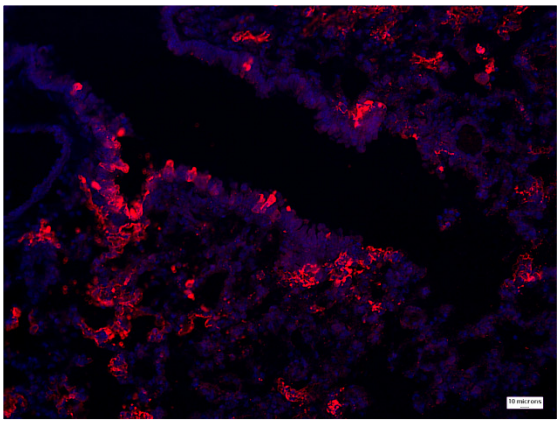

T3HA1

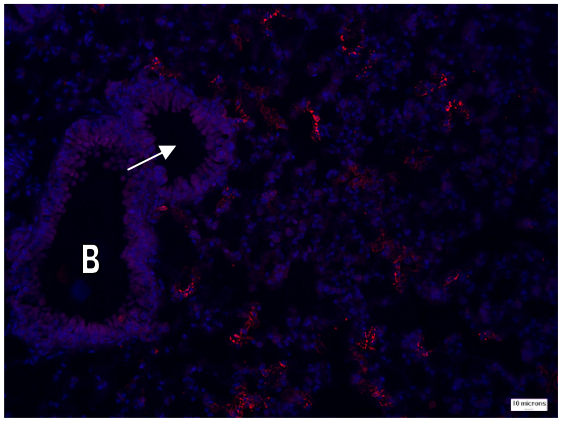

4.3.4 Infection of the Mouse Bronchial Epithelium is σ1s dependent

We have thus far shown that the extent of infection in the bronchial epithelium is primarily controlled by the T3D S1 gene segment. The S1 gene segment encodes two proteins, σ1 and σ1s. To further elucidate the role of these proteins in epithelial tropism, PKR-/- mice were infected with T3D strains that differ in their expression of σ1s. The T3C-84 strain expresses both σ1 and σ1s, whereas the T3C-84MA strain contains a termination mutation at the 6th amino acid position in the alternate reading frame, creating a σ1s null mutant (55).

When PKR -/- mice were infected with these two viruses, we observed that the T3C-84 strain resulted in a strong infection of the bronchial epithelium, as depicted by the staining of the cuboid-shaped cells lining the bronchiole (marked "B" in Figure 10). In contrast, the infection by the σ1s null mutant strain T3C-84MA did not infect the bronchial epithelium. The immunofluorescence images in Figure 10 showed that the infection of the primary lung epithelium in PKR -/- mice was dependent on the T3D σ1s protein.

Figure 10. Viral staining by Reoviruses that differ in their expression of σ1s. PKR-/- mice were infected with 10^5 pfu of T3C-84 (T3D expressing σ1s) and T3C 84 MA (T3D σ1s- null mutant). Lungs were harvested 5 days post infection for immunofluorescence staining of frozen lung tissue using a cocktail of anti-T1L plus anti-T3D primary antibody, followed by Cy3-conjugated (red) secondary antibody. Nuclei were stained with Hoechst (blue) or phase contrast images were obtained at 400x magnification; Figure shown is a representation of other stained regions. B, bronchioles.

PKR -/- Mice Lungs

T3C-84

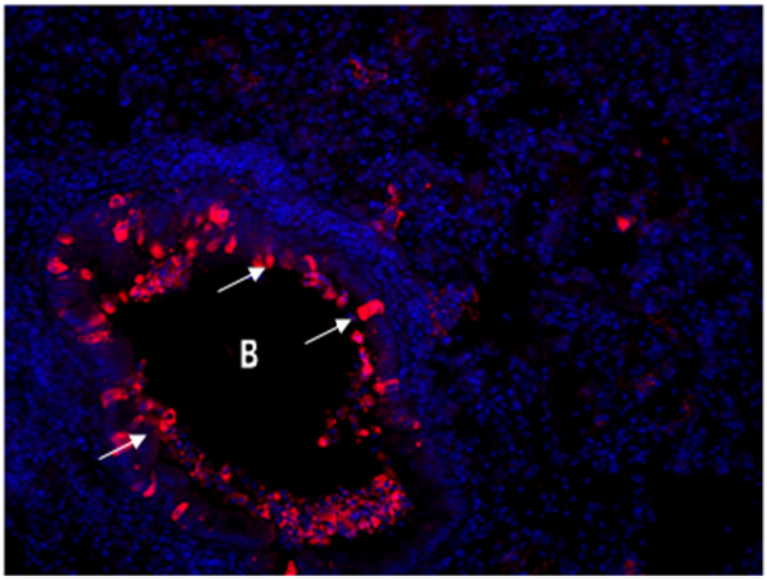

T3C-84 MA

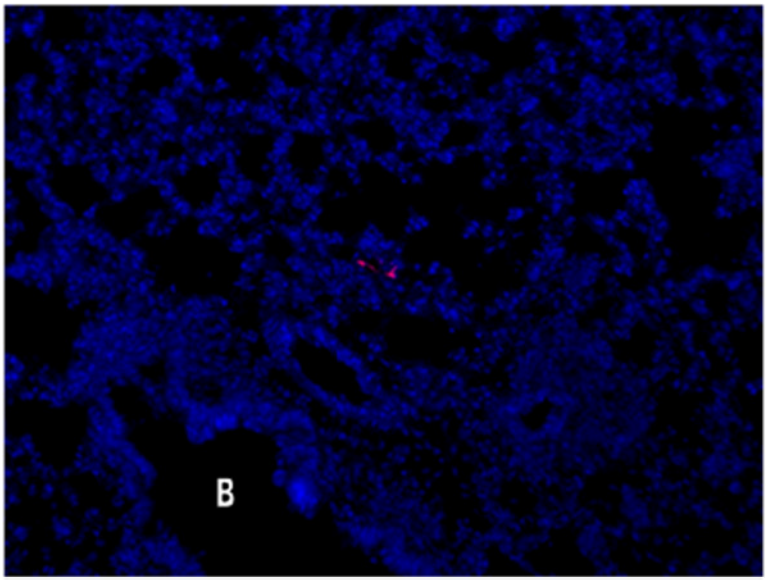

4.3.5 The effects of PKR on the Reovirus parental strains with respect to Reovirus-induced disease

To study the effect of PKR on Reovirus induced disease, groups of five Balb-c PKR+/+ and Balb-c PKR -/- mice were infected with 10^6 pfu/mouse of either parental serotypes T1L and T3D. Weight loss was monitored on a daily basis.

Given that the extent of weight loss is a measure of the extent of disease severity, infection of Balb-c PKR +/+ was more extreme that in Balb-c PKR -/- when infected with T1L. The lowest average weight for 5 mice was found to be at 75% of the original body weight in Balb-c PKR +/+ mice, compared to 85% in Balb-c PKR -/- mice at 9 days post infection. In contrast, upon infection with T3D, the average body weights for Balb-c PKR+/+ mice showed an increase of 11.2% over the course of two weeks post infection; whereas infection of Balb-c PKR -/- mice resulted in a 5% decrease in the average body weight loss.

When compared to infection by T3D, the effect of T1L infection was more dramatic, as demonstrated by the significant decrease in body weight loss after a week post infection in both Balb-c PKR+/+ and PKR -/- mice (Figure 11). This disease severity correlated with the growth effects seen in figure 6.

Figure 11. Average body weights in Balb-c (PKR+/+) and TIK (PKR-/-) mice after infection with parental Reoviruses T1L or T3D. Intranasal T1L and T3D infection of adult PKR+/+ Balb-c versus PKR -/- Balb-c mice shows both enhancement and protection against Reovirus-induced disease respectively. Groups of five mice were infected intranasally with 10^6 pfu of T3D or T1L, and body weight was monitored for 14 days. Mean percent body weight values are shown with standard plus or minus one standard deviation. PKR -/- mice infected with T3D did not show a significant decrease in body weight than PKR+/+ mice, but the converse was observed with mice infected with T1L, where infection by T1L led to significant weight loss.

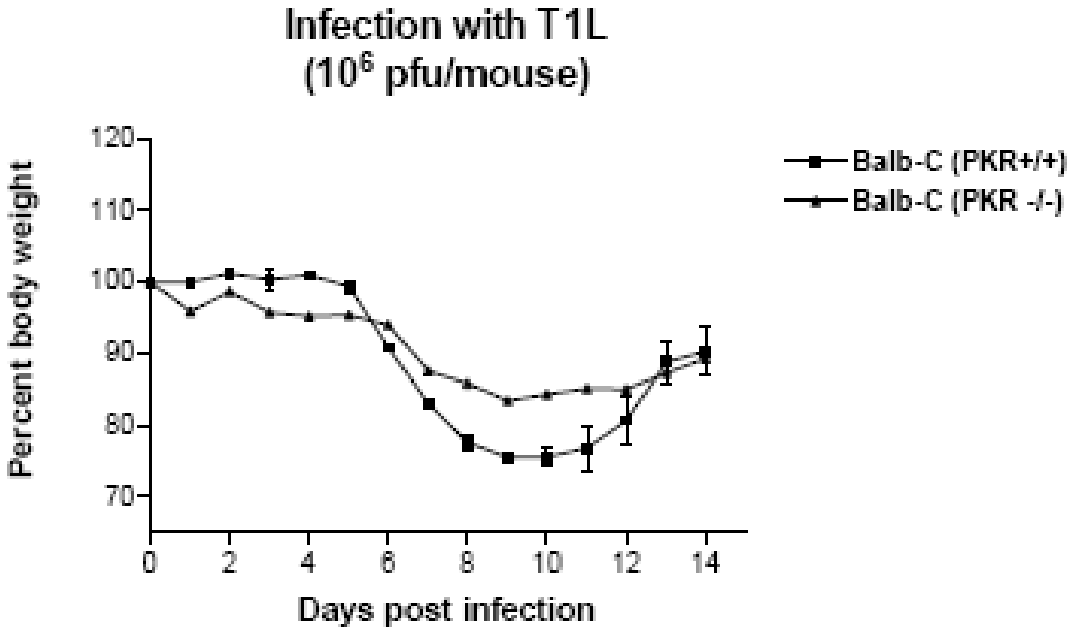
Infection with T1L
(10^6 pfu/mouse)
Percent body weight
120
110
100
90
80
70
0
2
4
6
8
10
12
14
Days post infection
Balb-C (PKR+/+)
Balb-C (PKR -/-)

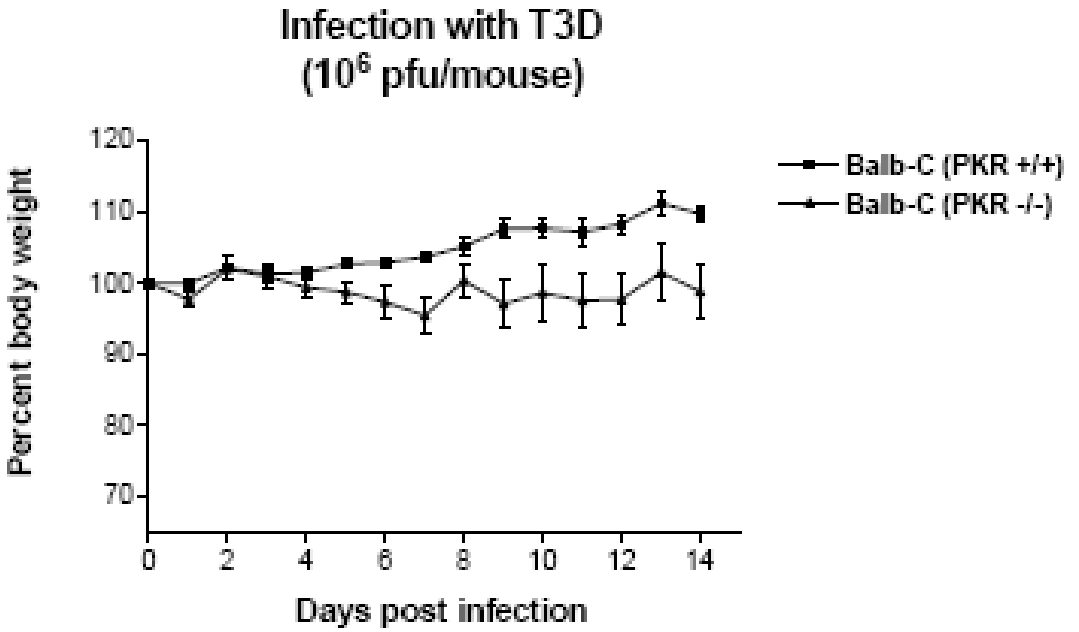
Infection with T3D
(10^6 pfu/mouse)
Percent body weight
120
110
100
90
80
70
0
2
4
6
8
10
12
14
Days post infection
Balb-C (PKR +/+)
Balb-C (PKR -/-)

4.3.6 Growth of Reoviruses and Reassortants in Balb-c and PKR -/- mice lungs and PKR sensitivity with respect to the S1 gene segment.

The growth of the reassortants that have been used for viral staining have also been studied with respect to replication in PKR+/+ and PKR -/- lungs. Groups of 3 wild type Balb-c and PKR-/- mice were infected with 10^5 pfu/mouse of Reovirus. Five days post infection, lungs were harvested and the infectious yield was determined by viral plaque assays (Figure 12).

As observed in our previous studies, T3D was more sensitive to PKR than T1L, as shown by the yield of the two parental reassortants in mouse embryo fibroblasts (figure 5). We observed the same where we found that the yield of T1L is minimally effected by PKR, where as the effect of PKR shows a 100-fold decrease in viral yield of T3D in PKR +/+ mice lungs (Figure 12). Although T1L and T3D differ in tropism for both fibroblasts and bronchiolar epithelium, the genes that control these differences differ both with respect to cell type and their relationship with PKR.

Although PKR inhibits both T1L and T3D growth in MEF, T1L grows better than T3D in MEF (in both PKR +/+ and PKR -/-), primarily due to properties of the T1L M1 gene (encoding the μ2 protein) and to lesser extent the L2 gene. The MEF pattern of growth of T1L versus T3D reflected in the viral yield in mice lungs, however, T1L replication was stimulated by PKR rather than inhibited (as shown in fibroblasts). This indicated that lung tissue differs from MEF in cellular factors that control Reovirus replication. The bronchiolar epithelium does not support T1L infection, indicating that T1L and T3D Reoviruses have serotype dependent differences in the ability to infect the various cell types that make up organs and presumably tumours. Although our studies raise more questions than they answer, they indicate that Reoviruses with altered cell tropism can be generated by reassortants between T1L and T3D.

No significant difference was observed when comparing the growth of T1HA3 in wild type Balb-c and PKR -/- mice lungs. T3HA1, which has its S1 gene segment from T1L, shows a decrease in viral yield in PKR -/- lungs from 10^8 to $10^{6.3}$ compared to T3D. This shows that in the absence of PKR, viral yield was reduced. Comparing the growth of T1L and T1HA3 (which has its S1 from T3D on an otherwise T1L background) in Balb-c PKR +/+ mice, we observed that the presence of S1 from T3D caused the reassortant to become sensitive to PKR, which resulted in a decrease in viral yield in Balb-c lungs from $10^{7.5}$ to $10^{6.3}$.

Both T3C-84 and T3C-84 MA had similar growth patterns, where the yield in PKR +/+ lungs was 50-100 fold lower compared to the growth in PKR -/- lungs. However, the viral yield of T3C-84 MA was 10 fold higher in PKR +/+ lungs than T3C-84.

Comparing the overall yields of Reoviruses and the reassortants, we found that the yields were generally lower in PKR +/+ mice lungs, except for T1L, where we find that the yield was 5-fold higher in PKR +/+ lungs than PKR -/- lungs.

4.4 Discussion

4.4.1 Lung PKR inhibits T3D and also prevents infection of bronchioles

The expression of PKR in the Balb-c mouse lung showed that the infection by both T3D and T1L was restricted to the alveolar region only. This was very interesting because infection via the intranasal route involves the delivery of inoculum through these airways and thus the bronchioles have been exposed to 10^5 pfu of Reovirus. However, in the PKR -/- mouse lung, T3D, but not T1L, was able to infect the mouse lung bronchiolar epithelium (Figure 7). This indicated a protective role played by PKR, where it protected the bronchiolar epithelium from infection by Reovirus T3D infection. We also observed this in Figure 12, where the yields of

Figure 12. Growth of Reovirus and Reassortants in Balb-c (PKR+/+) and Balb-c (PKR -/-) mice. Groups of 3 Balb-c and PKR-/- mice were intranasally infected with 10^5 pfu of T1L, T3D or any one of the four Reovirus reassortant strains. 5 days post infection; lungs were harvested and were homogenized. Viral titers were calculated. Mean results shown of three biological replicates, with standard errors.

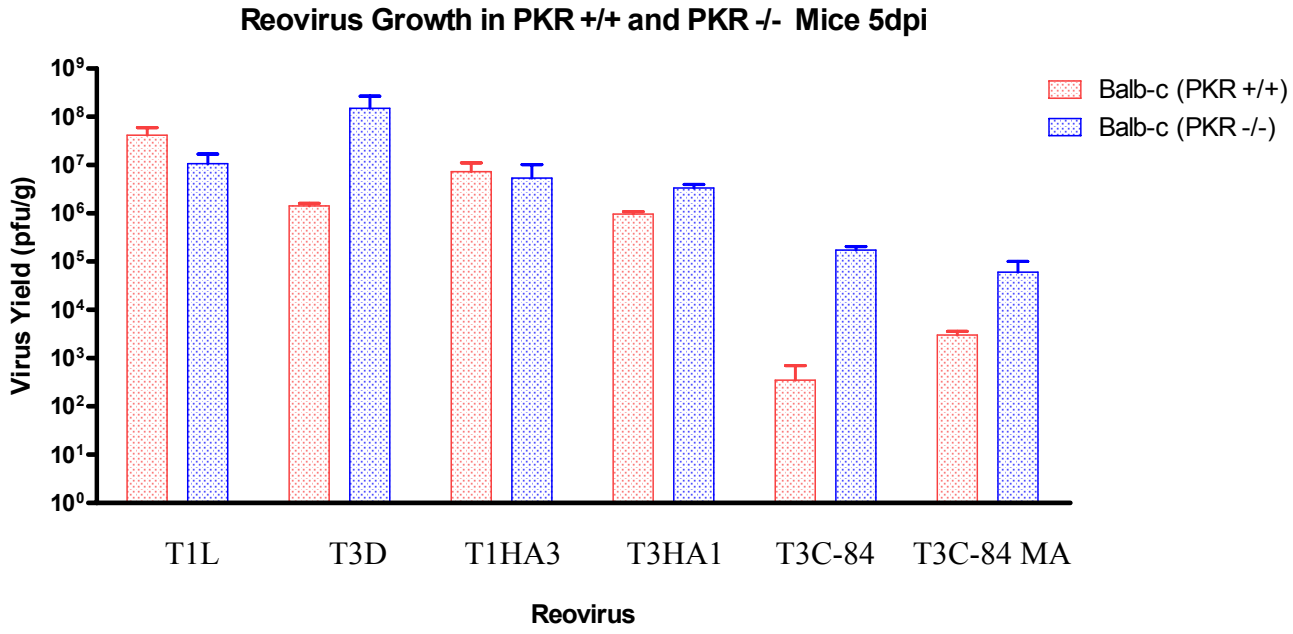
Reovirus Growth in PKR +/+ and PKR -/- Mice 5dpi
Virus Yield (pfu/g)
10^9
10^8
10^7
10^6
10^5
10^4
10^3
10^2
10^1
10^0
Balb-c (PKR +/+)
Balb-c (PKR -/-)
T1L
T3D
T1HA3
T3HA1
T3C-84
T3C-84 MA
Reovirus

most of the reassortant strains were higher in the PKR-/- mice lung than in wild type Balb-c (PKR +/+). The greatest yield was seen for T3D. We speculate this to be due to an increased replication in both the alveolar as well as the bronchiolar epithelium due to a lack of PKR-induced inhibition. In contrast, the yield of T1L was reduced in PKR -/- lungs, which indicates a beneficial role of PKR in T1L and T3D lung replication.

4.4.2 Lung PKR enhances T1L replication

PKR was shown to inhibit the replication of T3D, but PKR stimulated the replication of T1L, as depicted in Figure 11. In Balb-c mice, infection by T1L resulted in a greater weight loss when compared to PKR -/- mice, indicating greater disease, which was consistent with increased replication. In contrast, in PKR-/- mice, the T3D infectious yield was higher, reflecting an enhanced ability to replicate and therefore greater body weight loss than Balb-c. This explains our results where we found that T1L is more PKR resistant than T3D, which was in contrast more sensitive to PKR (Figures 5 & 6). Morin et al, 1996 showed that in a rat lung model of Reovirus-induced pneumonia, T1L grew to higher titers in the lung, and this was attributed to the S1 gene segment (47). Our results were the same in Balb-c mice, as T1L displays enhanced viral replication. However, T1L grew to lower titers than T3D in Balb-c PKR -/- lungs. We showed further that this was achieved due to a σ1s-dependent mechanism of infecting the bronchiolar epithelium of the lung. Thus, T3D was inhibited from replicating in bronchiolar cells because of an inhibitory effect of PKR. T1L, in contrast was inhibited from replicating in the bronchiolar epithelium by a loss of PKR, indicating that there may be another PKR-independent factor that inhibits replication in the bronchiolar epithelium. The Reovirus T1L lung infection may inhibit M1 gene effects in alveolar tissues (fibroblasts or epithelium).

In contrast to an inhibitory role for PKR in reovirus replication others have shown that PKR and RNase L are required for efficient shutoff of host protein synthesis for some reovirus strains and is thus associated with enhanced viral replication by 10- to 100-fold in PKR +/+ MEF (70, 71). It therefore appears that the reovirus host interactions involving the PKR response and viral gene expression are complex and may involve several competing or interacting virus and host components.

4.4.3 Differential Reovirus parental growth patterns in wild type and PKR -/- Balb-c lungs are attributed to the S1 gene segment

In contrast to its inhibitory effect on T3D, we propose that PKR is used by T1L to enhance its replication in lung alveolar epithelium. This was reflected in greater body weight loss in Balb-c mice after T1L infection (Figure 11) as well as decreased yield of T1L in TIK mice (Figure 12). However, T1L replication was limited to the alveolar region due to the properties of its S1 genome segment.

Previous studies in our lab showed that in mouse embryo fibroblasts, PKR protected the lung from infection against both parental serotypes T1L and T3D, with a greater inhibition of T3D replication than T1L (Figure 5). This difference has been attributed to the properties of their M1 genome segments, which encode the μ2 protein, which is involved in PKR resistance (21, 33, 78). The lung is mostly epithelium and therefore the difference in growth in lungs probably reflects the difference in growth among the different cell types (bronchiolar versus alveolar epithelium).

The S1 gene segment has been shown to control viral tropism in many studies (13, 35, 81). We showed that the genetic basis for the difference between T3D and T1L infection of the

PKR-/- mouse lung bronchiolar epithelium was attributed to the S1 gene segment of parental serotype T3D (Figures 8 & 9). The infection of the PKR-/- bronchiolar epithelium by T3D also required the expression of σ1s as a key protein in the tropism of the bronchiolar epithelium. While the functions of σ1s are not yet known, we can propose that one of its roles is involved in the mechanism of infection in the mouse bronchiolar epithelium. Although further work has to be done to understand the interactions of σ1s with host defense, such as PKR and other possible roles in host factor antagonism in the bronchiolar epithelium and interactions with PKR.

The Reovirus S1 genome segment has been identified in tissue tropism and is involved in the interaction between the host receptor and the virus. In addition, it is also the protein that the host directs neutralizing antibodies against, and it is one of the two Reovirus gene segments that encodes two proteins, σ1 and σ1s. When this S1 gene segment was interchanged between the two parental serotypes, we showed that the reassortant that possessed the S1 from T3D (T1HA3) resulted in the infection of the bronchiolar epithelium, contrary to T3HA1, which had its S1 from T1L (Figure 9). This showed clearly that the infection of the bronchiolar epithelium was due to the S1 gene from T3D, but not T1L.

In figure 12, when we compared the yield of T1L to T1HA3 (which has its S1 segment from T3D) we observed the reassortant to become more sensitive to PKR, since in a decrease in viral yield in wt Balb-c lungs was seen due to a single segment reassortment. Moreover, the S1 from T3D also allowed T1HA3 to grow to similar levels both in the presence and absence of PKR, implying a balance or trade-off between PKR sensitivity (from the T3D S1 segment) and PKR resistance (from the T1L M1 gene segment). This was mirrored by the viral yield of T1HA3 in both PKR +/+ and PKR -/- lungs. In contrast, T3HA1, which has the S1 from T1L, showed a decrease in viral yield in PKR-/- lungs compared to wild type T3D, further adding to

the notion that T1L employs PKR for its replication, possibly through the properties of its S1 gene.

Comparing the two variant strains T3C-84 and T3C-84MA, when σ1s was knocked out, the mouse bronchial epithelium was not infected. The T3 σ1s gene was therefore required for the infection of the bronchiolar epithelium, as seen by the lack of bronchiolar staining on T3C-84MA-infected lungs (Figure 10). This clearly maps the infection of the bronchial epithelium in PKR -/- lungs to the differences in the expression of the σ1s protein, suggesting that the infection of the bronchiolar epithelium in PKR -/- lungs was σ1s-dependant.

The two reassortants T3C-84 and T3C-84MA were competent in their infections, as shown in Figure 12. Both strains also showed a similar pattern for growth in wild type Balb-c (PKR +/+) and TIK (PKR -/- mice) lungs. The σ1 protein of T1L and T3D both bind the host protein Junction Adhesion Molecule as their receptor. However, the binding of the secondary carbohydrate differs between the two parental serotypes. T3D contains a receptor binding domain in its tail, which binds alpha-linked sialic acid residues. Other strains such as the T3C-84 fail to bind to sialic acid residues whereas T3C-84MA has regained the ability to bind to sialic acid (4, 10, 11, 79). Thus, binding to sialic acid is not absolutely necessary to infect the bronchiolar epithelium, as both T3C-84 and T3C-84MA are infectious, as shown by the viral yield in mouse lungs (Figure 12). However, compared to T3D, there was a significant difference in the viral yield between the T3C-84/T3C-84MA variant strains. The 3-log difference in virus yield is not attributable to the difference in the ability of the Reoviruses to bind sialic acid receptors in the mouse lung.

4.5 Summary of Conclusions

i. Upon Reovirus parental infection of Balb-c mice (PKR +/+), only alveolar regions were infected.

ii. PKR protected the bronchial epithelium from infection from Reovirus serotype T3D.

iii. In contrast, Reovirus T3D, but not T1L, was able to infect the PKR -/- mouse lung bronchiolar epithelium. This was attributed to the S1 gene segment of T3D.

iv. Infection of the PKR -/- mouse bronchiolar epithelium was dependent on the expression of T3D σ1s non-structural protein.

v. Reovirus T1L used PKR to enhance disease, whereas T3D growth and replication was limited by PKR.

CHAPTER FIVE
STUDY OF TUMOUR ONCOLYSIS BY PARENTAL REOVIRUSES T1L and T3D AND REASSORTANTS

5.1 Background and prior studies

Being naturally oncolytic, Reovirus has shown promise in the field of novel emerging cancer therapeutics, due to its preferential replication in transformed cell lines. Thus, in the last decade, mammalian Reoviruses, especially T3D, have been promoted and evaluated as oncolytic agents in experimental and clinical cancer therapy trials. Defects in PKR and IFN pathways are characteristics of many tumours and transformed cells. This enables replication of viruses that are sensitive to interferon to infect and replicate within these cells, with VSV and Reovirus being prime examples. Reovirus has been proposed to exploit the already activated *Ras* pathway in a variety of tumour cells that are deficient in their PKR and interferon responses, to result in their lysis. The mechanism of action may involve the ability of Reoviruses to induce cell death and apoptosis in tumour cells, but not in normal non-transformed cells (14, 15, 44, 66).

Oncolytics Biotech® is currently conducting clinical trials in the United States, Canada and United Kingdom, using Reolysin® as a cancer therapeutic. The current clinical program includes eight Phase I/II or Phase II human trials examining Reolysin® alone or in combination with radiation and chemotherapy. Reovirus acts as a systemic cancer therapeutic to treat a variety of Ras-mediated cancers.

Improving viral oncolysis is an exercise in applied pathogenesis, where aspects of viral infection are utilized for tumour destruction, rather than disease progression. Studies in our lab have shown the oncolytic ability of Reoviruses and their reassortants to be enhanced when certain gene segments are present on a specific parental backbone. A panel of 19 T1L x T3D Reovirus reassortants was screened for their ability to lyse tumours *in vivo*. Oncolysis was

assessed in a mouse lung tumour model, where the colon cancer cell line, CT26 localized to the mouse lung after intravenous injection in normal Balb-c mice. CT26 cells are susceptible to persistent infection by parental Reoviruses, but are resistant to lysis *in vitro*. This model has been used in our studies (see materials and methods section for more details).

Groups of 5 mice were injected with CT26 cells to establish lung tumours that result in fatality within 3 weeks of injection. Long term survival (over 45 days) was observed for four specific Reovirus reassortants (EB88, EB96, EB97 and EB123) after a single intra-nasal challenge of 10^7 pfu per mouse was administered, with two of the reassortants resulting in survival of over 250 days. (Figure 13)

These specific reassortants thus had enhanced oncolytic properties compared to their parental prototypes. When their genetic map was analyzed, it was found that these four reassortants possessed unique combinations of gene segments from either parental strain, specifically the L2 and the M1 from T3D as shown in Table 3.

Results from previous work in our laboratory have helped classify the four reassortants into two groups: EB88 and EB96, which possess the M2 gene segment from T1L versus EB97 and EB123, which possess their L1 from T3D. The differences in their growth, viral yield *in vivo* and the oncolysis have been studied, and been attributed to various gene segments. It was found that the possession of the M2 gene segment from T1L has shown greater oncolytic ability.

Figure 13: Survival curve of Balb-c mice bearing CT26 lung tumours following a single intranasal dose of Reovirus (1 x 10^7pfu/ml). A panel of T1L x T3D reassortants was used to treat Balb-c mice bearing CT26 lung tumours in order to assess survival post-treatment. Reassortants EB88, EB96, EB97 and EB123 were able to prolong survival for more than 45 days post treatment.

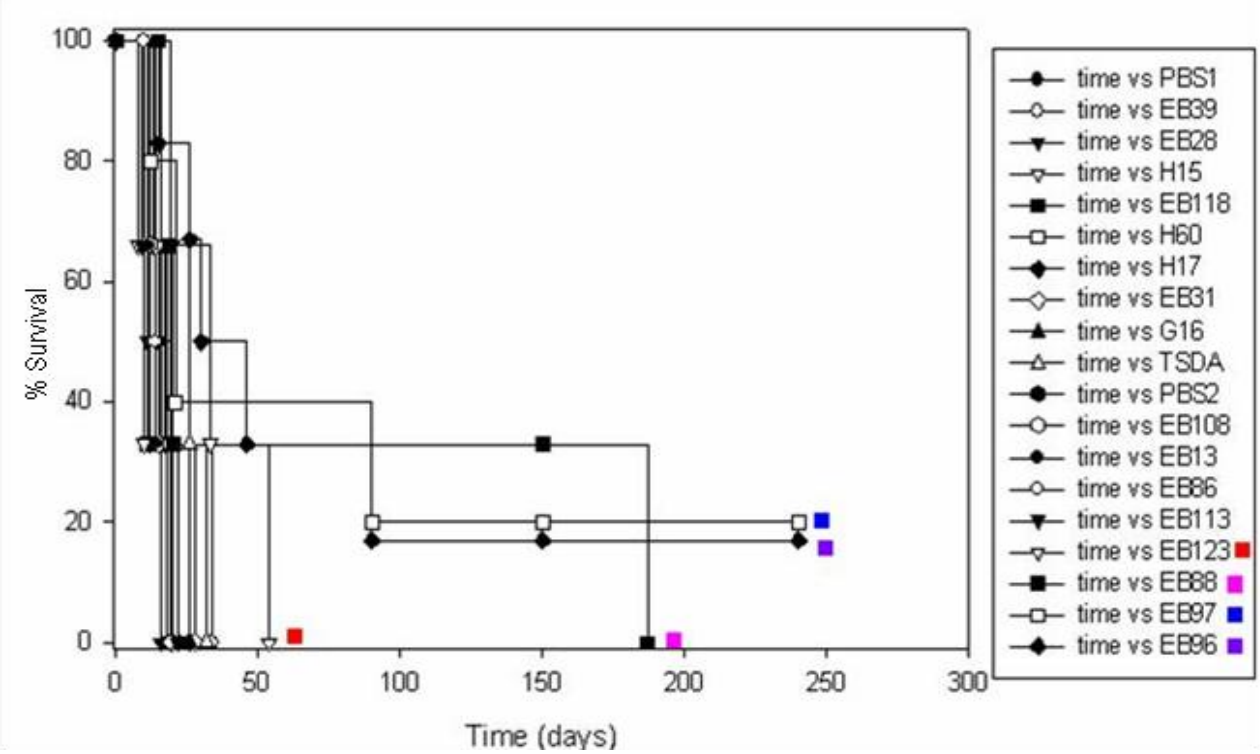
100
80
60
40
20
0
% Survival
0
50
100
150
200
250
300
Time (days)
time vs PBS1
time vs EB39
time vs EB28
time vs H15
time vs EB118
time vs H60
time vs H17
time vs EB31
time vs G16
time vs TSDA
time vs PBS2
time vs EB108
time vs EB13
time vs EB86
time vs EB113
time vs EB123
time vs EB88
time vs EB97
time vs EB96

Table 3: Genetic Map of Reovirus parental and four reassortants

Virus	L1	L2	L3	M1	M2	M3	S1	S2	S3	S4
T1L	L	L	L	L	L	L	L	L	L	L
T3D	D	D	D	D	D	D	D	D	D	D
EB88	D	D	D	D	L	D	D	D	D	D
EB96	L	D	L	D	L	L	L	L	D	L
EB97	D	D	L	D	D	D	D	D	D	L
EB123	D	D	L	D	D	D	D	D	L	D

5.2 Specific Objectives

Preliminary results suggested that there were several contributing factors for improving oncolysis and that specific reassortant viruses possessed enhanced oncolytic abilities relative to their parental prototype strains. There is therefore a need to determine the genetic basis for Reovirus oncolysis.

To study the ability of the four Reovirus reassortants (EB88, EB96, EB97 and EB123) and their effect on the survival of mice, we tested different treatment regimes and doses to observe survival of CT26 tumour bearing-mice.

The M1 gene segment plays a key role in Reovirus biology and pathogenesis, such as transcription/ translation, viral growth, tropism and disease (8). We intended to understand the impact of the M1 gene, which expresses the μ2 protein, in the context of viral oncolysis. The M1 gene segments of T1L and T3D were encoded in VSV, which is a known oncolytic virus, to create a recombinant VSV-chimera that expresses the μ2 proteins from parental strains T1L and T3D. The VSV chimera strains were used to study the survival of CT26 tumour-bearing mice, relative to VSV controls.

5.3 Results

5.3.1 Treatments with Reoviruses at 10^9 pfu are fatal to CT26 tumour-bearing mice

Various *in vivo* studies were carried out to see if increased Reovirus doses would enhance tumour regression of CT26 Balb-c mice lung tumours. After tumour implantation, during the course of treatment with 10^9 pfu of Reovirus and reassortants, we observed that the PBS treated mice survived 2 to 4 days longer than those treated with parental Reoviruses or reassortants. The mice treated with the parental Reoviruses T1L and T3D reached their respective end-points

earlier than those treated with the reassortants, indicating virus-induced pathology or toxicity (see figure 14).

It was also observed that two days after the treatment with Reoviruses, the mice began showing physical signs of sickness, such as hunching, huddling as well as the presence of rough/oily looking fur. Decreases in body temperatures as well as weight loss were observed as early as three to four days post Reovirus infection. Endpoints were declared when weight loss was greater than 20% of the original mouse weight, and breathing rates were high, indicating respiratory distress. This was observed within five to six days after infection of 10^9 of Reovirus treated mice. These symptoms occurred in PBS treated mice (untreated control group) eight to nine days after treatments began.

Upon harvesting the lungs of the euthanized mice, we observed that there were a large number of tumours present on the surface of the lungs, and very few to no flattened tumours. The tumour morphology therefore resembled the lungs of PBS treated (uninfected controls) mice.

5.3.2 Treatments with 10^8 pfu of Reoviruses and reassortants in CT26 tumour-bearing mice

Since doses of 10^9 pfu decreased survival of CT26 tumour-bearing Balb-c mice, we decreased the treatment dose by 10-fold. Treatments of CT26-tumour bearing mice with 10^8 pfu of parental Reovirus or reassortants showed that the average survival time (in days) had increased on average by a day or two, compared to the 10^9 dose. However, it was still observed that untreated mice (PBS group) survived longer compared to the Reovirus-treated group. The lung morphology was no different from that observed from the higher dose, where the harvested

Figure 14: Survival curve of Balb-c mice bearing CT26 lung tumours, infected with a single dose of 1 x 10^9 pfu Reovirus or Reassortants. All treatment groups reached endpoints before the control group, suggesting that the increased death was due to the high dose of the virus treatment.

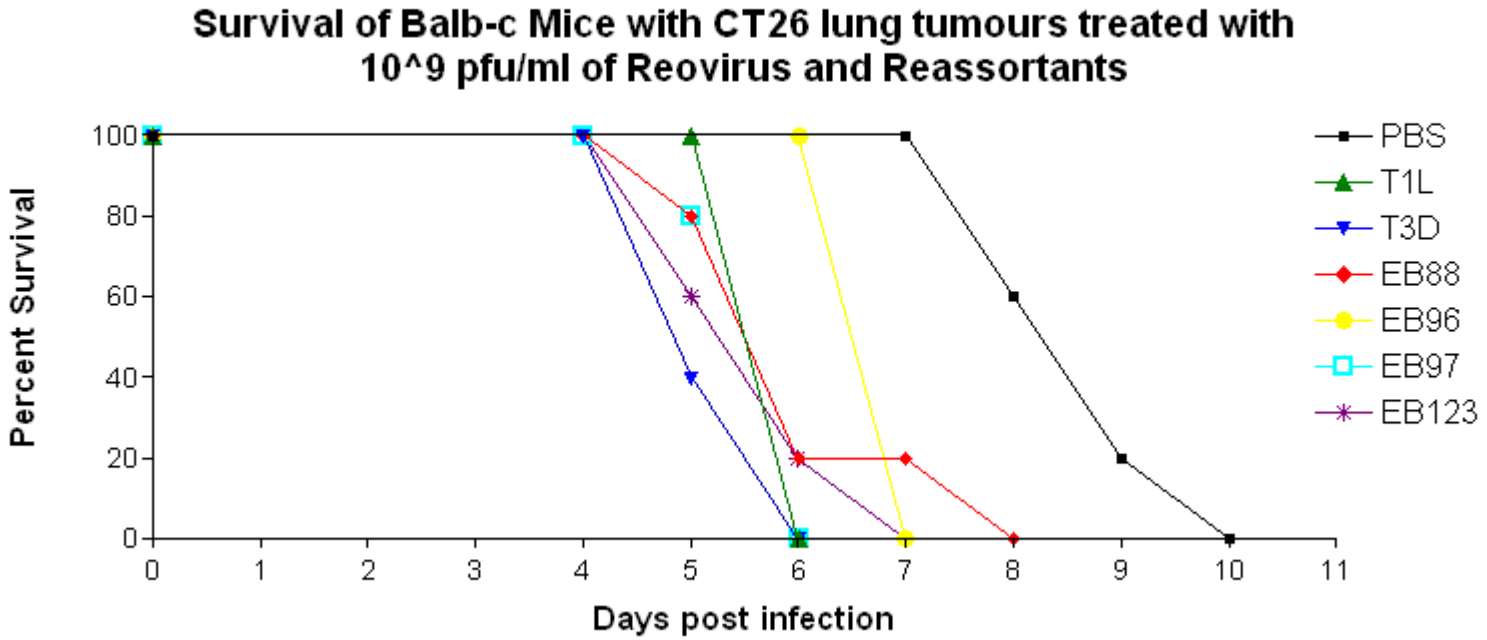
Survival of Balb-c Mice with CT26 lung tumours treated with 10^9 pfu/ml of Reovirus and Reassortants
Percent Survival
100
80
60
40
20
0
0
1
2
3
4
5
6
7
8
9
10
11
Days post infection
PBS
T1L
T3D
EB88
EB96
EB97
EB123

lungs of the treated mice lungs were similar looking to the PBS treated mice group. The tumours were present all around the lungs, with very little to none that were flattened (Figure 18).

Although these results do show that lowering the Reovirus treatment dose from 10^9 to 10^8 results in an increase on the mouse survival by a few days, the results we observed were not significant with respect to PBS (untreated) mice. We therefore continued to lower the treatment dose to 10^7.

5.3.3 Treatments with multiple doses of Reoviruses at 10^7 does not enhance mouse survival, but does show early signs of viral oncolysis

Our initial screen was carried out with a single treatment dose of Reoviruses at 10^7 pfu/mouse, where we found that treatments with the four Reovirus reassortants (EB88, EB96, EB97 and EB123) resulted in long term survival (Figure 13). We intended to study if a treatment regime that consisted of multiple treatments at this dose would enhance the survival of mice. Therefore mice were infected with 10^7 of these Reovirus reassortants at days 1, day 4 and day 7 to observe tumour regression and survival.

Figure 16 showed that multiple treatments increased the median time to death, but did not enhance overall survival. It is however, noteworthy to mention that upon harvesting the lungs of some of these mice, a small portion of the tumours on the surfaces of mice lungs showed signs of flattening (data not shown). Although survival was not significantly enhanced, the observations from the lung morphology showed effects and signs of tumour oncolysis.

Figure 15: Survival curve of Balb-c mice bearing CT26 lung tumours, infected with a single dose of 1 x 10^8 pfu Reovirus or Reassortants. Median time of death (in days) - PBS: 8.3 days; T1L: 6.5 days; T3D: 9.3 days; EB88: 8.5 days; EB96: 8.2 days; EB97: 8.5 days; EB123: 8.4 days. All treatment groups, with the exception of T3D reached their endpoints before the control (PBS) group.

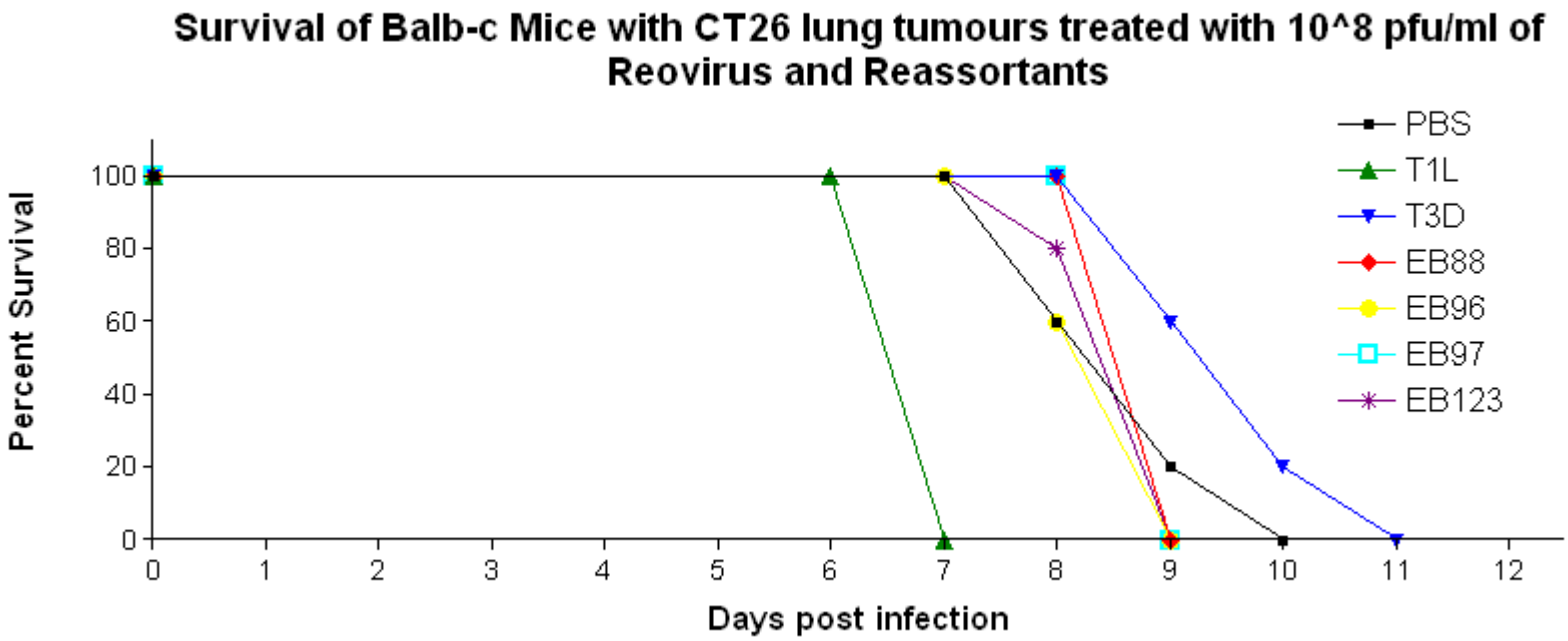
Survival of Balb-c Mice with CT26 lung tumours treated with 10^8 pfu/ml of Reovirus and Reassortants
Percent Survival
100
80
60
40
20
0
0
1
2
3
4
5
6
7
8
9
10
11
12
Days post infection
PBS
T1L
T3D
EB88
EB96
EB97
EB123

5.3.4 Treatments with multiple doses of Reoviruses at 10^6 enhances mouse survival and evidence of viral oncolysis

Since we observed significant mouse death with multiple doses at 10^7 pfu/mouse, we investigated the possibility of a lower dose, but retaining the multiple treatment regimes. Tumour-bearing mice were intra-nasally infected with 10^6 pfu per mouse, at days 1, 4 and 7, (Figure 17).

The mice in the PBS control group all reached their endpoints by day 10. We also saw that the mice that were treated with EB97 showed a similar trend, resulting in 100% death by day 10. Mice treated with EB96 showed an average increase in survival by one day. EB123 showed a slight increase, with 20% of the mice surviving by day 14. Treatment with EB88 showed a significantly enhanced survival of 20% of the mice surviving up to 30 days.

When the lungs for mice treated with EB88 (from the mice euthanized at earlier time points, 8dpi) were harvested and observed, we found that there were fewer numbers of large tumours, and several tumours that were flattened throughout the outer surface of the mouse lung. The harvested lungs of other mice showed a greater number of smaller tumours. In contrast, the mice lungs in the PBS control (untreated) group had a lot of large and small tumours spread throughout the surface (Figure 18).

Figure 16: Survival curve of Balb-c mice bearing CT26 lung tumours, infected with three doses of 1 x 10^7 pfu Reovirus or Reassortants. Arrows indicate the days of infection. Median time of death (in days) - PBS: 8.3 days; T3D: 10.5 days; EB88: 9.2 days; EB96: 9.9 days; EB97: 10.0 days; EB123: 10.9 days. Average time of death (per mouse) - PBS: 8.4 days; T3D: 10.0 days; EB88: 8.4 days; EB96: 8.5 days; EB97: 9.5 days; EB123: 9.3 days. Despite multiple treatment doses, enhanced survival was not observed, suggesting death due to virus overdose/respiratory arrest due to lung tumours (like the PBS control group).

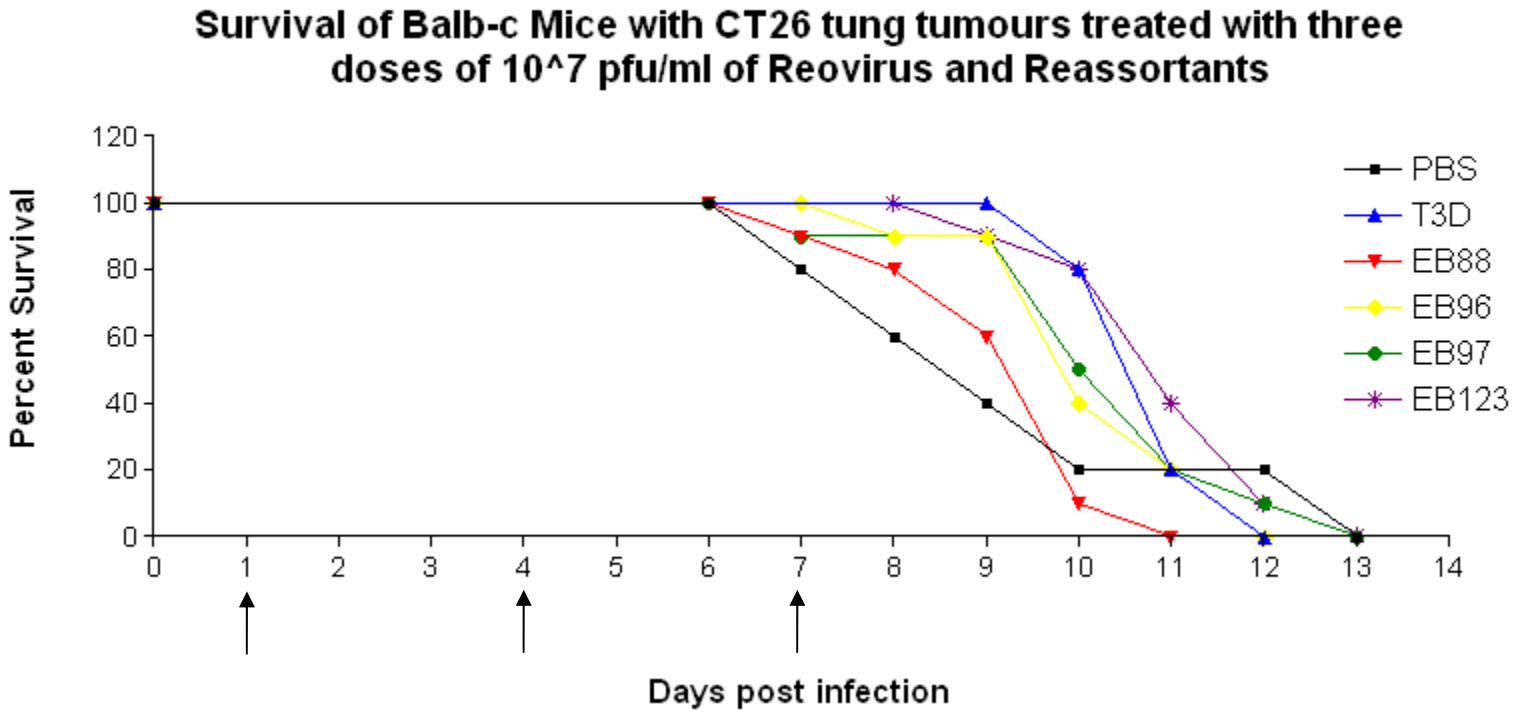
Survival of Balb-c Mice with CT26 tung tumours treated with three doses of 10^7 pfu/ml of Reovirus and Reassortants
Percent Survival
120
100
80
60
40
20
0
0
1
2
3
4
5
6
7
8
9
10
11
12
13
14
Days post infection
PBS
T3D
EB88
EB96
EB97
EB123

5.3.5 Treatments with transgenic VSV expressing Reovirus T3D M1 gene enhanced survival

While we do observe a relationship between the dose and the treatment regime of Reovirus, we intended to also study the effect of the Reovirus μ2 protein encoded by the M1 gene segment in enhancing oncolytic ability. VSV has shown great potential as an oncolytic virus (5). We therefore introduced the Reovirus M1 gene that expresses the μ2 protein into VSV, to observe the effect of a single protein in enhancing oncolysis.

VSV strains expressing both T1L and T3D M1 genes (VSV-T1M1 and VSV-T3M1, respectively), along with a VSV-control virus expressing GFP (VSV-GFP) were used to infect groups of 5 (for PBS and VSV-GFP) and 10 (for VSV-T1M1 and VSV-T3M1) tumour bearing Balb-c mice, at a single dose of 10^7 pfu/mouse (Figure 19).

Figure 17: Survival curve of Balb-c mice bearing CT26 lung tumours, infected with three doses of 1 x 10^6 pfu of Reovirus reassortants. All reassortants gave enhanced survival, except EB97 treatment group, which had the same survival rate as the control group. Median time of death (in days) - PBS: 8.5 days; EB88: 11.0 days; EB96: 9.0 days; EB97: 8.0 days; EB123: 10.0 days. Average time of death (per mouse) - PBS: 7.8 days; EB88: 15.2 days; EB96: 8.2 days; EB97: 7.6 days; EB123: 9.4 days. Treatment with EB88 resulted in the longest survival post treatment, at 31 days post initial treatment. Arrows indicate the days of infection.

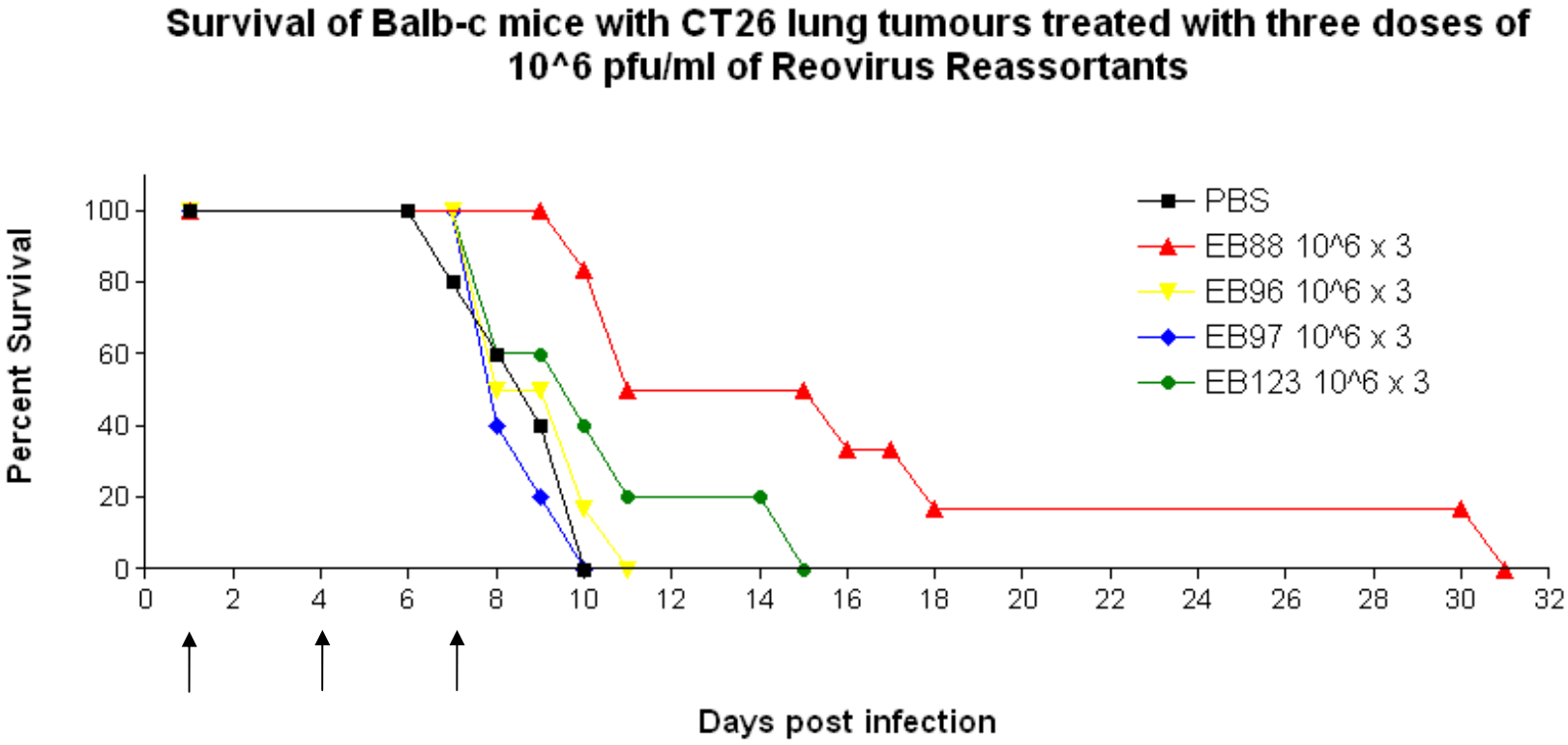
Survival of Balb-c mice with CT26 lung tumours treated with three doses of 10^6 pfu/ml of Reovirus Reassortants
Percent Survival
100
80
60
40
20
0
0
2
4
6
8
10
12
14
16
18
20
22
24
26
28
30
32
Days post infection
PBS
EB88 10^6 x 3
EB96 10^6 x 3
EB97 10^6 x 3
EB123 10^6 x 3

Figure 18: Balb-c tumour bearing lungs of mice treated with PBS (top left) and with 10^7 pfu/mouse of reassortant treatment groups (EB88, EB97 and EB123), 8 days post treatment. Mice treated with Reovirus reassortants displayed tumour flattening on the lung surface.

PBS

EB88

EB97

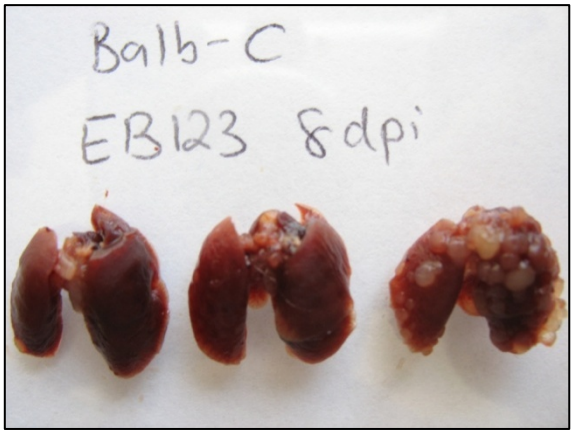

EB123

Figure 19: Survival curve of Balb-c mice bearing CT26 lung tumours, infected with 1 x 10^7 pfu/mouse of transgenic VSV expressing the Reovirus M1 gene from either parental strain. VSV-T3M1 (transgenic VSV strain expressing M1 gene segment from Reovirus T3D) showed enhanced survival at 125 days post treatment. Average time of death (per mouse) - PBS: 7.8 days; VSV-GFP: 20.4 days; VSV-T1M1: 18.2 days; VSV-T3M1: 35.7 days. All VSV transgenic strains displayed significantly longer survival of tumour bearing mice compared to the control group ($p < 0.001$ for VSV-GFP, 2-tailed, equal variance; $p < 0.001$ for VSV-T1M1, 2-tailed, unequal variance; $p < 0.05$ for VSV-T3M1, 2-tailed, unequal variance).

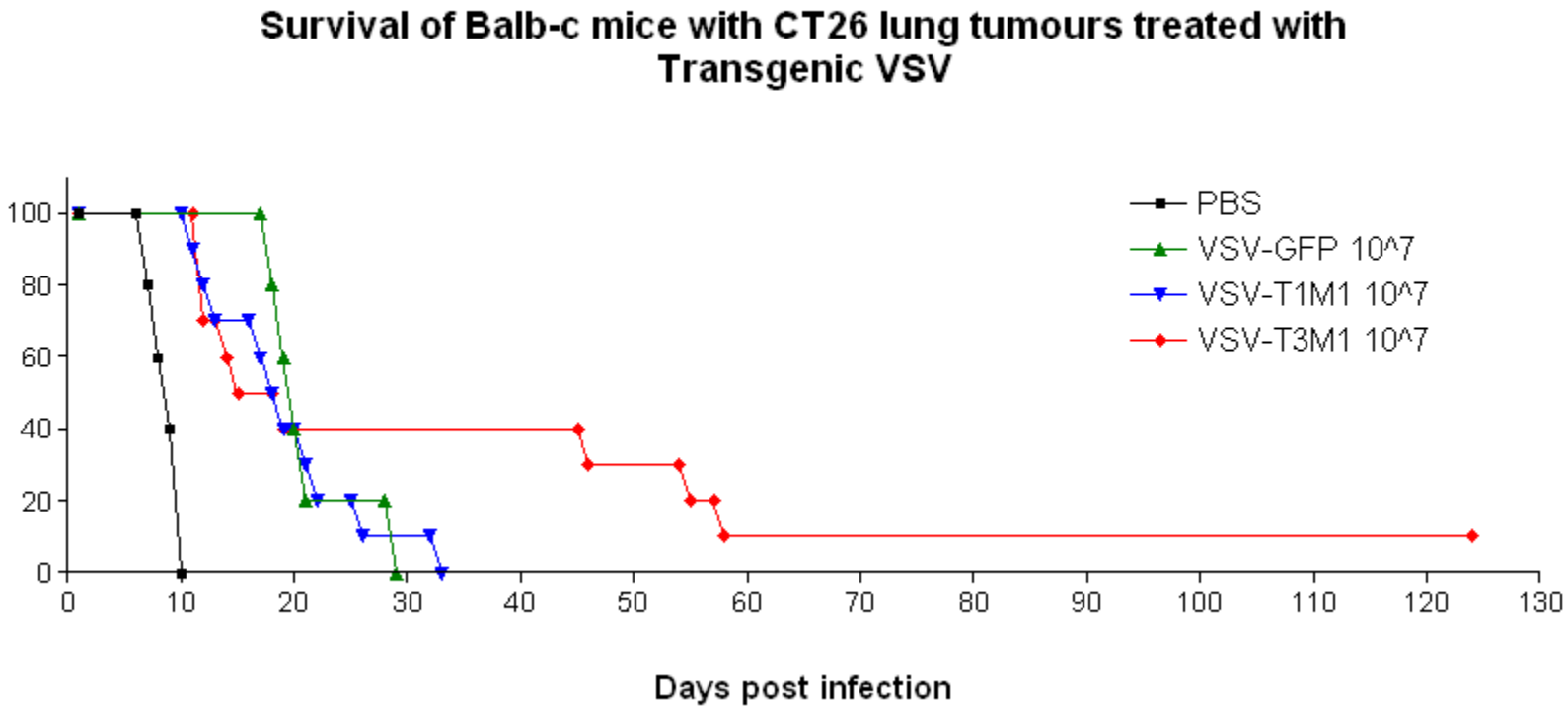
Survival of Balb-c mice with CT26 lung tumours treated with Transgenic VSV
PBS
VSV-GFP 10^7
VSV-T1M1 10^7
VSV-T3M1 10^7
100
80
60
40
20
0
0
10
20
30
40
50
60
70
80
90
100
110
120
130
Days post infection

We observed that the untreated (PBS) group showed 100% death of the mice by day 10 post virus treatment. The treatment by VSV-GFP showed increased survival of the tumour-bearing mice to 29 days. This increase in survival by VSV-GFP without any additional Reovirus proteins was used as a baseline to observe the effect of the addition of Reovirus proteins to VSV. When the M1 from T1L is expressed on a VSV backbone, we saw that the mice survival was similar to VSV-GFP, but was increased by 2 to 3 days. However, when the M1 from T3D was expressed on a VSV backbone, survival of one mouse was increased to 125 days for one mouse, compared to 33 days for VSV-T1M1, 29 days for VSV-GFP, and only 10 days for PBS treated. Although the percentage of mice that survived was only 10%, the overall survival curve showed enhanced survival compared to the other treatment groups.

The lungs harvested from this treatment group showed a very small number of tumours and also flattened nodules on the surface of the lung (data not shown). Also, when the lungs from the last mouse were harvested, traces of flattened tumours were observed.

5.4 Discussion

The ability of parental serotype T3D to lyse tumours *in vivo* has been successfully shown in several studies, we have extended these studies to include T1L x T3D reassortants (Figure 13). The aim of this part of the project was to investigate a variety of treatment regimes that vary in doses and number of treatments of Reovirus in CT26-tumour bearing mice. This was sought to assess the toxicity and effectiveness of reassortants EB88, EB96, EB97and EB123 in treating CT26 lung tumours.

When Balb-c mice were infected at higher doses of 10^8 and 10^9 pfu, we found that they died from enhanced virus toxicity, rather than the lung tumours. The symptoms we observed for

the PBS treated mice around day 8, was what we observed for the Reovirus treated mice at days five and six after infection. The fact that these symptoms were observed a lot earlier in virus treated mice in both doses suggests that the mice developed these symptoms from Reovirus infection, rather than the effect of the tumours. Therefore, the possibility of higher doses for Reovirus treatment may be counterproductive, as lung pathology due to virus infection and induced inflammation induced fatal responses.

Four reassortants from the data of our preliminary study at 10^7 pfu of viral lysates resulted in the longest survival (EB88, EB96, EB97 and EB123). We therefore sought to study if administering multiple treatments at this dose of purified viruses over a week would further enhance survival of CT26 tumour bearing mice. The survival curve for this treatment regime gave us very contrasting results from a single dose infection. None of the mice survived more than 2 weeks after the initial treatment. Moreover, we observed the death of a few mice in the EB88 and EB97 treatment groups before the final treatment was administered. Multiple treatments within a week can cause the immune response to be heightened and may have contributed due to decreased oncolytic response. In addition to increased lung infection, the increased anti-viral response, including the production of interferon, could have caused the mouse immune system to become sensitive, and therefore treatments over a short period of time could have overwhelmed their immune system, which may have caused their death. Cytotoxic and immunotherapeutic effects of Reovirus in tumour bearing mice therefore need to be further studied.

When the treatment dose was reduced to 10^6 pfu per mouse, with multiple treatments administered, we observed an improvement in survival. Although the survival rate was not high, the difference compared to a higher dose was significant – 11 days for 10^7 pfu of EB88

compared to 31 days for 10^6 pfu ($p < 0.05$, 2-tailed, equal variance). The extent of virus-induced pathology is an important factor to be considered when considering treatment of Reoviruses. It may therefore be necessary to lower the dose and increase the time between subsequent treatments.

The EB88 reassortant that demonstrated the best survival in CT26 tumour-bearing mice possessed the M2 gene segment from T1L, with the rest of its genome segments come from T3D (ref table 3). It possesses the T3D S1 gene segment that may enhance infection of lung epithelium (from chapter 4); T1L L2 and T3D M3 for viral yield and protein production (E.G. Brown et al, unpublished). Moreover, the observation that it does significantly better in the treatments than T3D suggests an important role of the T1L M2 gene segment in viral oncolysis.

In previous experiments performed in our laboratory, it was found that EB88 and EB96 yielded lower viral titers, whereas EB97 and EB123 gave higher viral yields in CT26 cell infections. Moreover, EB88 and EB96 differ from EB97 and EB123 in the possession of their M2 gene segments, possessing the M2 from T1L or T3D, respectively. The M2 gene segment plays a role in virus penetration, forming bulk of the virion outer capsid, potential roles in transcriptase activation, as well as in apoptosis (21). This, along with the observation that EB96 possesses its S1 from T1L, may also contribute to better oncolysis and suggests that the unique combination of these gene segments may play important roles in viral oncolysis, ranging from initial infection to the ability to grow and replicate in a tumour environment.

The M1 gene segment was chosen to study the effect of one Reovirus gene in enhancing oncolysis because of its role in growth in both PKR +/+ and PKR -/- MEF. When this was expressed in VSV, which is also an oncolytic virus, we noticed a dramatic increase in survival of mice treated with a recombinant VSV that expressed the μ2 protein from T3D (average time of

survival of 35.7 days for VSV-T3M1 treated mice, compared to 7.8 days for untreated (PBS) mice). In fact 10% of the mice showed survival up to over 120 days. But it is noteworthy to mention that by 35 days post treatment initiation, we observed less than 40% survival from all the other treatment groups except those treated with VSV-T3M1. This continued till the end of two months. Although this was a preliminary study, we hope to use the VSV-Reovirus chimera to increase the immune attack of the injected tumours, and then treating with Reovirus and reassortants to increase immune attack of infected tumours. While using oncolytic virus chimeras is in its preliminary stage, we do see promising results and hope for future studies.

CHAPTER SIX
COMPARISON OF REOVIRUS PROTEIN PRODUCTION IN L929 FIBROBLAST AND CT26 EPITHELIAL CELLS

6.1 Background and previous studies

The L929 mouse fibrosarcarma cell line is a common cell system for the molecular characterizations of Reovirus growth and gene expression. The growth and protein synthesis of Reovirus parental serotypes in L929 fibroblast cells have been previously analyzed over a 24-hour time period following infection at an MOI of 10. Reovirus results in high yields of viral replication (over 10^7 pfu/ml) in L929 cells (Figure 20). The rate of replication increased around 15 hours post infection, where 10 infectious virions are produced per cell with almost 10-fold increase by the 18^{th} hour post infection, and with moderate increases after this time point. Using western blotting, the levels of accumulation of viral proteins were determined over the time span using antibodies against μ2, μNS and σNS. Infection of fully permissive L929 cells by parental Reovirus serotypes results in a transient degradation of viral proteins μ2, μNS and σNS at 18 hours post infection. This was followed by a general boost in viral protein synthesis, as well as a 10-fold increase in viral yield 18 hours post infection. In addition, the pattern of transient breakdown and re-synthesis of the viral proteins also correlated with a similar pattern of transient destruction of PKR, followed by its re-synthesis. This was more prominent in T3D infected cells (Figure 20). The degradation pattern of total PKR was also associated with reduced levels of phosphorylated PKR and eIF2α (data not shown), which may be involved in the mechanism that enhances viral replication.

Preliminary work in studying the overall growth of Reoviruses in the mouse colon carcinoma epithelial cell line, CT26 cells, has been initiated in our lab. This is of particular

Figure 20: Reovirus growth and protein synthesis in L929 mouse fibroblasts. Western blots Reovirus infection of fully permissive L929 cells show a transient degradation of μ2, μNS and σNS that coincides with a general burst in viral protein synthesis, a 10 fold increase in titer that coincides with a transient destruction of PKR especially for T3D. The loss of PKR is associated with reduced levels of phosphorylated PKR and eIF2α (not shown).

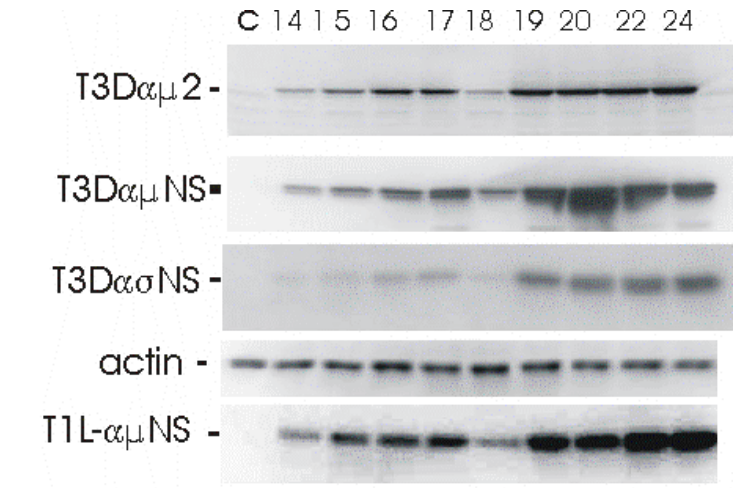
C 14 15 16 17 18 19 20 22 24
T3Dαμ2 -
T3DαμNS-
T3DασNS -
actin -
T1L-αμNS -

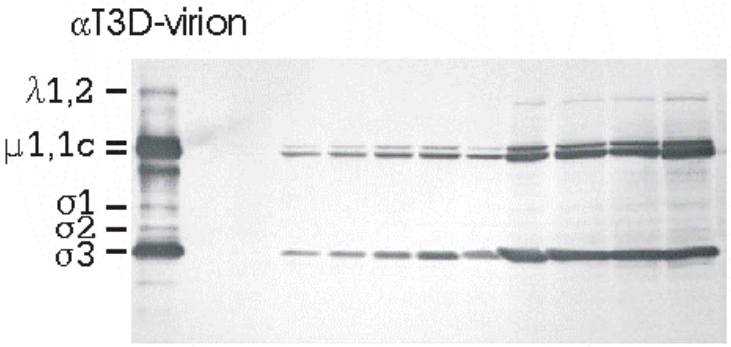
αT3D-virion
λ1,2 –
μ1,1c =
σ1 –
σ2 –
σ3 –

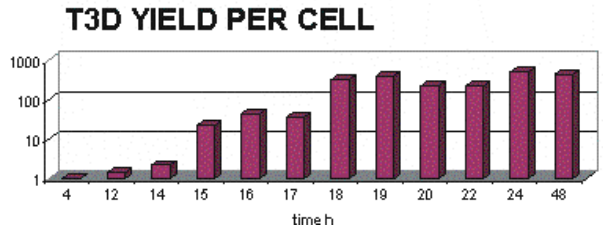
T3D YIELD PER CELL
1000
100
10
1
4 12 14 15 16 17 18 19 20 22 24 48
time h

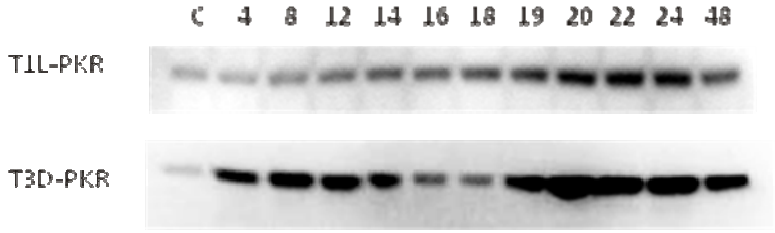
C 4 8 12 14 16 18 19 20 22 24 48
T1L-PKR
T3D-PKR

interest with respect to Reovirus infections because we have employed the CT26 mouse-colon tumour model as a test system for assessing Reovirus oncolysis. We have observed that 3 days post infection of CT26 cells, the growth and protein production differed between the two parental Reoviruses. T3D had higher protein production than T1L. In fact, T1L had the lowest protein production when compared to the ability of viral protein production post-infection of a panel of Reovirus reassortants, which was consistent with the ability of T1L to replicate in CT26 cells at 10^7 pfu/ml. (Figure 21).

6.2 Specific Objectives

Since Reovirus is naturally oncolytic in its nature and most tumours are epithelial, we sought to determine the growth and protein production in a carcinoma cell line. Our data from Reovirus infection of L929 fibroblast cells led us to investigate viral and host protein synthesis and accumulation due to infection of the parental serotypes in the mouse colon carcinoma epithelial cell line, CT26. The CT26 cell line is a tumour cell line, which we will also use to implant tumours in Balb-c mice in our future experiments.

Our key objective was to assess if productive infection was also associated with similar patterns of Reovirus and host protein production in CT26 cells, as was observed in the L929 fibroblast cells. We aimed to observe the effect of Reovirus infection on several host proteins and the overall production of viral proteins. We studied the effect of Reovirus infection on the following host proteins over a 24 hour period post infection: Protein Kinase R (PKR), eukaryotic Initiation Factor 2α (eIF2α), and Interferon Regulatory Factors -3 and -7 (IRF-3 & IRF-7). The production of the viral structural proteins and the inner capsid protein μ2 was also studied over a 24 hour period post infection.

Figure 21: Protein synthesis of parental Reovirus and reassortant in CT26 cells, 3 days post infection (MOI = 10), as assessed by western blotting using a cocktail of rabbit anti-T1L and anti-T3D antisera. The secondary antibody was alkaline phosphatase conjugated goat anti-rabbit IgG developed with BCIP/NBT.

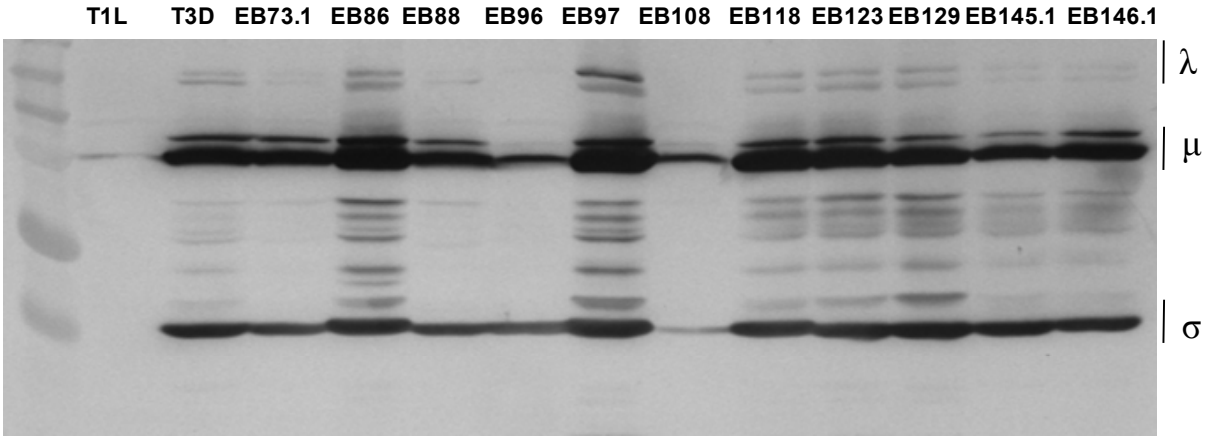
T1L
T3D
EB73.1
EB86
EB88
EB96
EB97
EB108
EB118
EB123
EB129
EB145.1
EB146.1
λ
μ
σ

6.3 Results

6.3.1 Effect of Reovirus infection on total viral protein production and the inner capsid protein μ2 in CT26 epithelial cells.

We assessed the protein production of parental Reovirus strains in CT26 cells over a 24 hour time period. CT26 cells were infected with an MOI of 10 with either parental strain T1L or T3D. SDS-PAGE samples were collected hourly from 15 hours to 24 hours post infection, and gel electrophoresis was performed, followed by immunoblotting for viral proteins. Results are shown in figure 22.

After T1L infection of CT26 cells, we did not observe any virus proteins until the 24 hour time point, when strong staining bands were detected using both anti-virus and anti-μ2 antibodies. However, with infection by T3D, a gradual increase in overall virus protein production was evident at the 15 hour time point, which progressed with time to the 24 hour time point. It is also noteworthy that there was an abrupt increase in viral proteins at 18 hours and then again at 22 hours.

Blotting for the Reovirus inner capsid protein μ2, we also observed a similar trend as seen for the total virus proteins. Infection with T1L did not result in the appearance of this structural protein till 24 hours post infection. However, as early as 15 hours post infection of CT26 cells with T3D, we observed a faint band that steadily and gradually increased in intensity by the 24 hour time point. Comparing the intensity of μ2 in L929 fibroblasts, we find that there was a noticeably lower production of μ2 in CT26 epithelium.

These studies of the synthesis of viral proteins in infected CT26 cells showed that T1L virus infection does not result in accumulation of detectable proteins until 24 hours post infection. T3D infection however resulted in a gradual accumulation with transition to high

Figure 22: Protein synthesis of parental Reovirus T1L and T3D in CT26 cells. Western blotting was done against viral proteins using anti-T1L or anti-T3D antisera (top panel) or anti-actin (bottom panel). Goat anti-rabbit IgG conjugated to Horse-Radish Peroxidase was used as the secondary antibody. Gels show total Reovirus proteins, inner capsid protein μ2, and actin levels in CT26 cells over a 24 hour time course post viral infection. FB, fibroblast; C, uninfected cells.

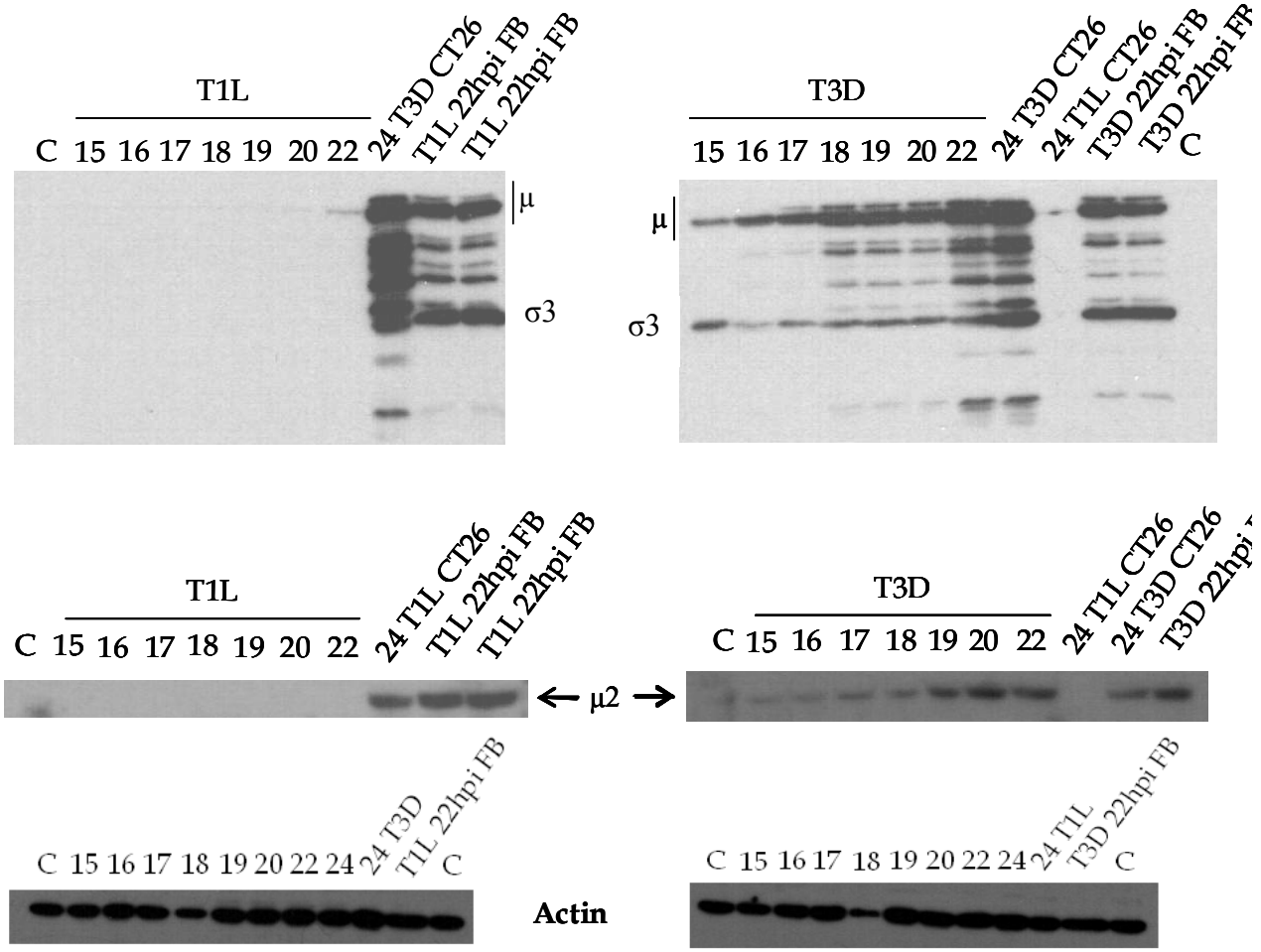
T1L
C 15 16 17 18 19 20 22 24 T3D CT26 T1L 22hpi FB T1L 22hpi FB
μ
σ3
T3D
15 16 17 18 19 20 22 24 T3D CT26 24 T1L CT26 T3D 22hpi FB T3D 22hpi FB C
μ
σ3
T1L
C 15 16 17 18 19 20 22 24 T1L CT26 T1L 22hpi FB T1L 22hpi FB
T3D
C 15 16 17 18 19 20 22 24 T1L CT26 24 T3D CT26 T3D 22hpi
μ2
C 15 16 17 18 19 20 22 24 T3D T1L 22hpi FB C
C 15 16 17 18 19 20 22 24 T1L T3D 22hpi FB C
Actin

accumulation seen at 18 hours and 22 hours post infection. Interestingly, the levels of actin that was used as a loading control also demonstrated a sharp reduction at the 18 hour time point for both T1L and T3D infection. The reduction was more prominent for T3D infection; however, it is clear from inspection of the T3D protein blot that the dip in actin intensity was not due to loss of material from this sample time point.

6.3.2 Effect of Reovirus infection on total and phosphorylated PKR in CT26 epithelial cells

Our preliminary studies on Reovirus infection of L929 fibroblast cells have shown that the parental serotypes T1L and T3D had different effects on host PKR levels post infection. We assessed the expression levels of PKR and phosphorylated PKR in the mouse colon tumour carcinoma cell line, CT26. CT26 cells were seeded in 6-well plates and then infected with Reovirus T1L or T3D at an MOI of 10, along with uninfected CT26 cells as controls. Samples were collected hourly from 15 hours to 24 hours post infection, before collecting proteins for SDS-PAGE electrophoresis, followed by western blotting.

Figure 23 showed the effect of virus infection on total cellular PKR and phosphorylated-PKR. Infection of CT26 cells by T1L showed that by the 15 hour time point, the total PKR available in the host cell had been diminished to a lower level than the uninfected control collected at the same time. This was followed by a sudden increase of PKR production at the 16 hour time point, and then a large drop in total PKR at the 17 hour time point. Following this, a gradual increase in total PKR production was observed at each hour up to the 24 hour time point. The levels of PKR at the 24 hour time point was similar to the amount present in the L929

Figure 23: Protein synthesis of host proteins PKR and phosphorylated-PKR over 24 hours post infection with Reovirus T1L and T3D in CT26 cells. Western blotting was performed against host proteins using commericial antibodies against PKR and pPKR. Goat anti-rabbit IgG conjugated to Horse-Radish Peroxidase was used as the secondary antibody. Gels show actin levels in CT26 cells over a 24 hour time course post viral infection as a loading control. FB, fibroblast; C, uninfected cells.

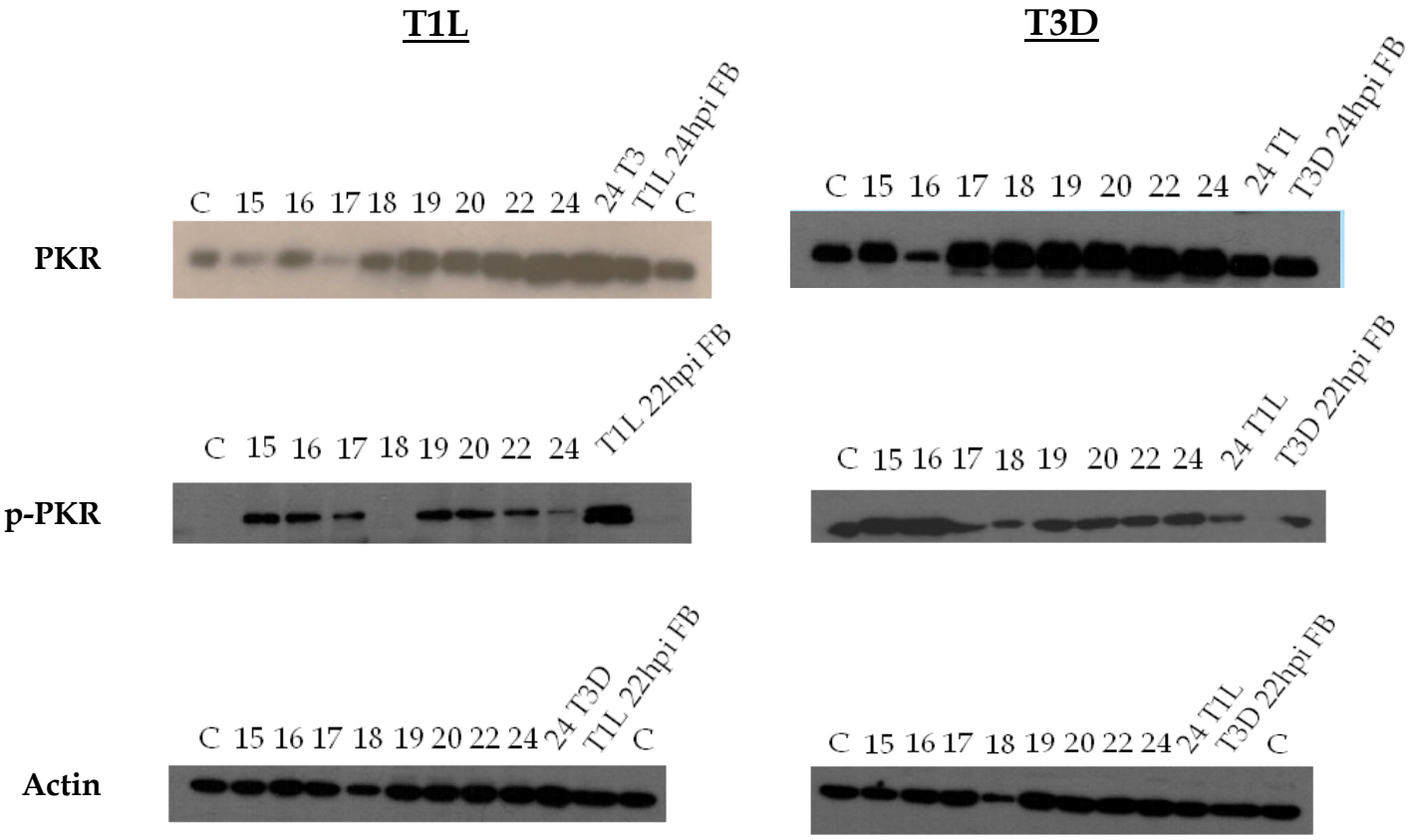
T1L
T3D
PKR
p-PKR
Actin
C 15 16 17 18 19 20 22 24 24 T3 T1L 24hpi FB C
C 15 16 17 18 19 20 22 24 24 T1 T3D 24hpi FB
C 15 16 17 18 19 20 22 24 T1L 22hpi FB
C 15 16 17 18 19 20 22 24 24 T1L T3D 22hpi FB
C 15 16 17 18 19 20 22 24 24 T3D T1L 22hpi FB C
C 15 16 17 18 19 20 22 24 24 T1L T3D 22hpi FB C

fibroblast cells at the same time. The PKR level in T3D infected CT26 cells showed a slightly different pattern of transient degradation followed by increases in PKR production. An increase in total PKR production was seen at the 15 hour time point, followed by a transient degradation in PKR at the 16 hour time point that was followed by an increasing amount of total PKR thereafter to the 24 hour time point. When the total PKR induced at the 24 hour time point in T1L infected CT26 cells or in L929 cells is compared to T3D infected cells, we observed that Reovirus T3D induces a greater amount of total PKR in CT26 cells.

Observing the effect of Reovirus infection on the active phosphorylated form of PKR, we saw that at 15 hours after T1L infection, pPKR was much higher than the uninfected control cells, which was followed by a gradual decrease of the phosphorylated form of PKR up to the 18 hour time point, where phosphorylated-PKR was barely detectable. Following this, we observed a general increase of phosphorylated-PKR up to the 20 hour time point, followed by a slight decrease at 22 hours post infection. Finally, at the 24 hour time point, the level of phosphorylated-PKR was once again decreased. Infection of CT26 cells by Reovirus T3D showed a slightly different pattern of induction and reduction in CT26 cells. The pPKR level was elevated at 15 and 16 hours post T3D infection. After the 17 hour time point, we observed a large decrease in phosphorylated-PKR (but not totally absent). However, the amount of phosphorylated-PKR gradually increased by the 24 hour time point. The amount of phosphorylated-PKR 24 hours following T3D infection was much higher than that resulting from 24 hours post T1L infection in CT26 cells or in L929 cells.

6.3.3 Effect of Reovirus infection on the total and phosphorylated eukaryotic initiation 2-alpha in CT26 cells

After studying the effects of T1L and T3D on PKR, we observed the effect of parental Reovirus infection on the substrate of PKR, the eukaryotic initiation 2-alpha (eIF2α). Upon activation, PKR phosphorylates eIF2α, which inhibits and eventually results in the shutdown of protein synthesis.

When CT26 cells were infected, the samples collected over a 24 hour time period, were blotted for total eIF2α and phosphorylated eIF2α (p-eIF2α). In figure 23 we observed that the total cellular eIF2α also fluctuated throughout the course of infection by T1L and T3D. Large decreases in total eIF2α were seen at the 18 hour time points for both T1L and T3D infected CT26 cells.

When probed for phosphorylated eIF2α, we found that with T1L infection, there was a detectable decrease in p-eIF2α at the 18 hour time point, followed by an increased accumulation up to 24 hours post infection (to the level of the uninfected control sample). We also observed that the amount of p-eIF2α at this time point in CT26 cells was lower than the same in L929 fibroblast cells. However, for T3D infected CT26 cells, we found there was a dramatic decrease in phosphorylated eIF2α at the 18 hour time point, followed by a large increase for the next 2 hours and then a subsequent decrease at 22 and 24 hours post infection. This therefore is quite striking, and mirrors the time and the effect seen in L929 cells.

Figure 24: Protein synthesis of host proteins showing total eIF2*α*, phosphorylated- eIF2*α*, Interferon Regulatory Factors (IRF) -3 and -7 over 24 hours post infection with Reovirus T1L and T3D in CT26 cells. Western blotting was performed against host proteins using commericial antibodies. Goat anti-rabbit IgG conjugated to Horse-Radish Peroxidase was used as the secondary antibody. Gels show actin levels in CT26 cells over a 24 hour time course post viral infection as a loading control.

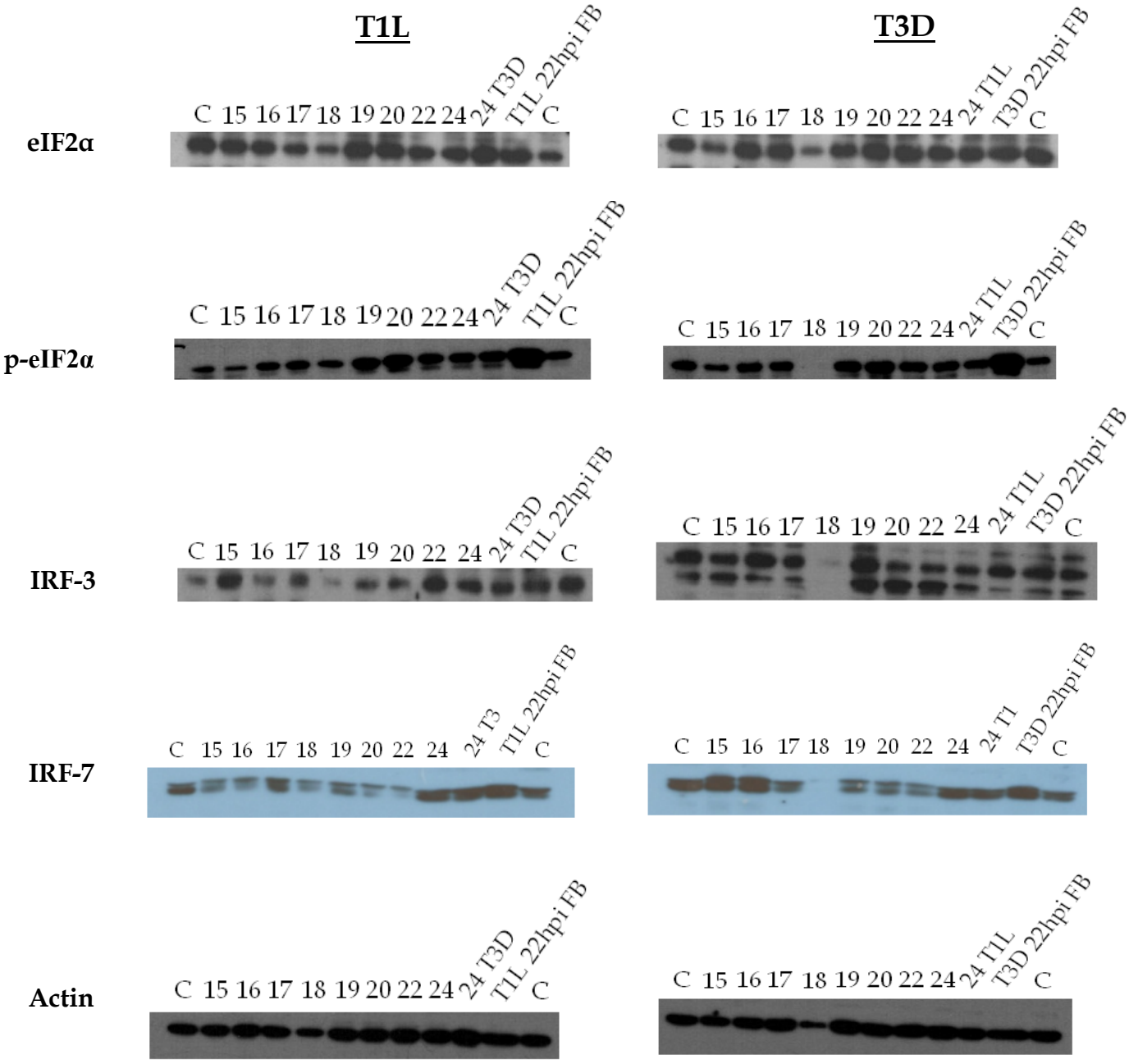
T1L
T3D
eIF2α
p-eIF2α
IRF-3
IRF-7
Actin
C 15 16 17 18 19 20 22 24 24 T3D T1L 22hpi FB C
C 15 16 17 18 19 20 22 24 24 T1L T3D 22hpi FB C
C 15 16 17 18 19 20 22 24 24 T3 T1L 22hpi FB C
C 15 16 17 18 19 20 22 24 24 T1 T3D 22hpi FB C

6.3.4 Effect of Reovirus infection on Interferon regulatory factors-3 and -7 in CT26 epithelial cells

Interferon regulatory factors (IRF) -3 and -7 are transcription factors that interact to play an important role in the early and late induction of interferon, respectively, that thus results in the transcription of interferon genes, PKR being one of the main ones (3, 57). We therefore studied the effect of Reovirus infection on the production of IRF-3 and IRF-7 over the 24 hour time course of infection in CT26 cells.

In figure 24, we observed that upon T1L infection of CT26 cells, IRF-3 levels were low at early times and then alternated from high to low levels for each hour between 15 and 19 hour time points, followed by an abrupt increase from the 22 to the 24 hour time point. In contrast, the levels of total IRF-3 remained relatively more stable when CT26 cells are infected with Reovirus T3D, except at the 18 hour time point, where there was a large and dramatic drop in the amount of IRF-3. This was followed by a subsequent boost in accumulation and another reduction in IRF-3 up to the 24 hour time point. This pattern of accumulation and reduction was very similar to that observed with p-eIF2α (Figure 24).

The pattern of IRF-7 was very similar to that of IRF-3. T1L infection of CT26 cells resulted in a slight decrease of IRF-7 intensity by 16 hours post infection relative to the control, but at the 17 hour time point there was an increase in accumulation. This again reduced and then fluctuated back up at the 19 hour time point, followed by a subsequent decrease in the intensity and finally a boost by the 24 hour time point post infection. These varied levels of accumulation and reductions were seen as fluctuations in time and suggest cycles of formation and degradation. Infection of CT26 cells by T3D showed a different pattern. IRF-7 levels remained high up to the 16 hour time point, followed by a slight decrease at 17 hours post infection, and a

dramatic reduction at the 18 hour time point. This was followed by an increase at the 19 hour point, marginally decreasing through the 20 and 22 hour time points, followed by an increase to the level of the cellular level, as shown by the uninfected control sample.

The actin levels were also seen to be reduced at 18 hours that were consistent with a degradation of host proteins at this point. The previous blot of viral proteins (Figure 22) indicated that this time point was not associated with a loss of viral proteins for T3D.

6.4 Discussion

In this section, we assessed in general Reovirus gene expression as well as the effects of infection on host defenses. The infected host cell senses Reovirus infection, and upon infection, IFN is induced, which causes the induction of antiviral effectors, including PKR. After activation and phosphorylation of its substrate eIF2α, PKR acts to shut down host protein synthesis.

Infection of CT26 cells by serotypes T1L and T3D seemed to have varying effects on the kinetics of host and viral protein production between the two parental Reoviruses. We have previously shown that T3D had higher protein production than T1L. In fact, T1L had the lowest protein production when compared to the ability of viral protein production post-infection of a panel of Reovirus reassortants (Figure 21).

Our results show that for T3D, there was a major increase in viral proteins at 18 hours. At the same time, we observed that infected cells have reduced (or degraded) pPKR, as well as its substrate eIF2α at 18 hours post infection. At the same time-point, other proteins also break down, showing similar kinetics, as seen by the decrease in actin, eIF2α, IRF-3 and IRF-7 levels. Therefore, this time point is a crucial stage where viral protein synthesis is enhanced at the cost

of the degradation of cellular/host proteins. We therefore conclude that parental serotype T3D induces degradation of pPKR at 18 hours to result in the enhanced viral protein synthesis.

It is noteworthy that the total PKR is reduced one hour before pPKR is reduced upon both T1L and T3D infection. Reovirus T1L infection shows a decrease in total PKR levels at 17 hours and phosphorylated PKR at 18 hours post infection, whereas T3D infection shows a decrease in total PKR levels as early as 16 hours post infection and a decrease in phosphorylated PKR at 17 and 18 hours post infection. We also observed that actin is reduced at 18 hours, as was IRF-3 and IRF-7.

At this juncture, it is important to mention that μ2 is a ubiquitinated protein that may be involved in this process. The Reovirus μ2 protein is encoded by the M1 gene segment. The ubiquitinated μ2 protein has been shown to be present in Reovirus inclusions together with components of the ubiquitin proteosome pathway (Brown, unpublished). Parker et al, 2002 have shown that the Reovirus μ2 protein is a microtubule-associated protein, and it plays a crucial role in the formation and the structural organization of Reovirus inclusion bodies (52).

Therefore, based on our results, we show that there is an enhanced effect of the virus infection leading to the 18 hour time point, where the virus induces the breakdown of host factors, which thus may be affecting host degradation systems. In addition, at the 18 hour time point, after the organization of microtubules, resulting in the formation of the viral inclusion bodies (mirrored by the decrease in actin levels at 18hpi), we found an increase in total viral proteins (figures 22-24). All the fluctuations in host proteins PKR, eIF2α, IRF-3, IRF-7 and actin may represent aspects of how the virus activates the cell to achieve sufficient breakdown – i.e. cycles of effects that increase with time until they can reduce host PKR. We therefore propose

that T3D induces the degradation of host inhibitors (such as PKR) to result in enhanced viral gene and protein expression, possibly through a μ2 protein dependent mechanism.

Comparing the effects of T1L with T3D, we showed that T1L did not grow very well in CT26 cells (figures 21 and 22). Although it does induce cycles of degradation and resynthesis of host proteins, it does not replicate and synthesize viral proteins in the CT26 epithelium in the same dramatic manner as T3D does (compare T1L and T3D viral protein levels in figure 22). The effects of T1L on CT26 cells are not as effective, suggesting that T1L therefore does not work well as T3D, at least not up to 24 hours post infection. We therefore conclude that T1L is not an overall effective virus in terms of growth and protein synthesis in CT26 epithelial cells.

CHAPTER SEVEN
ASSESSING THE INTERFERON SENSITIVITIES AND EMERGENT PROPERTIES OF ONCOLYTIC REOVIRUS AND REASSORTANTS IN FIBROBLAST AND EPITHELIAL CELLS

7.1 Background

Interferons (IFNs) are members of a multi-gene family of inducible cytokines. IFNs have a broad range of biological activities in addition to their well known anti-viral properties. The interferon system includes those cells which are able to produce IFN upon an external stimulus, such as virus infection, that allows the cells to respond by inducing and establishing an antiviral state. Infection by viruses such as Influenza, Vesicular Stomatitis Virus (VSV), and Reoviruses lead to the induction of IFN, and these viruses are also sensitive to the antiviral actions of IFN (57).

IFN-induced signaling occurs via the Jak-STAT pathway. Binding of IFN to these receptors result in the activation of Jak and STAT transcription factors on the cell surface via tyrosine phosphorylation, followed by dimerisation and subsequent translocation with IRF-9 to the nucleus to induce interferon stimulated genes (57, 89).

Interferons are categorized into two types: type I and type II. Type I IFNs include four subtypes: IFN-α, IFN-β, IFN-ω and IFN-τ. These are also known as viral IFNs, as they are induced by virus infection. Type II IFN is induced by an antigenic stimulus, and is also known as IFN-γ, or immune IFN (25). IFN-γ is synthesized only by certain cells of the immune system, such as natural killer cells, CD4 Th1 cells and CD8 cytotoxic suppressor cells. Figure 25 illustrates the schematic of the summary of the IFN system, from Samuel, CE, 2001 and Tyler et al, 1998. (57, 78)

Figure 25: Schematic summary of the IFN system. Virion particles are illustrated as open hexagons and IFN proteins as open circles. The IFN-producing cell on the left illustrates a cell induced by virus infection to produce IFN-α or IFN-β or stimulation by an antigen or a mitogen to produce IFN-γ. The IFN treated cell on the right shows paracrine IFN action in a cell that is induced to an antiviral state by the production of IFN-regulated proteins. This would result in the inhibition of virus replication. Adapted from Samuel, C. E. 1998. Reoviruses and the interferon system. Curr Top Microbiol Immunol 233:125-45.

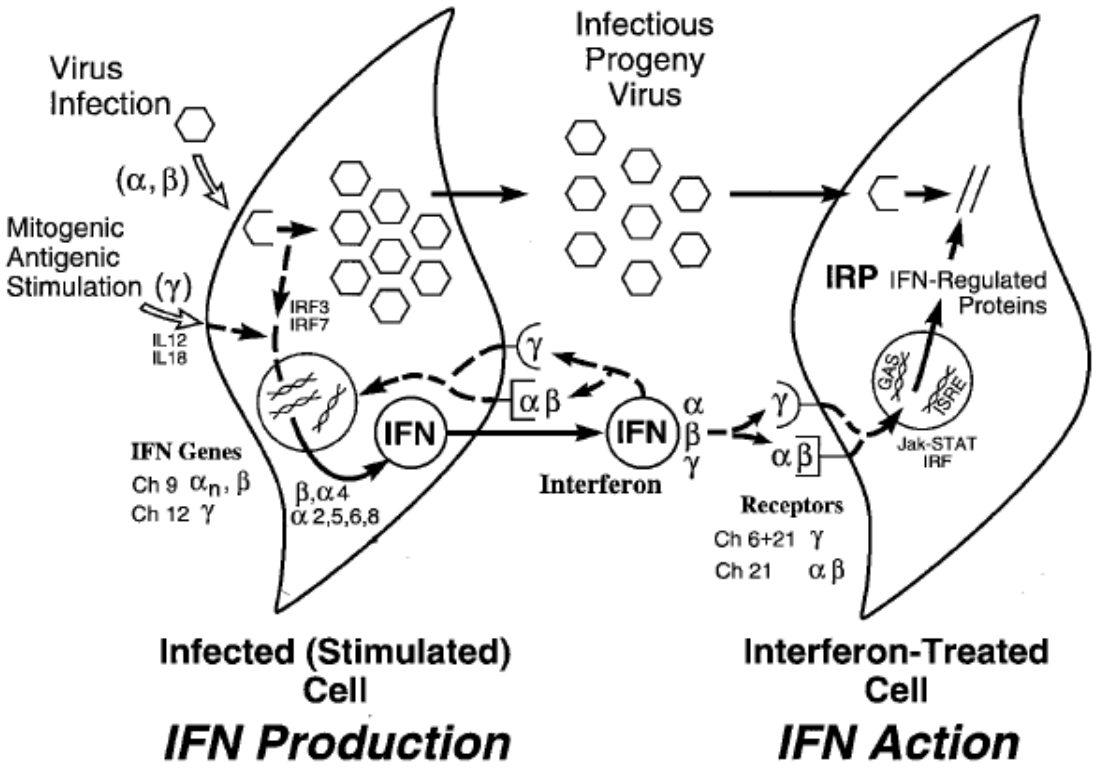
Virus
Infection
(α, β)
Mitogenic
Antigenic
Stimulation (γ)
IL12
IL18
IRF3
IRF7
IFN Genes
Ch 9 αn, β
Ch 12 γ
β,α4
α 2,5,6,8
IFN
γ
αβ
Infectious
Progeny
Virus
IFN
α
β
γ
Interferon
Receptors
Ch 6+21 γ
Ch 21 αβ
IRP IFN-Regulated
Proteins
GAS
ISRE
Jak-STAT
IRF
Infected (Stimulated)
Cell
IFN Production
Interferon-Treated
Cell
IFN Action

Infection of animal cells by Reoviruses leads to the induction of IFN. All Reovirus serotypes induce interferon; however, the degree to which IFN is induced varies between Reovirus strains as well as the type of cell that is infected. Several groups have researched the effect of IFN on Reovirus growth, replication and sensitivities (16, 38, 56, 59, 73, 89). Sharpe and Fields, 1983 demonstrated that in mouse fibroblasts, Reovirus T3D induces IFN to a much greater extent than T1L (61). Wieber and Joklik, 1975, have reported that T3D viral replication was reduced nearly 100-fold upon treatment of mouse L-cells with type-1 IFN (83). Moreover, Jacobs and Ferguson, 1991, showed that the replication of the Reovirus Type 3 Dearing strain was reduced by 17- to 100-fold, and that of the Lang strain was reduced by 2- to 3- fold in IFN pre-treated mouse L cells (38). In addition to varying in induction capacities, the parental serotypes, T1L and T3D, also differed in their sensitivities to IFN-β. Sherry et al, 1998, have shown that strain-specific differences in the induction and sensitivity to type I IFNs have been attributed to the M1, S2 and L2 gene segments, that encode the μ2, σ2 and λ2 proteins (64).

Interferon pre-treatment has shown to selectively inhibit Reovirus growth and protein synthesis in different cell lines (6, 38). Previous data in my research has shown varying effects of parental serotypes T1L and T3D on cell tropism, host cell and virus protein breakdown and re-synthesis between fibroblasts and epithelial cell lines, as well as the different oncolytic potentials of Reoviruses and reassortants. Interferon induction and sensitivity thus remains an integral part of understanding the molecular virology of Reovirus pathogenesis.

7.2 Specific Objectives

Tumours are usually epithelial in their origin, but they also contain cells with fibroblastic properties, due to the epithelial-mesenchymal transition. Since tumours are generally deficient in their PKR and IFN responsiveness pathways, we sought to investigate the interferon sensitivities of parental Reoviruses (T1L and T3D) and the four reassortants (EB88, EB96, EB97 and EB123) as well as the emergent properties of oncolytic reassortants in fibroblast and epithelial cells.

Due to the possibility that interferon sensitivity is a factor in Reovirus oncolysis, our main objective was to study the effects of interferon pre-treatment in one fibroblast cell line (L929 cells) and three epithelial cell lines (CV-1, Vero and CT26 cells). Viral replication and protein synthesis levels were analysed in IFN pretreated and untreated cells at 16, 24, 48 and 72 hours post infection of these four cell lines with parental T1L and T3D and the four reassortants. Viral titers in untreated and IFN pretreated cells were also analysed at 72 hours post infection, to understand the relative sensitivities of Reovirus and reassortants to interferon. Our specific aims were :

- To assess the production of IFN-β in L929 and CT26 cells upon infection by parental Reoviruses and the four reassortants
- To study the effects of interferon pre-treatment in L929 cells, CV-1 cells, Vero cells, and CT26 cells after infection with parental Reoviruses and the four reassortants that have enhanced oncolytic ability
- To assess viral protein production and titers after infection with the Reoviruses

7.3 Results

7.3.1 T3D induced IFN-β to a greater level than T1L in L929 cells, while the oncolytic Reassortants have varying levels of IFN-β induction.

Twenty-four hours post infection of L929 cells with parental Reoviruses T1L and T3D and the four reassortants, it was observed that IFN-β was greatly induced by parental Reovirus T3D to 975pg/ml, as detected by ELISA, whereas the induction of IFN-β by T1L was much lower at 130pg/ml (Figure 26). The four reassortants differed in IFN-β induction 24-hours post infection, where EB88 showed the highest amount of IFN-β induction of 357pg/ml, followed by EB97, which induced IFN-β to 216pg/ml. Reassortant viruses EB96 and EB123 showed the least induction of IFN-β, to similar levels as parental Reovirus type T1L, at 130pg/ml. Therefore T3D induced IFN-β to a greater level than T1L.

The differences in the ability to induce interferon between the reassortants are attributed to their gene segments (refer to Table 3 for genetic map). Based on the data and the genetic map from Table 3, EB88 has the M2 gene segment from T1L, on a T3D background, which rendered its ability to induce interferon to be dramatically reduced by a third. EB97 has its M2 from T3D, but its L3 and S4 gene segments are from T1L that causes it to induce IFN-β to an intermediate level. EB96 has gene segments L2, M1 and S3 from T3D, but its ability to induce interferon was greatly reduced presumably due to the remaining genome segments from T1L. The decrease in IFN-β induction of EB96 could be attributed to its S2 gene segment, which is from parental prototype T1L. Reassortant EB123 has its L3 and S3 gene segments from T1L, which resulted in the ability of the virus to induce IFN-β to a lower level than T3D (Figure 26).

Figure 26: IFN-β induction by Parental Reovirus (T1L and T3D) and Reassortants (EB88, EB96, EB97 and EB123) 24 hours post infection in L929 cells. T3D induces IFN-β to ~10-fold higher levels than T1L. All reassortants have different levels of IFN-β induction, varying between the two parental serotypes. Values indicate means with standard errors of duplicate sets of experiments.

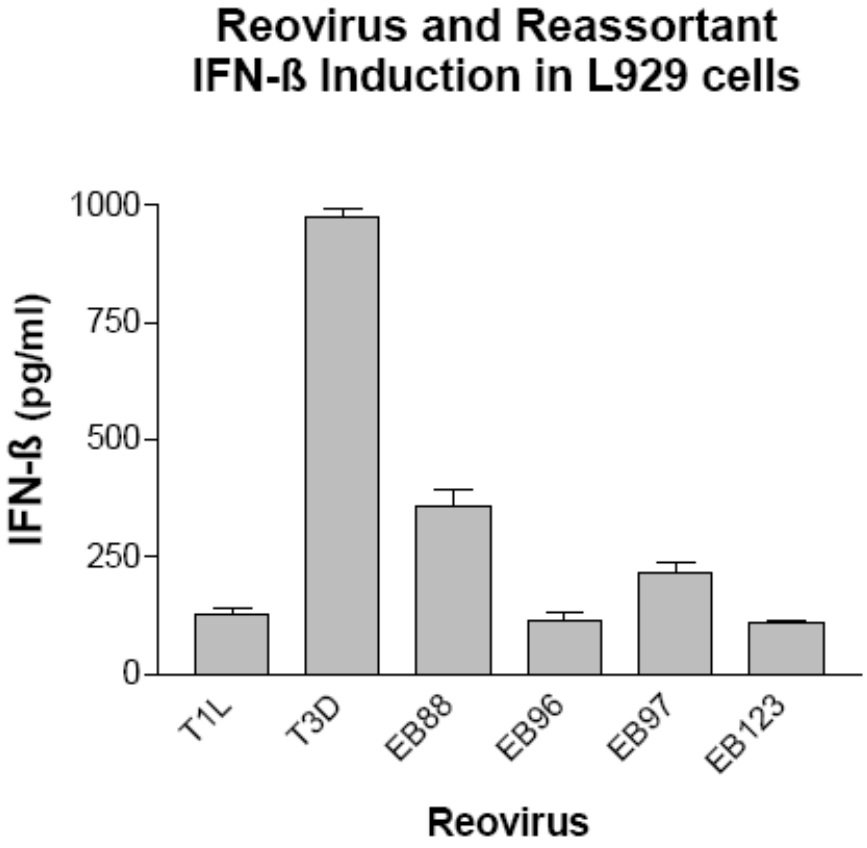
Reovirus and Reassortant
IFN-ß Induction in L929 cells
IFN-ß (pg/ml)
1000
750
500
250
0
T1L
T3D
EB88
EB96
EB97
EB123
Reovirus

It is known that the M1 gene segment is the primary genetic determinant of Reovirus strain-specific differences in the IFN response in cardiac cells (64). All these reassortants possess the M1 gene from T3D, and yet have reduced IFN-β production dramatically compared to the parental T3D Reovirus, indicating that other genes are influencing IFN- β induction. Therefore, our results imply that M1 plays a role in IFN-β induction in L929 cells through various interactions with other Reovirus gene products.

7.3.2 EB88 induced 4-fold more IFN-β than parental serotype T3D, while T1L and oncolytic Reassortants have low or undetectable levels of IFN-β induction in CT26 cells.

The CT26 mouse colon tumour cell line is the cell line used in our *in vivo* tumour challenge model. Twenty-four hours following infection with parental Reoviruses T1L and T3D and the four reassortants, IFN-β production was measured using ELISA. We found that between the two parental serotypes, T3D induced IFN-β to 25pg/ml, whereas the level of IFN-β for T1L was below the limit of detection of the ELISA assay (Figure 27).

Among the four reassortants, EB88 induced IFN-β to 100pg/ml, whereas EB97 and EB123 induced IFN-β to very low levels, at ~1pg/ml, while IFN-β induction for reassortant EB96 was below the limit of detection for the assay. Comparing the levels of induction between T3D and EB88, the reassortant induced IFN-β to 4-fold higher level than the parental serotype, due to the function of the individual M2 gene segment and its interactions with the T3D backbone.

Figure 27: IFN-β induction by Parental Reovirus (T1L and T3D) and Reassortants (EB88, EB96, EB97 and EB123) 24 hours post infection in CT26 cells. EB88 induces IFN-β to ~4-fold higher levels than T3D. All reassortants have different levels of IFN-β induction. EB97 and EB123 have very low levels of IFN-β induction, whereas the IFN-β induction of parental serotype T1L and reassortant strain EB96 were below the detection limit of the assay. Values indicate means with standard errors of duplicate sets of experiments.

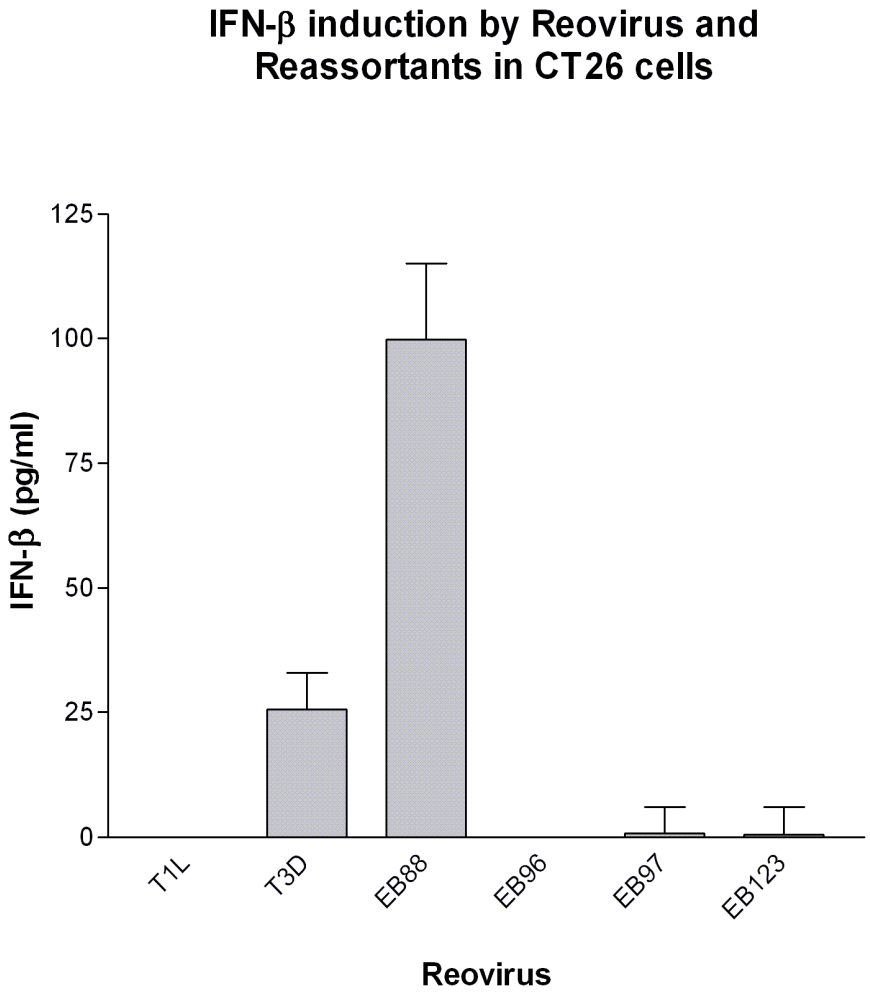
IFN-β induction by Reovirus and Reassortants in CT26 cells
IFN-β (pg/ml)
125
100
75
50
25
0
T1L
T3D
EB88
EB96
EB97
EB123
Reovirus

7.3.3 Reovirus reassortants displayed different yield and interferon sensitivity properties compared to their parental strains in L929 cells

To study the effect of IFN pre-treatment on the viral production of Reovirus and the four oncolytic reassortants, IFN pretreated and untreated L929 cells were infected with the Reovirus parental serotypes (T1L & T3D) and the four reassortants (EB88, EB96, EB97, EB123) at an MOI of 10. Each viral infection was repeated in triplicate for untreated and following twenty-four hour treatmentwith 200U of mouse IFN-β. Viral titers were measured by plaque assays on each sample to determine the viral yields 72 hours post infection, as shown in Figure 28.

In all cases, the untreated viral yields were higher than IFN-β treated titers. The T1L and T3D parental serotypes had untreated yields of 3×10^8 pfu/ml and 4×10^8 pfu/ml. The reassortants all had lower untreated yields with EB88 having the lowest yield at 6×10^6 pfu/ml and the other three reassortants having yields ranging from 2×10^7 pfu/ml to 4×10^7 pfu/ml (Figure 28). Upon IFN pretreatment, parental Reovirus T3D showed a 1.5-log decrease in viral titers which was significant compared to that of T1L, which was minimally effected by IFN pretreatment. Reassortant strains EB88 and EB123 showed between 2 to 5 fold decreases in viral yield, whereas EB96 showed a 10-fold decrease in viral yield after IFN pretreatment. EB97 was the only reassortant that showed a minimal effect of IFN pretreatment on viral yield, being similar to that of T1L.

Figure 28: Reovirus titers at 72 hpi in L929 cells that were pretreated and untreated with IFN. IFN treatments were with 200U/ml per well or without interferon for 24 hours before infection (MOI=10). Results are shown as a mean of triplicate experiments with standard errors for each virus.

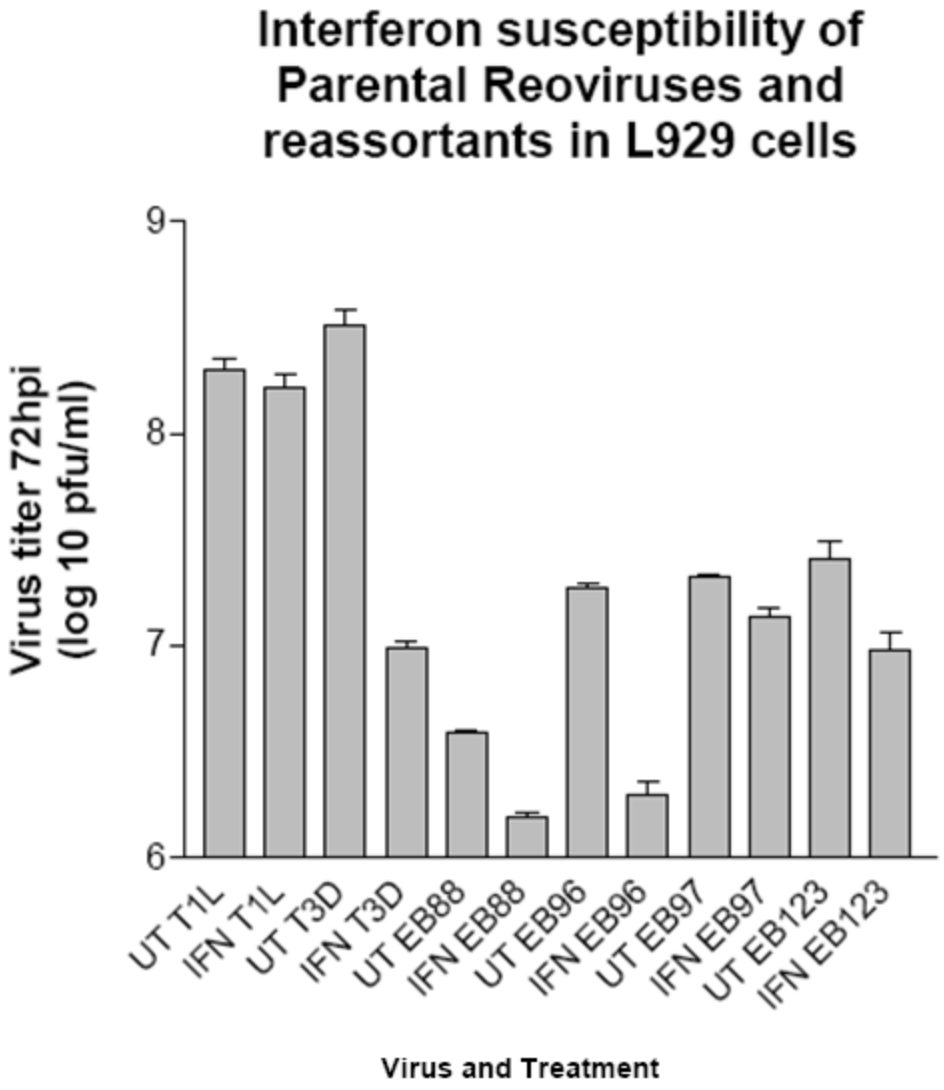
Interferon susceptibility of Parental Reoviruses and reassortants in L929 cells
Virus titer 72hpi (log 10 pfu/ml)
9
8
7
6
UT T1L
IFN T1L
UT T3D
IFN T3D
UT EB88
IFN EB88
UT EB96
IFN EB96
UT EB97
IFN EB97
UT EB123
IFN EB123
Virus and Treatment

To better compare the interferon sensitivity of the different Reovirus strains, a graphic representation was made by dividing the untreated viral yield with the interferon-treated yield for each virus (Figure 29). T1L was almost interferon resistant with a yield ratio of 1.2 while T3D was the most sensitive, showing an 11.2 fold decrease in viral yield after the interferon pretreatment. The reassortants had varying levels of interferon sensitivity. EB88 and EB123 showed intermediate relative sensitivities, at 2.5 and 2.7, respectively, which resembled the yield ratio more closely to parental prototype T1L. With the yield ratio of 1.2, EB97 displayed very similar resistance to interferon as T1L. On the contrary, EB96 was the only reassortant with a similar level of interferon sensitivity as the T3D parental serotype with a yield ratio of 9.5.

Therefore, parental serotype T1L was the most interferon resistant, where as serotype T3D was very sensitive to the effect of IFN pretreatment. The reassortant strains showed sensitivities to IFN ranging from being very similar in resistance to the T1L parental strain and others showing intermediate sensitivities in L929 fibroblast cells. De Benedetti et al, 1985, also show treatment of L929 cells with IFN resulted in the reduction of viral mRNA synthesis by 75 to 80% after infection with Reovirus, although protein synthesis was not inhibited (16).

Figure 29: Relative IFN-sensitivity of Reovirus and reassortants in L929 cells.
Reovirus reassortants have varying levels of interferon sensitivity that are different from both parental strains. Values were calculated by dividing the average untreated titer with the average interferon-treated titer for each reovirus.

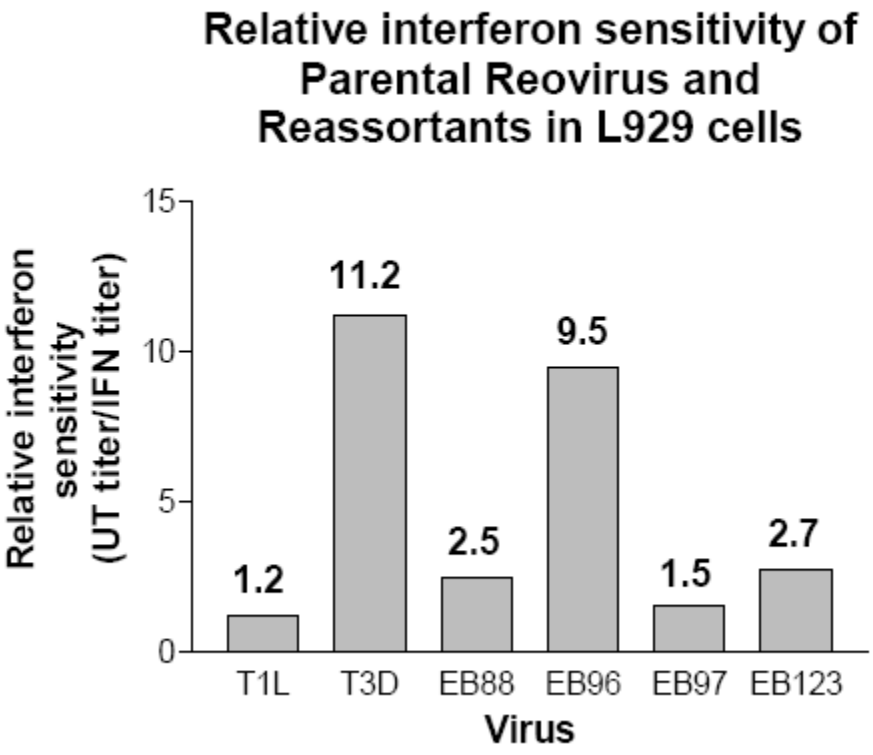
Relative interferon sensitivity of Parental Reovirus and Reassortants in L929 cells
Relative interferon sensitivity (UT titer/IFN titer)
15
10
5
0
1.2
11.2
2.5
9.5
1.5
2.7
T1L
T3D
EB88
EB96
EB97
EB123
Virus

7.3.4 Reovirus reassortants displayed interferon dependent protein synthesis patterns in L929 cells

To study the effects of interferon pretreatment on the protein synthesis of Reovirus in L929 cells, samples were collected in SDS-PAGE sample buffer at 16, 24, 48 and 72 hours post infection (hpi). Mock infections were done with PBS on untreated (–) and interferon-pretreated (+) cells and were loaded as negative controls. Actin was probed as a loading control. Western blot analysis with a cocktail of anti-T1L and anti-T3D antibodies showed the different trends of protein synthesis for the various Reoviruses (Figure 30).

T1L protein synthesis was sensitive to interferon at all times post infection with the least effect seen at 48 hpi. Although μ1 protein and cleavage products were the most prominent at 48 and 72 hpi, more σ3 was produced in the IFN treated samples than the untreated samples. Actin was present at control levels at 16 hpi, but by 24 and 48 hpi, actin production was boosted, following its degradation by the 72 hour time point.

T3D protein synthesis showed sensitivity to interferon that remained consistent over time. However, the host protein actin pattern showed stimulation by both infection and IFN treatment even at 16 hpi, where upon IFN pretreatment, actin production was boosted compared to the untreated. However, by 24 hours, actin levels remained higher than background. By 48 and 72 hpi, actin was degraded to levels below the controls.

The protein synthesis patterns for all the oncolytic reassortants were similar to T3D as they all showed interferon sensitivity over time.

Figure 30: Reovirus and reassortant protein production at 16, 24, 48 and 72 hours post infection in IFN pretreated and untreated L929 cells. Polyclonal rabbit anti-T1L and anti-T3D antisera were used to detect viral proteins. Goat anti-rabbit IgG conjugated with HRP was used as a secondary antibody. Controls include mock infected L929 cells with (+) or without (-) interferon pretreatment. Actin bands are shown as loading controls.

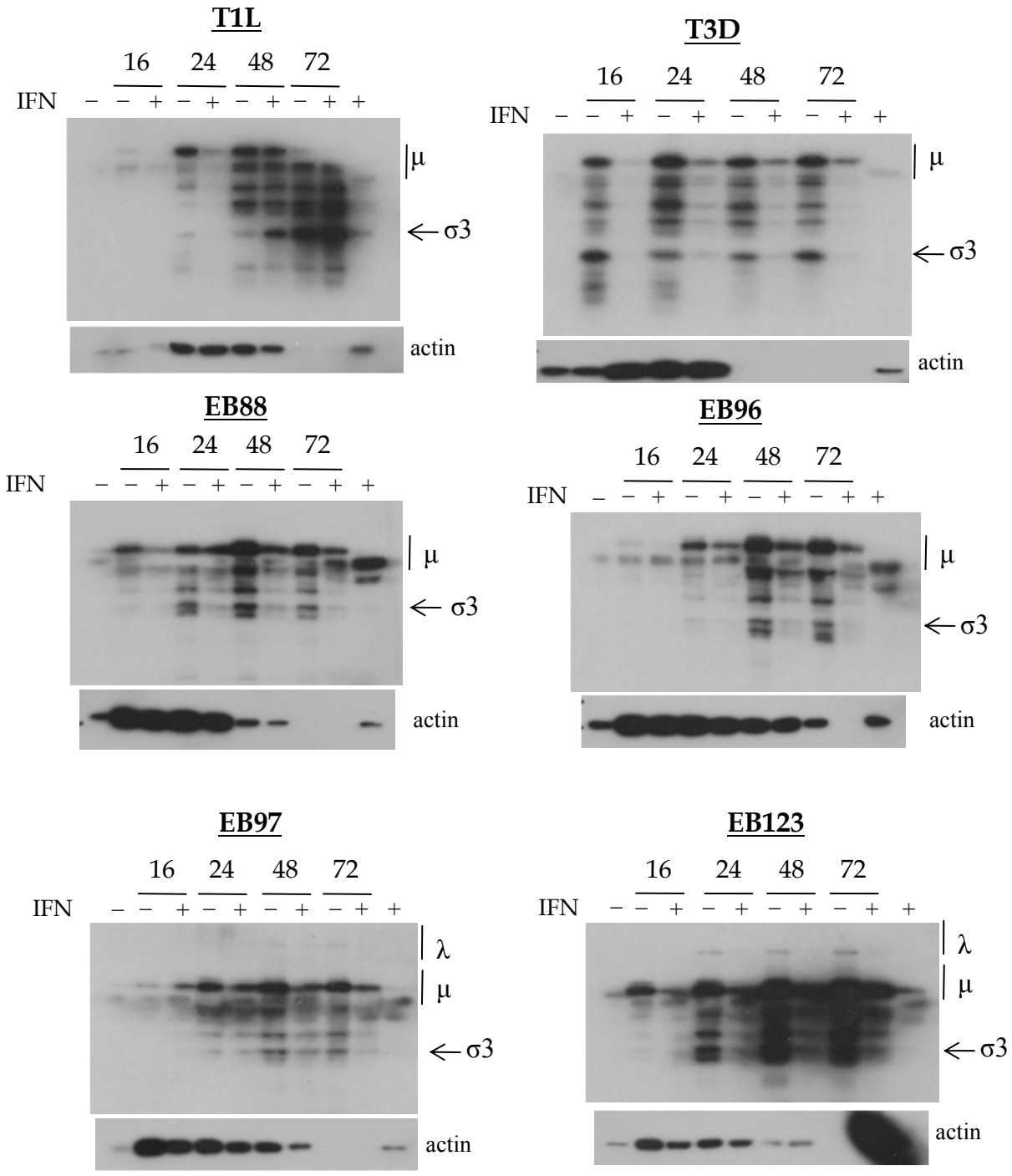
T1L
16 24 48 72
IFN – – + – + – + – + +
μ
← σ3
actin
T3D
16 24 48 72
IFN – – + – + – + – + +
μ
← σ3
actin
EB88
16 24 48 72
IFN – – + – + – + – + +
μ
← σ3
actin
EB96
16 24 48 72
IFN – – + – + – + – + +
μ
← σ3
actin
EB97
16 24 48 72
IFN – – + – + – + – + +
λ
μ
← σ3
actin
EB123
16 24 48 72
IFN – – + – + – + – + +
λ
μ
← σ3
actin

Actin levels were also observed to be boosted at early time points, followed by complete degradation at later time points. In addition, production of Reovirus λ proteins was also visible on the EB123 blot as early as 24 hpi, in untreated samples, indicating a higher level of protein production by EB123 relative to other reassortants.

Therefore the IFN effect on protein synthesis patterns of Reovirus reassortants correspond to the virus yields reported in 7.3.3, and were intermediate between the patterns shown by the two parental serotypes in L929 cells.

7.3.5 Reovirus reassortants displayed emergent properties of yield and interferon sensitivity compared to the growth of the parental strains in CT26 cells

To assess the growth of the parental serotypes and the four reassortants in CT26 cells over a 72 hour period, mouse colon carcinoma cells, CT26 cells, were pretreated with IFN. Following a 24 hour incubation, cells were infected with parental Reoviruses and reassortants at an MOI of 10. Cells untreated with IFN were also used to compare the effect of IFN on Reovirus growth and protein production.

The protein synthesis of Reovirus parental strains has been studied in chapter six over a 24 hour period and it was found that T1L did not express protein as well as T3D in CT26 cells (Figures 21 and 22). Contrary to the growth of the parental serotypes in L929 cells, the viral yield of T3D seems to be minimally effected by IFN pretreatment, whereas the yield of T1L was reduced by 2-fold upon IFN pretreatment in CT26 cells. Therefore, T3D was less sensitive to IFN in CT26 cells than L929 cells.

The ability of the four reassortants to grow in CT26 cells were comparable or greater than the parental serotypes, while the untreated yields of EB88 and EB96 are lower than T1L and

T3D. The viral yields of oncolytic reassortants EB88, EB96 and EB97 in CT26 cells were enhanced from 10- to 100-fold upon IFN pretreatment. EB88 appeared to be benefiting from IFN pretreatment the most, giving over a 100-fold increase in viral yield. The only exception to this trend was the growth of EB123, which was shown to be decreased by the pretreatment of IFN by 30-fold. Reassortants EB88, EB96 and EB97 did not behave like either of the parental strains, suggesting that their IFN stimulation in CT26 cells was an emergent property due to reassortment and due to the unique combination of the gene segments (see Figure 31).

When assessing the relative sensitivities of the Reovirus and reassortants to IFN (Figure 32), we found that in CT26 cells, parental serotype T3D was almost IFN resistant with a yield ratio of 1.3, while T1L showed slightly more sensitivity to IFN with a yield ratio of 2.0. Reassortants EB88, EB96 and EB97 showed viral yield ratios of 0.008, 0.05 and 0.05 respectively, which showed the viral yields to be 25-fold to 162-fold higher than T3D. This indicates that IFN benefits the viral yield of these three reassortants, rather than inhibiting their production in CT26 cells. On the contrary, EB123 showed the most sensitivity against IFN pretreatment, with a yield ratio of 30.8 (figure 32).

Figure 31: Reovirus titers at 72 hpi in CT26 cells that were pretreated and untreated with IFN. IFN treatments were with 200U/ml per well or without interferon for 24 hours before infection (MOI=10). Results are shown as a mean of triplicate experiments with standard errors for each virus.

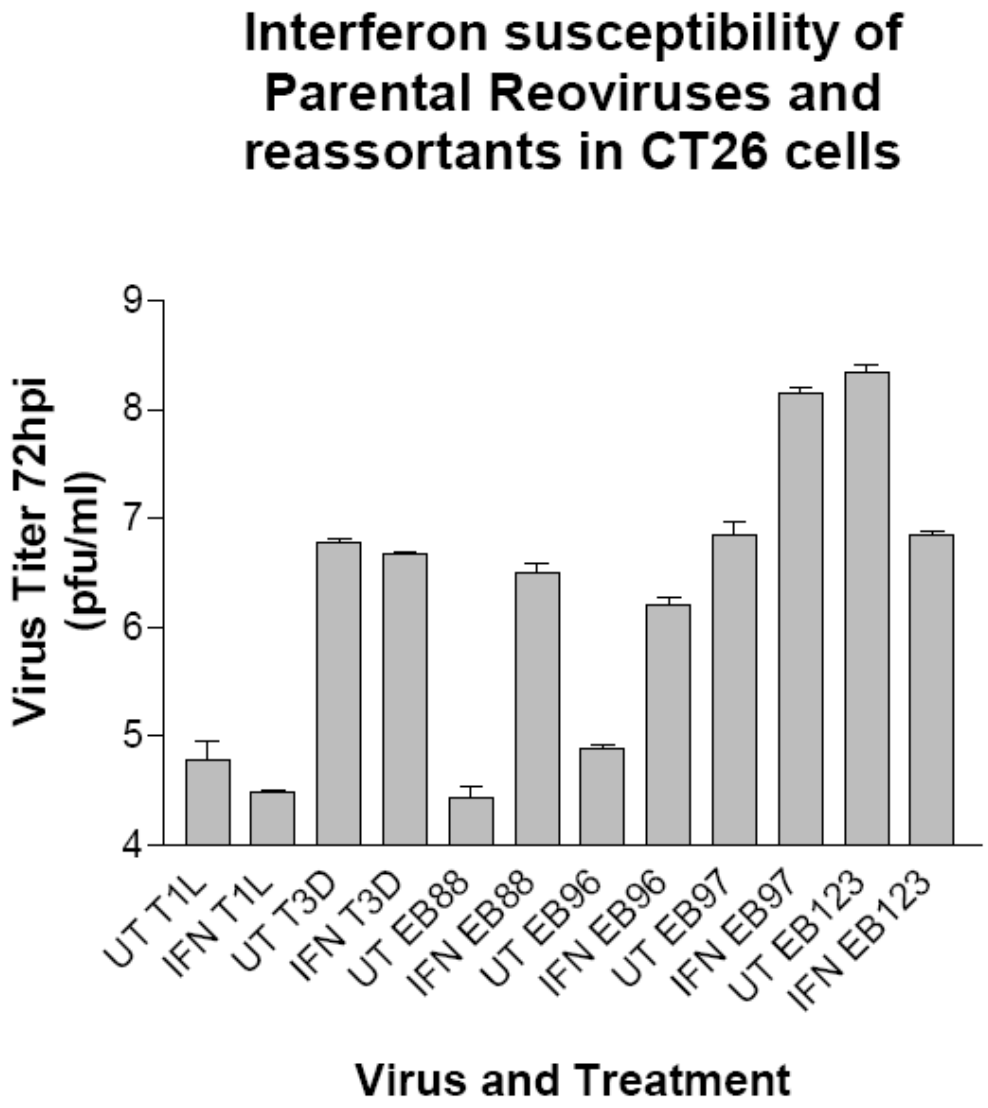
Interferon susceptibility of Parental Reoviruses and reassortants in CT26 cells
Virus Titer 72hpi (pfu/ml)
9
8
7
6
5
4
UT T1L
IFN T1L
UT T3D
IFN T3D
UT EB88
IFN EB88
UT EB96
IFN EB96
UT EB97
IFN EB97
UT EB123
IFN EB123
Virus and Treatment

Figure 32: Relative IFN-sensitivity of Reovirus and reassortants in CT26 cells. Reovirus reassortants have varying levels of interferon sensitivity that are different from both parental strains. Values were calculated by dividing the average untreated titer with the average interferon-treated titer for each reovirus.

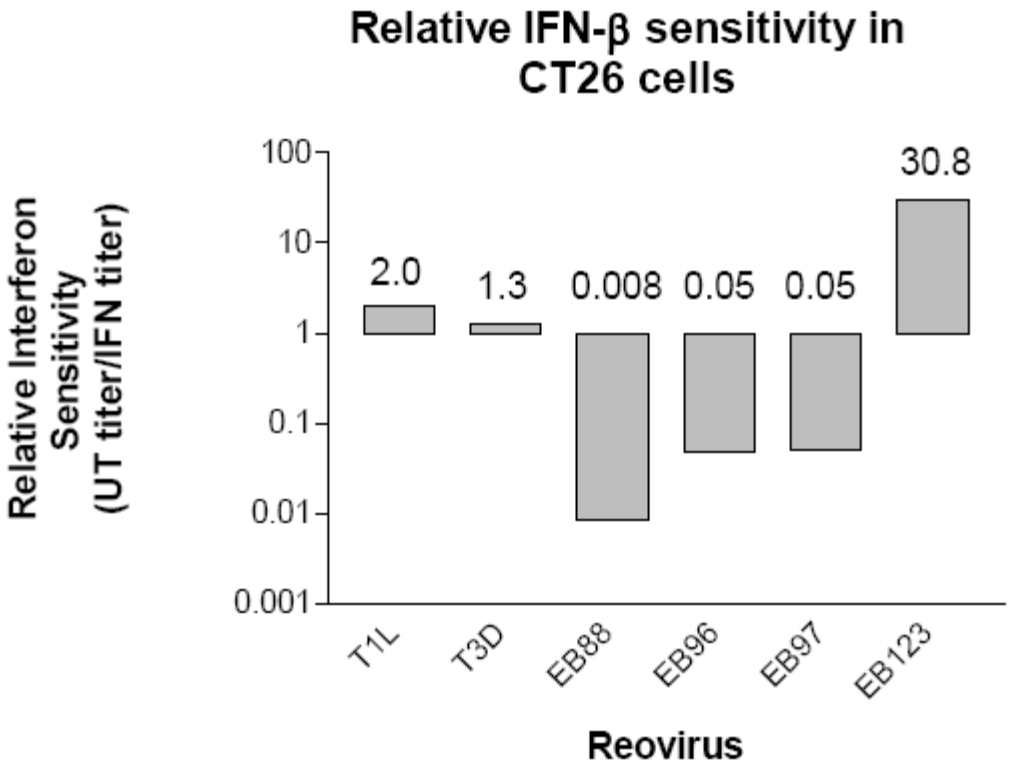
Relative IFN-β sensitivity in CT26 cells
Relative Interferon Sensitivity (UT titer/IFN titer)
100
10
1
0.1
0.01
0.001
2.0
1.3
0.008
0.05
0.05
30.8
T1L
T3D
EB88
EB96
EB97
EB123
Reovirus

7.3.6 IFN either enhanced or inhibited viral protein production of different Reoviruses in CT26 lung epithelial cells

To study the effects of IFN pretreatment on viral protein synthesis of parental Reoviruses and reassortants in CT26 cells, SDS-PAGE samples were collected at 16, 24, 48 and 72 hours. Mock infections with PBS were done on untreated and interferon pretreated CT26 cells as negative controls. Actin was used as a control of host protein levels. Western blot analysis was performed against Reovirus proteins using anti-Reovirus antibodies. Figure 33 shows the trends of viral protein synthesis.

There seemed to be two distinct trends that were observed at a first assessment of the blots on figure 33, where the degree of protein synthesis of T1L, EB88 and EB96 showed less viral protein production, than T3D, EB97 and EB123 that showed enhanced viral protein synthesis. Moreover, infection with T3D, EB97 and EB123 also showed the production of Reovirus λ3 polymerase protein, as early as 16 hours for EB123 and 48 hours for T3D and EB97 (Figure 33).

Comparing the protein synthesis of the two parental serotypes, T3D had much better protein synthesis in CT26 cells than T1L, where longer exposures were required that were associated with background staining of a prominent host band below μ1c and σ3 proteins. Also, both parental strains were enhanced by IFN at twenty-four hours post infection, but sensitive thereafter. In addition, Reovirus T3D was more resistant to the effect of IFN than T1L, as indicated by the intensity of μ1 bands at 48 and 72 hours post infection. This was also mirrored in the viral titers at 72 hours post infection from figure 31.

Figure 33: Reovirus and reassortant protein production at 16, 24, 48 and 72 hours post infection in IFN pretreated and untreated CT26 cells. Polyclonal rabbit anti-T1L and anti-T3D antisera were used to detect viral proteins. Goat anti-rabbit IgG conjugated with HRP was used as a secondary antibody. Controls include mock infected CT26 cells with (+) or without (-) interferon pretreatment. Actin bands are shown as loading controls.

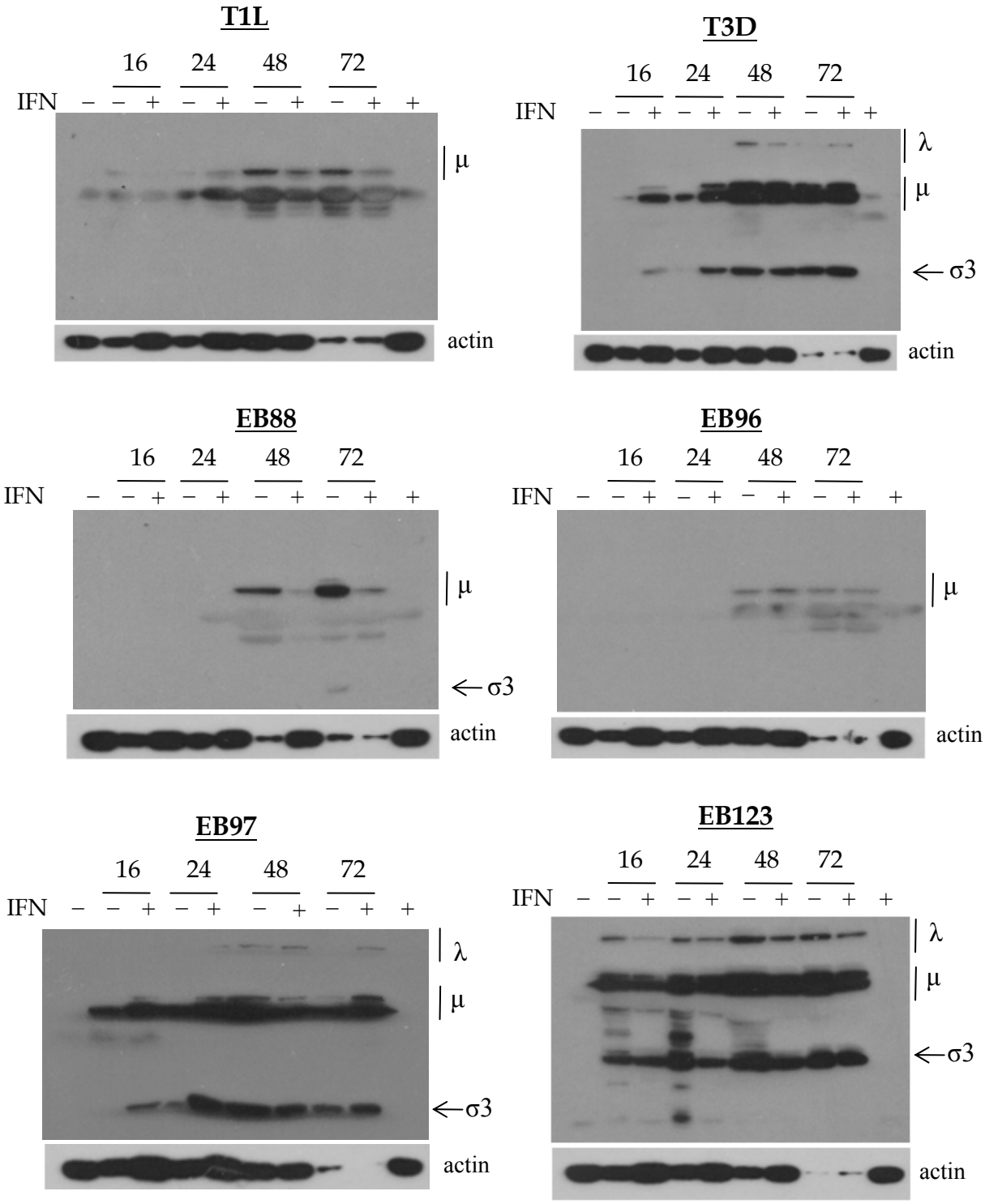
T1L
16 24 48 72
IFN – – + – + – + – + +
μ
actin
T3D
16 24 48 72
IFN – – + – + – + – + +
λ
μ
←σ3
actin
EB88
16 24 48 72
IFN – – + – + – + – + +
μ
←σ3
actin
EB96
16 24 48 72
IFN – – + – + – + – + +
μ
actin
EB97
16 24 48 72
IFN – – + – + – + – + +
λ
μ
←σ3
actin
EB123
16 24 48 72
IFN – – + – + – + – + +
λ
μ
←σ3
actin

Reassortants EB88 and EB96 were shown to grow to lower titers in CT26 lung tumours, whereas EB97 and EB123 grew to higher titers (unpublished data, Brown lab). This was also reflected in the CT26 cells blots, where no viral protein is detected up to the 48 hour time point for EB88 and EB96, whereas high amounts of viral protein were synthesized as early as the 16 hour time point in EB97 and EB123. In addition, IFN enhanced the synthesis of viral proteins for EB97, as shown by the increased intensity of μ1 bands in IFN treated CT26 cells at 24, 48 and 72 hours, but not EB123 (Figure 33).

Although reassortant viruses EB88 showed greater sensitivity to IFN than EB96 in terms of protein production, their viral yield are 100-fold (for EB88) and 25-fold (for EB96) higher in the presence of IFN than EB97 and EB123 (which is in fact sensitive to IFN in terms of viral yield) (Figure 31). Therefore it is interesting to note that higher viral protein synthesis may not necessarily correlate with increased viral yield.

The other interesting aspect of Reovirus growth in CT26 cells was the breakdown of actin at later time points. Infection by all Reoviruses and reassortants resulted in actin degradation by the 72 hour time point. EB88 infection, however, causes actin degradation earlier, at 48 hours. It is also worth noting that actin production was generally higher in the presence of IFN (Figure 33).

Therefore, there seems to be an interaction with Reovirus proteins, IFN and host proteins such as actin, which consequently plays a role in the synthesis of viral proteins and viral yield. The effect of IFN was different in CT26 epithelial cells compared to L929 mouse fibroblast cells.

Figure 34: Reovirus titers at 72 hpi in Vero cells that were pretreated and untreated with IFN. IFN treatments were with 200U/ml per well or without interferon for 24 hours before infection (MOI=10). Results are shown as a mean of triplicate samples with standard errors for each virus.

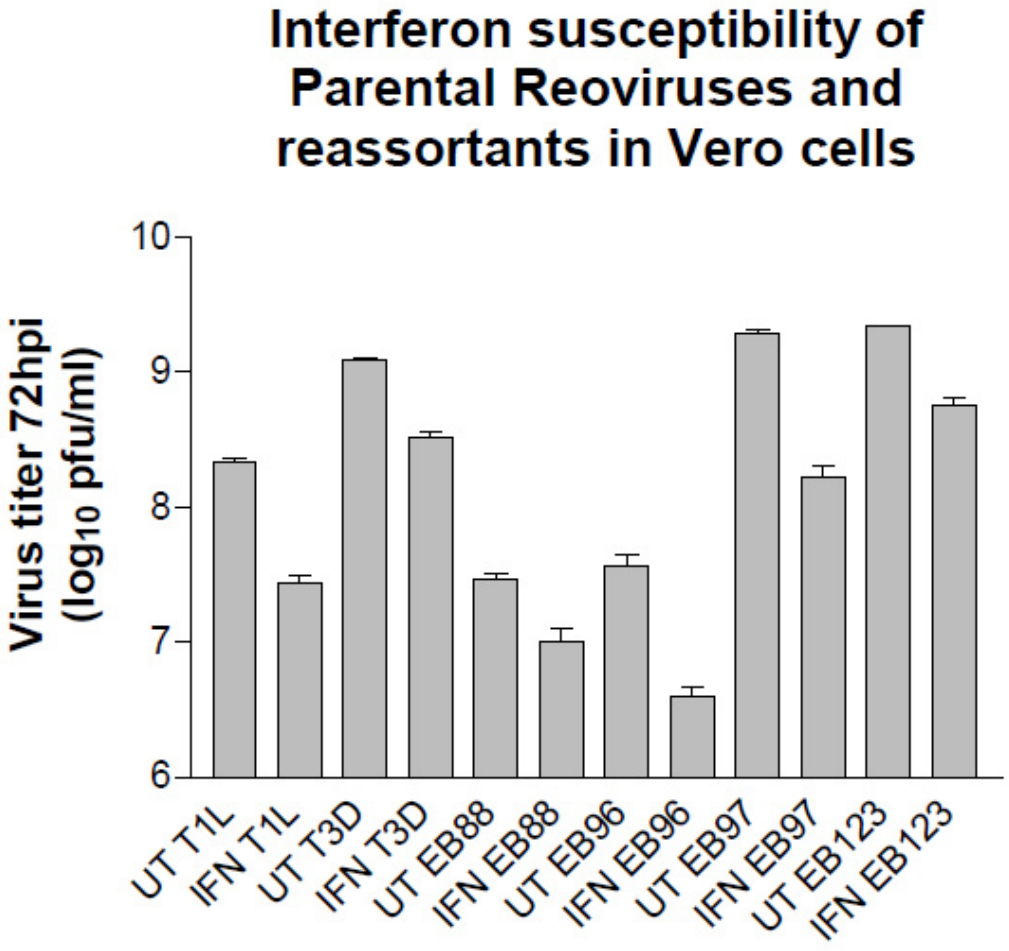
Interferon susceptibility of Parental Reoviruses and reassortants in Vero cells
Virus titer 72hpi (log10 pfu/ml)
10
9
8
7
6
UT T1L
IFN T1L
UT T3D
IFN T3D
UT EB88
IFN EB88
UT EB96
IFN EB96
UT EB97
IFN EB97
UT EB123
IFN EB123

7.3.7 Reovirus and Reassortant yield and IFN sensitivity in Vero cells mapped to the M2 and the S4 gene segments, respectively.

After studying the effect of IFN on Reovirus growth and protein production in L929 mouse fibroblast cells and CT26 epithelial cells, we next investigated these properties in Vero monkey kidney epithelial cells to monitor differences in replication or protein synthesis levels in a cell that cannot produce IFN. The same yield experiments were performed by infecting Vero cells with T1L and T3D wildtypes and EB88, EB96, EB97, and EB123 oncolytic reassortants at an MOI of 10. The experiment was repeated in triplicate for each viral infection with or without interferon pretreatment for 24 hours with 200U of human IFN-α-2b. Viral yields after 72 hours were determined by plaque assays and plotted on a bar graph (Figure 34).

We observed that the yields of both parental serotypes and all four reassortants were decreased upon IFN pretreatment, indicating IFN sensitivity. In IFN untreated cells, Reovirus serotype T1L grew to 3 x 10^8 pfu/ml compared to T3D, at 1 x 10^9 pfu/ml, which is a 10-fold relative decrease in viral yield. We also observed that reassortants EB88 and EB96 had lower yields, ranging from 2 x 10^7 to 4 x 10^7 pfu/ml in untreated Vero cells, which were even lower than T1L. EB97 and EB123 had very similar yields to T3D, 1-2 x 10^9 pfu/ml. The similarities in the lower viral yields of T1L, EB88, and EB96 and the higher viral yields of T3D, EB97, and EB123 can be mapped to the M2 gene segment. EB88 and EB96 possess the M2 gene segment from T1L, whereas EB97 and EB123 possess the M2 gene segment from T3D (Figure 34 and Table 3).

The interferon sensitivity graph was generated using the previously described method of dividing the average untreated titer with the average interferon pretreated titer for each Reovirus infection of Vero cells (Figure 35). T1L was more sensitive to interferon, with a yield ratio of

Figure 35: Relative IFN-sensitivity of Reovirus and reassortants in Vero cells.
Reovirus reassortants have varying levels of interferon sensitivity that are different from both parental strains. Values were calculated by dividing the average untreated titer with the average interferon-treated titer for each reovirus.

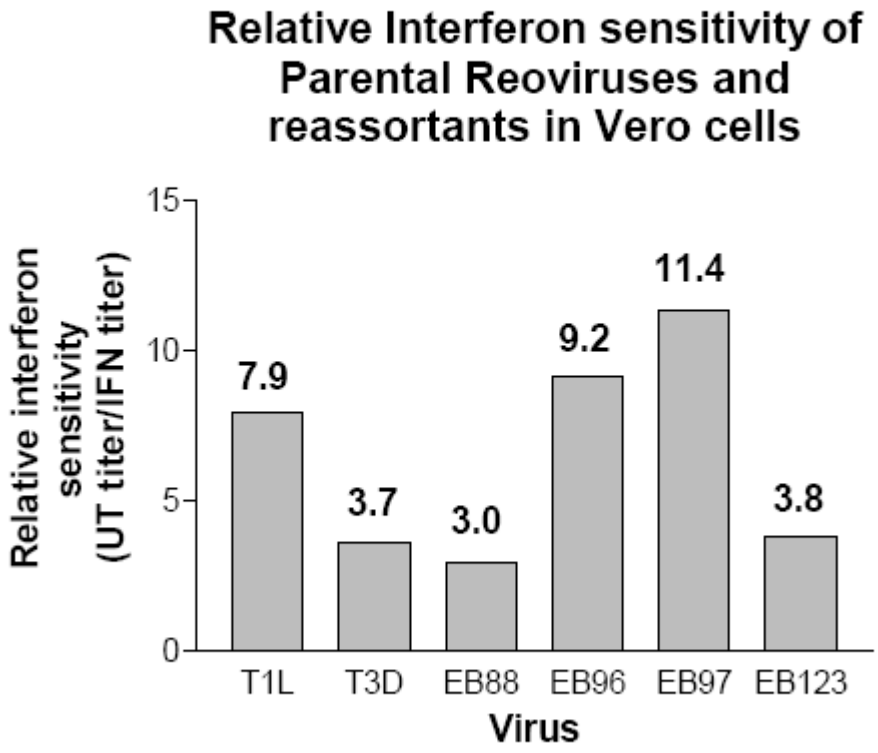
Relative Interferon sensitivity of Parental Reoviruses and reassortants in Vero cells
Relative interferon sensitivity (UT titer/IFN titer)
15
10
5
0
7.9
3.7
3.0
9.2
11.4
3.8
T1L
T3D
EB88
EB96
EB97
EB123
Virus

7.9, than T3D, with a yield ratio of 3.7. This interferon sensitivity in Vero cells was the opposite of what was seen in L929 fibroblast cells where T1L was more resistant to interferon than T3D. Moreover, compared to their sensitivities in CT26 cells, where both T1L and T3D seemed less sensitive to IFN, in Vero cells, we found T1L being more sensitive than T3D. The reassortants also behaved differently with respect to one another suggesting, once again, that improved reassortant oncolysis is likely not just due to interferon sensitivity, but due to cell type (fibroblast versus epithelial). EB88 and EB123 gave yield ratios of 3.0 and 3.8, respectively, which were more similar to T3D, where as the yield ratios of EB96 and EB97, of 9.2 and 11.4, respectively, were closer to T1L. This pattern where T1L, EB96, and EB97 displayed an increased sensitivity to interferon pretreatment compared to T3D, EB88 and EB123 mapped to their S4 genome segment (Figure 35 and Table 3).

7.3.8 Parental Reoviruses and reassortants displayed interferon dependent protein synthesis patterns in Vero cells that mapped to the M2 gene segment

The protein synthesis levels of reovirus parental serotypes and reassortants in Vero cells were analyzed by using the same protocol that was used for the infections in the L929 and CT26 cells. SDS samples were collected at four time points after infection and western blots were generated by probing for Reovirus proteins with polyclonal anti-T1L and anti-T3D antibodies (Figure 36).

Between the two parental serotypes, we found that T3D synthesized proteins earlier and to greater levels in Vero cells than T1L. Reovirus T1L was sensitive to IFN throughout the time course of the experiment, which corresponded to the viral yield decrease of 10-fold in Figure 34. In contrast, T3D protein synthesis was IFN sensitive at 24 hpi, and resistant by the 72 hour time

Figure 36: Reovirus and reassortant protein production at 16, 24, 48 and 72 hours post infection in IFN pretreated and untreated Vero cells. Polyclonal rabbit anti-T1L and anti-T3D antisera were used to detect viral proteins. Goat anti-rabbit IgG conjugated with HRP was used as a secondary antibody. Controls include mock infected Vero cells with (+) or without (-) interferon pretreatment. Actin bands are shown as loading controls.

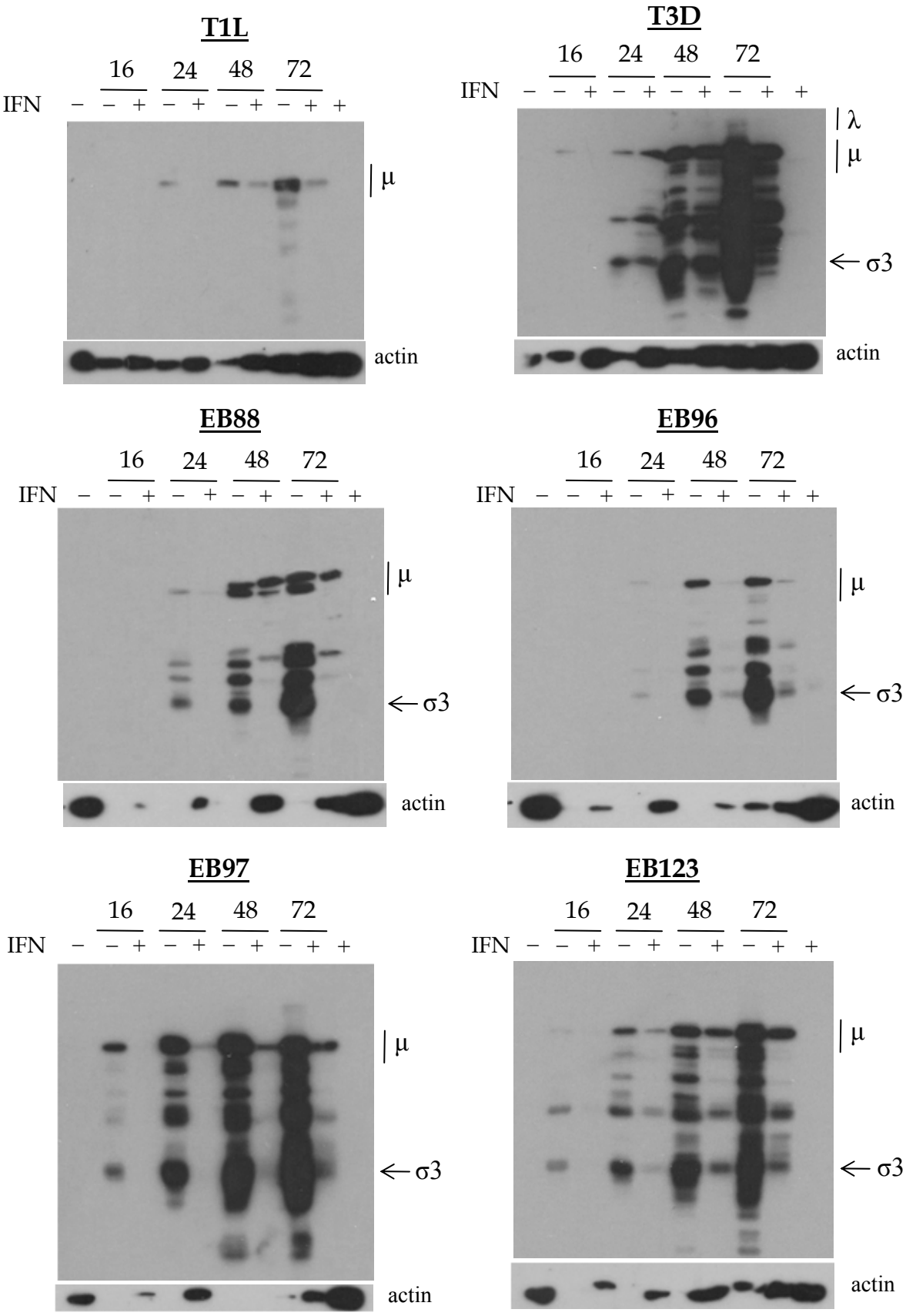
T1L
16 24 48 72
IFN – – + – + – + – + +
μ
actin
T3D
16 24 48 72
IFN – – + – + – + – + +
λ
μ
← σ3
actin
EB88
16 24 48 72
IFN – – + – + – + – + +
μ
← σ3
actin
EB96
16 24 48 72
IFN – – + – + – + – + +
μ
← σ3
actin
EB97
16 24 48 72
IFN – – + – + – + – + +
μ
← σ3
actin
EB123
16 24 48 72
IFN – – + – + – + – + +
μ
← σ3
actin

point, consistent with a slight decrease of 2-fold in viral yield observed upon IFN pretreatment (Figure 34 and Figure 36). In the case of the four reassortants, we observed that they were all sensitive to the effect of IFN on protein production, to varying levels – where EB96 was the most sensitive, and EB123 was the least sensitive (Figure 36).

The western blots, T3D, EB97 and EB123 showed earlier synthesis and greater amounts of protein products, suggesting that in Vero cells, these Reoviruses generated more viral proteins than T1L, EB88, and EB96. This same pattern of virus protein production was also observed in CT26 cells. This relative difference in protein synthesis levels between the Reoviruses also corresponded with the yield data which showed that T1L, EB88 and EB96 have lower yields compared to T3D, EB97, and EB123 (Figure 34 and Figure 36). These differences in protein levels can also be attributed to their M2 genome segment.

In contrast to normal mammalian cells, Vero cells are interferon-deficient and therefore they do not secrete type-1 interferon when infected by viruses. However, they still possess the IFN-α/β receptor, which allows them to respond to interferon when added to the culture (17, 20).

When observing the pattern of actin production, we find that actin is maintained at low levels in the absence of IFN pretreatment, whereas actin production was increased when Vero cells were pretreated with IFN. Therefore, the interferon-induced state prevents viral protein synthesis in Vero cells. This suggests some interaction between Reovirus proteins, IFN and actin, which consequently plays a role in the synthesis of viral proteins and/or viral yield, as was observed with CT26 cells.

Figure 37: Reovirus titers at 72 hpi in CV-1cells that were pretreated and untreated with IFN. IFN treatments were with 200U/ml per well or without interferon for 24 hours before infection (MOI=10). Results are shown as a mean of triplicate samples with standard errors for each virus.

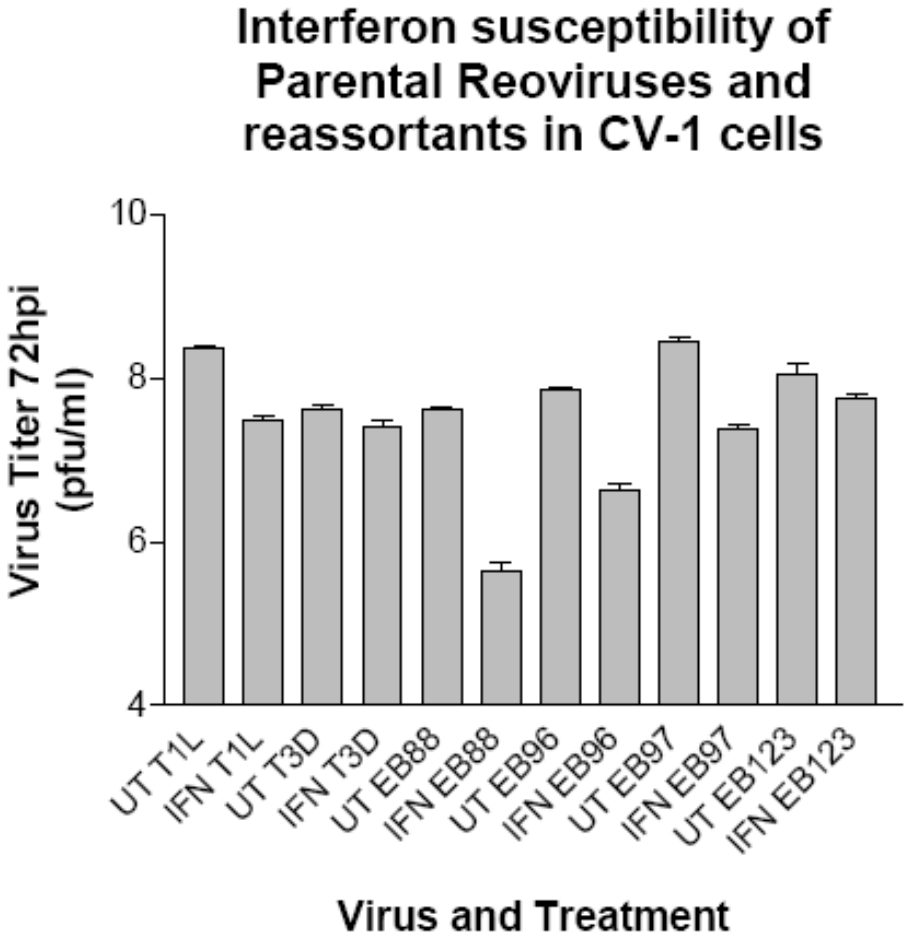
Interferon susceptibility of Parental Reoviruses and reassortants in CV-1 cells
Virus Titer 72hpi (pfu/ml)
10
8
6
4
UT T1L
IFN T1L
UT T3D
IFN T3D
UT EB88
IFN EB88
UT EB96
IFN EB96
UT EB97
IFN EB97
UT EB123
IFN EB123
Virus and Treatment

7.3.9 Reovirus and Reassortant yields in CV-1 cells were similar to Vero cells

The third and final epithelial cell line that was assessed was the African green monkey kidney cell line CV-1. This specific cell line was used because unlike Vero cells, CV-1 cells are able to secrete type-1 IFN. Hence we wanted to assess the ability of a cell line that is endogenously capable to produce IFN upon viral infection. The samples were repeated in triplicate for each viral infection with or without interferon pretreatment. Viral yields after 72 hours were determined by plaque assays and plotted on a bar graph (Figure 37).

In untreated CV-1 cells, T1L grew to 2.3 x 10^8 pfu/ml, where as T3D grew to 4.1 x 10^7 pfu/ml. It was observed that IFN-pretreatment caused the decrease in yield of parental reovirus and reassortants. Although T1L grew better in CV-1 cells, T3D was the least affected by the effect of IFN pretreatment, with its IFN treated viral yield at 2.6 x 10^7 pfu/ml, compared to an almost 10-fold decrease of IFN treated yield of T1L at 3 x 10^7 pfu/ml. IFN pretreatment affected the yield of EB88 by almost 100-fold, from 4.3 x 10^7 pfu/ml to 4.4 x 10^5 pfu/ml. EB96 and EB97 had a 10- to 15-fold decrease, similar to that of T1L. EB123 resembled T3D the most, as it was one of the reassortants that was least effected by the IFN pretreatment on viral yield (Figure 37). With the exception of the differences in the growth and viral yields of the parental serotypes, the trends observed with the four Reovirus reassortants in CV-1 cells more closely resembled what was observed in Vero cells (Figure 34 and Figure 37).

To better visualize the relative interferon sensitivity of the different reovirus strains in CV-1 cells, the interferon sensitivity graph was generated (Figure 38). From all the strains, Reovirus T3D and reassortant EB123 showed to be the least sensitive to the effect of IFN on viral yield, with viral yield ratios of 1.6 and 2.0, respectively. Parental serotype T1L had a yield ratio of 7.3, making it more sensitive than T3D. Reassortants EB86 and EB97 had higher

Figure 38: Relative IFN-sensitivity of Reovirus and reassortants in CV-1 cells. Reovirus reassortants have varying levels of interferon sensitivity that are different from both parental strains. Values were calculated by dividing the average untreated titer with the average interferon-treated titer for each reovirus.

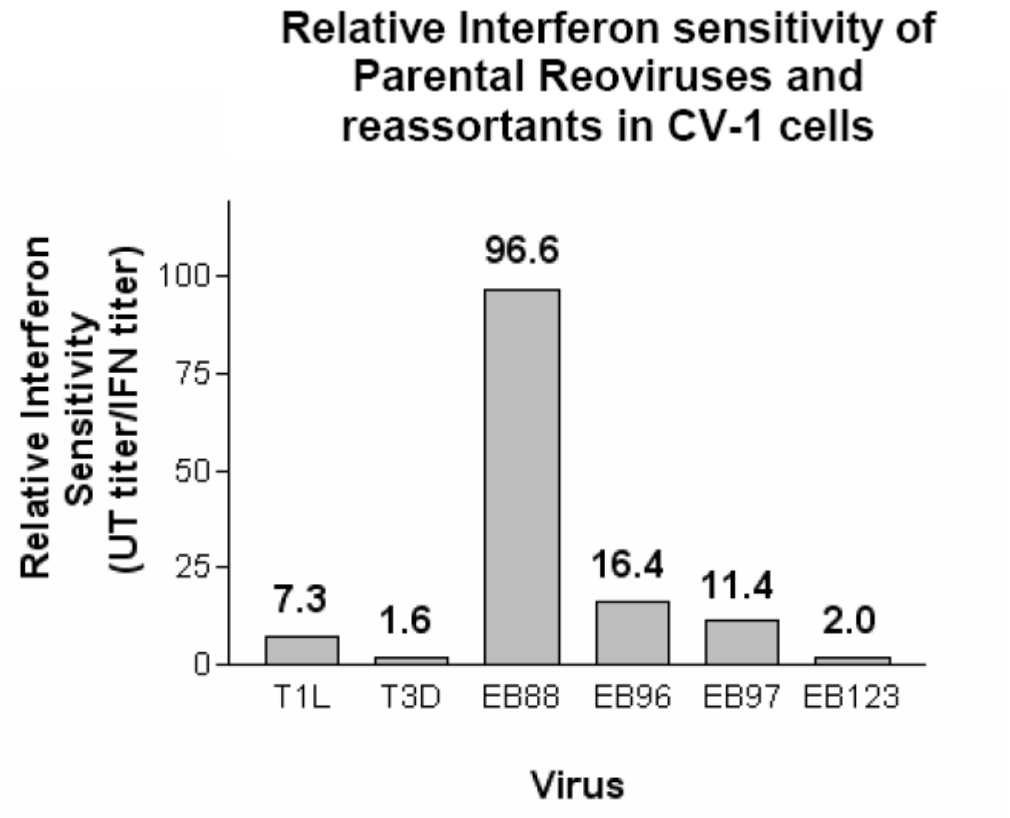
Relative Interferon sensitivity of Parental Reoviruses and reassortants in CV-1 cells
Relative Interferon Sensitivity (UT titer/IFN titer)
100
75
50
25
0
7.3
1.6
96.6
16.4
11.4
2.0
T1L
T3D
EB88
EB96
EB97
EB123
Virus

sensitivities to IFN than the two parental serotypes, whereas EB88 was the most sensitive to IFN pretreatment, having a yield ratio of 96.6. This was the first time EB88 had been observed to be the most sensitive to IFN (Figure 38). In Vero cells and L929 cells, EB88 had lower sensitivity to IFN, at 3.0 and 2.5 yield ratio, whereas in CT26 cells, EB88 had a yield ratio of 0.008, indicating enhanced viral yield upon IFN pretreatment. The production of endogenous IFN in a non-cancerous epithelial cell therefore seems to have a great impact on the sensitivity of EB88.

7.3.10 Reovirus and Reassortants displayed differences in interferon dependent protein synthesis in CV-1 cells

The protein synthesis levels of Reovirus parental serotypes in CV-1 cells (Figure 39) indicated that both parental strains were sensitive to IFN at the 16 hour time points, T3D being more sensitive than T1L; however, after 48 hours, both parental serotypes showed reduced resistance to IFN, having bands of similar intensities at 48 and 72 hour time points. Differences in protein production were most evident at early time points where T1L, T3D and EB123 were high inducers relative to EB88, EB96 and EB97, that were lower inducers of protein synthesis in CV-1 cells. EB88, EB96 and EB97 also displayed an interferon-sensitive protein synthesis, and a slower rate of protein synthesis where EB88 and EB96 produced undetectable viral proteins at early time points of 16 hours post infection. In addition, they both displayed sensitivity at 24 hours, followed by increased resistance by the 48 and 72 hour time points. In contrast, EB123 showed high levels of protein synthesis that was resistant at the earliest 16 hour time point, as shown by a stronger μ1 and σ3 band intensity. This was different than what was observed for both T1L and T3D with IFN pretreatment, suggesting gene interaction effects to produce IFN

Figure 39: Reovirus and reassortant protein production at 16, 24, 48 and 72 hours post infection in IFN pretreated and untreated CV-1 cells. Polyclonal rabbit anti-T1L and anti-T3D antisera were used to detect viral proteins. Goat anti-rabbit IgG conjugated with HRP was used as a secondary antibody. Controls include mock infected CV-1 cells with (+) or without (-) interferon pretreatment. Actin bands are shown as loading controls.

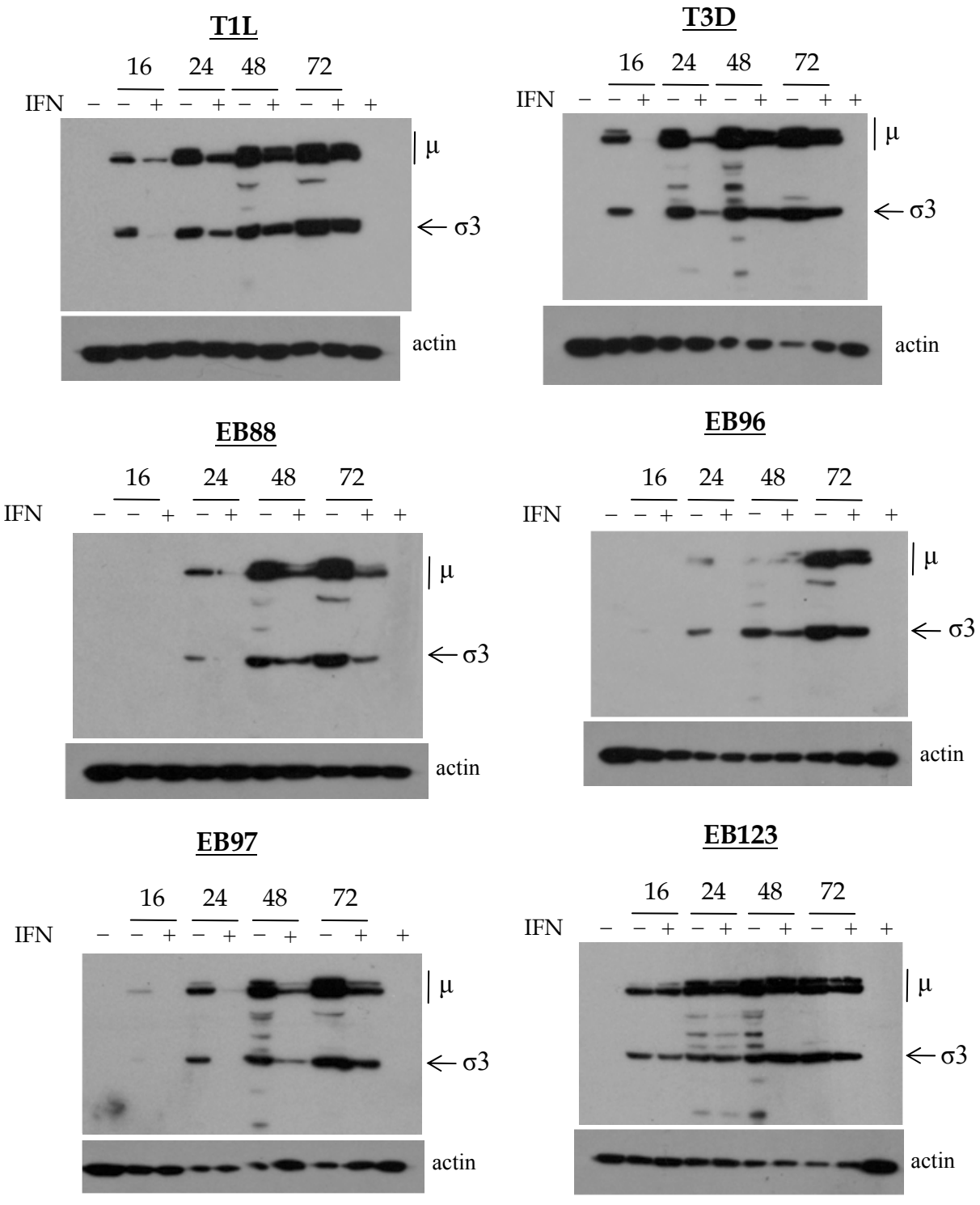
T1L
16 24 48 72
IFN – – + – + – + – + +
μ
← σ3
actin
T3D
16 24 48 72
IFN – – + – + – + – + +
μ
← σ3
actin
EB88
16 24 48 72
IFN – – + – + – + – + +
μ
← σ3
actin
EB96
16 24 48 72
IFN – – + – + – + – + +
μ
← σ3
actin
EB97
16 24 48 72
IFN – – + – + – + – + +
μ
← σ3
actin
EB123
16 24 48 72
IFN – – + – + – + – + +
μ
← σ3
actin

resistance. EB123 resistance to IFN pretreatment was also reflected in an insignificant decrease in viral yield from figure 37 and low relative interferon sensitivity from figure 38.

Another interesting aspect of CV-1 cell infection was that actin levels remained relatively constant throughout the time course of the experiment. We had observed profound degradation of actin at later time points in L929 and CT26 cells. Actin production was boosted during infection of interferon pretreated Vero cells. A relatively stable level of actin was observed throughout the 72 hour time course of T1L and EB88 infection, but was reduced at later times for T3D, EB96, EB97 and EB123 (Figure 39). This suggests that a functioning endogenous interferon system of a cell plays an important role in the effect virus infection has on the biology of the cell, but this effect is dependent on the cell type and virus strain. The biology of Reovirus and its interactions with native host proteins such as actin therefore needs to be further studied in depth.

7.4 Discussion

The primary purpose of this study was to investigate the replication and protein synthesis of Reovirus and reassortants that had properties of enhanced oncolytic ability. In addition, because deficits in IFN response are proposed to be central to tumour susceptibility and viral oncolysis, the effects of interferon pre-treatment of several cell types: L929 fibroblast cells, CV-1 cells, Vero (IFN-deficient) cells, and CT26 (cancer); therefore cells were infected with parental Reoviruses and the four oncolytic reassortants. It is known that T3D is naturally oncolytic, having activity for a wide range of cancers (42). There are, however, Reovirus resistant cancer cell lines (such as CT26) that require novel approaches in treatment with oncolytic Reoviruses. Genetic reassortment can yield progeny viruses that have novel and enhanced properties

compared to either of their parental strains (45). Therefore by studying the effect of IFN on viral yield, IFN sensitivity and protein synthesis, in fibroblast and epithelial cell lines, we identified specific aspects of reovirus reassortant strains that may be responsible for their improved oncolysis or other related properties.

We have gathered from our results that Reovirus oncolysis seems to be a complicated interplay between viral replication, protein synthesis, the growth environment and the antiviral response within various cell types. It is known that the interferon response is not only involved in the cellular response to viral infection, but it also plays a role in a variety of other cellular pathways, including the control and regulation of cellular growth as well as the induction of apoptosis, mediated by numerous factors, including PKR. Tumours are, in general, defective in both their IFN and PKR response, and the apoptosis pathways of most cancer cells are also compromised, rendering them to become highly susceptible targets by interferon-sensitive viruses such as Reoviruses. Oncolysis therefore targets cells due, at least in part, to the defects in the IFN pathways of the infected cells. In addition, tumours are epithelial in origin, but also possess fibroblastic cells. We therefore sought to analyze our data, emphasizing the various aspects that influence the biology of Reovirus. Therefore the replication and protein synthesis of parental Reoviruses T1L and T3D and the four reassortants (EB88, EB96, EB97 and EB123) were studied in cell lines that differ in their IFN-β induction abilities, morphology (fibroblast versus epithelium), and whether the cells are cancerous or normal.

7.4.1 Ability to induce IFN-β in L929 fibroblast and CT26 epithelial cells.

Reovirus parental serotype T3D induced IFN-β to high levels in both L929 and CT26 cells, which has been previously known to be the case in L929 cells, by Gaunt et. al, 1985 and

Jacobs et. al., 1991 (27, 38). In contrast, T1L induced IFN-β to lower or undetectable amounts in L929 and CT26 cells, respectively (figures 26 and 27). The ability of a virus to induce IFN-β will consequently affect its growth properties in the cell, which is a function of its susceptibility to IFN-mediated inhibition. Thus we saw that T1L has the ability to down-regulate the induction of IFN-β in L929 and CT26 cells. In addition, upon IFN pretreatment, T1L displayed almost complete resistance to IFN-β in both cell lines (figures 29 and 32). In contrast, T3D behaved differently in both cell lines, where it induced IFN-β 10-fold higher than T1L in L929 cells. Not only that, but T3D also displayed IFN sensitivity in L929 cells, where viral replication was reduced by 11-fold upon IFN-pretreatment (figures 28 and 29), but not in CT26 cells. T1L was relatively resistant to inhibition by IFN-β in both cell types. Thus both parental Reoviruses T1L and T3D had different abilities to induce IFN-β and to resist its antiviral effects.

Among the reassortants, EB88 produced IFN-β to high levels in both L929 and CT26 cell lines (figures 26 and 27). EB88 has its M2 gene segment from T1L (low inducer of IFN) on aT3D backbone (high inducer of IFN), which resulted in a 4-fold higher IFN-β level than T3D in CT26 cells. In addition, the induction of IFN-β reduced viral growth in L929 and CT26 cells, compared to the other Reoviruses (figures 28 and 31). However, upon IFN pre-treatment, reassortants EB88, EB96 and EB97 seem to display an unusual benefit from an induced antiviral state, since viral replication was enhanced by 10- to 100-fold in CT26 cells (figure 31). This sheds light on a possible interplay between various gene segments (involving the interaction between the M2 gene and other Reovirus genes) in these reassortants in the context of a cancer cell, which enables the virus to exploit the already compromised IFN-pathway to grow better in the presence of IFN in CT26 cells.

7.4.2 Reovirus replication and protein synthesis between fibroblasts and epithelium cell lines

Reovirus replication varies among the four cells lines (L929 fibroblasts, CV-1, Vero and CT26 epithelial cells). We saw that in CV-1 cells, the parental and the reassortant strains have similar relative replication levels (figure 37). In L929 fibroblasts, there was an increased difference between the relative replication of the parental and the reassortants, where the parental strains grew to titers higher than 10^8 pfu/ml, and the overall growth of the reassortants was reduced by roughly 10-fold (figure 28). This sheds some light onto the gene interactions that may be involved in the various replication systems such as those between fibroblast and epithelial cell lines. These observations were further emphasized when we study the replication in Vero and CT26 cells, where one system was deficient in its native IFN pathway, and the other was a cancerous cell line. When comparing T3D growth, we observed that it grew better than T1L in both Vero and CT26 cell lines. Moreover we also observed the relatively enhanced viral yields of reassortants EB97 and EB123 compared to EB88 and EB96 in both CT26 and Vero cells (figures 31 and 34). We speculate that these differences were due to the presence of T3D gene segments that are common to both EB97 and EB123, such as M2, M3, S1 and S2. These genes may be involved to achieve the observed differences in viral yields. The observed growth properties correlated with viral protein synthesis, where we saw that overall protein synthesis was enhanced when both CT26 cells and Vero cells were infected with T3D, EB97 and EB123 (figure 33 and 36).

We also showed in our previous studies (chapter 4) where T1L grew 10-fold higher in MEF cells, whereas T3D grew better in the lung. The difference in growth in MEF cells was attributed to the M1 and L2 genome segments. In contrast, the infection of the Balb-c mouse

lung was dependent on the S1 genome segment and the presence of PKR, which protected the bronchiolar epithelium from Reovirus infection. Moreover, within the lung T1L infection was restricted to the alveolar epithelium, whereas T3D was able to infect the bronchiolar epithelium using a σ1s-dependent mechanism.

Our results here mirror those found in prior studies of Reovirus growth in L929 cells (chapter 6, figure 20), where a relatively low rate of viral protein production was observed at earlier time points, followed by a general burst in viral protein synthesis (proteins μ2, μNS and σNS) as well as viral yield 18 hours post infection. This time-point was crucial, as several host proteins (such as p-PKR, eIF2α, IRF-3, IRF-7 and actin) underwent transient degradation and re-synthesis, followed by an overall increase in viral protein synthesis in CT26 epithelial cells (Figures 22-24).

7.4.3 IFN sensitivity amongst the Parental T1L and T3D and the oncolytic reassortants in the four cells types – protein synthesis and replication

We have shown that T3D grew to very high levels in L929 fibroblasts, and was also the most sensitive to IFN-pre-treatment. In contrast, T1L showed resistance to IFN pre-treatment, which also correlated with viral protein synthesis (figure 28). With the reassortants, we had varying sensitivities to IFN in L929 fibroblasts (figure 29), which further indicated the interplay of the combined gene segments from either parental serotype, creating a different phenotype than either parent.

We observed that in CV-1 cells, parental Reovirus strain T1L was more sensitive to IFN-pretreatment than T3D. Among the four reassortants, EB88 displayed the greatest sensitivity to IFN-pretreatment, almost 14- and 60-fold more sensitivity than T1L and T3D, respectively

(figures 37 and 38). This correlateed with protein synthesis of EB88 in CV-1 cells, which also showed great sensitivity to IFN at earlier and later time points (figure 39). Sensitivity to IFN seems to be an important characteristic in viral oncolysis. Here we have identified an oncolytic virus that displays sensitivity that is much greater than either parental strain.

Interferon pretreatment inhibited viral replication of parental Reoviruses and oncolytic reassortants in L929 cells, Vero cells and CV-1 cells. However, oncolytic reassortant strains EB88, EB96 and EB97 actually benefited from the IFN pre-treatment in CT26 colon tumour epithelial cells, where viral yield was enhanced (figures 31 and 32). It can be speculated that this emergent property of these oncolytic reassortants is what allows them to enhance survival in CT26- tumour bearing mice. We can therefore infer that for treatments of cancer with certain reassortant strains, co-treatment with IFN could allow enhanced viral replication, and therefore enhanced viral oncolysis. Moreover, the viral phenotype for EB88 was significantly different from T3D, considering the only difference between the two was the presence of gene segment M2 from T1L. Therefore, the presence of the M2 gene segment on two different viral gene backgrounds, T1L or T3D, changes the phenotype remarkably, which further indicates the involvement of multi-gene interactions in a tumour microenvironment.

7.4.4 Mapping Reovirus biological properties to individual gene segments

Our results have shown that the effect of specific Reovirus genome segments vary differently amongst the reassortants in the different cell lines. In L929 cells, the reassortants all display protein synthesis patterns that were sensitive to IFN pre-treatment, therefore more similar to T3D than to the resistant T1L trend. Interferon sensitivity is mapped to the L2 and the M1 gene segments of T3D (64). The L2 genome segment encodes the λ2 protein which plays a role

in particle assembly and in mediating enzymatic activities in capping of viral mRNA (21). The M1 gene encodes the μ2 protein, which has been shown to have multiple functions, ranging from RNA binding, transcription, growth, replication and disease properties (21, 45, 89). Sherry et al., 1998 showed that Reovirus interferon sensitivity to beta-interferon has been previously mapped to the L2 and the M1 gene segments (64). Our results also support the notion that the L2 and the M1 gene segments play an important role for the IFN-β sensitivity in L929 cells.

In CT26 epithelial cells, the reassortants EB88 and EB96 grew to levels that were comparable to T1L in the absence of IFN-β pre-treatment, whereas EB97 and EB123 grew to levels comparable to T3D. The difference in yield was mapped to the M2 gene segment, for this particular epithelial cell line that is cancerous in origin. A similar observation can be made when looking at viral protein synthesis, which renders an important role to the M2 gene segment. The M2 gene segment encodes the μ1 protein, which is found in the viral outer capsid, and plays a role in virus penetration and transcriptase activation (21). When comparing IFN-β sensitivity of the Reoviruses in CT26 cells, we found that with the exception of EB123, all the other reassortants did not behave like either parental serotype, suggesting emergent properties in cancer cells.

In Vero cells, virus yields were higher for T3D, EB97, and EB123 compared to lower yields for T1L, EB88, and EB96. These differences in yield mapped to the M2 genome segment. The IFN-β pre-treatment effects on yield showed that all the Reoviruses were sensitive to interferon to varying degrees. The differences between the more sensitive (T1L, EB96, EB97) and less sensitive (T3D, EB88, EB123) mapped to the S4 genome segment which encodes the σ3 protein, forming one of the major protein of the outer capsid, dsRNA binding, as well as its role in the cleavage of μ1 to μ1c (6, 21). Bergeron et al, 1998 found through their studies of

temperature sensitive Reoviruses that the lack of σ3 association with μ1, and/or the increased dsRNA-binding activity of σ3, could result in the partial resistance to interferon treatment (6). This implicates the role of the S4 gene segment encoding the σ3 protein in IFN resistance.

When studying the protein synthesis in Vero cells, the data revealed similar trends of increased yields and interferon sensitivities in certain Reovirus reassortants. T3D, EB97 and EB123 had bands of higher intensity, which imply increased protein synthesis relative to T1L that had much lower protein synthesis and yet similar virus yields. This correlated with their increased yields previously observed. These observations fit with the yield experiment showing that the differences in replication and protein synthesis levels under normal conditions map to the M2 genome segment.

T3D, EB88, and EB123 were relatively more resistant to IFN-β pretreatment at the level of protein synthesis while, on the other hand, T1L, EB96, and EB97 displayed greater sensitivities to IFN-β in Vero cells, because its origin (T1L or T3D) correlated with this property. This interferon sensitivity mapped to the S4 genome segment. The identical mappings made for both yield and protein synthesis experiments strengthen the idea that these genome segments play a role in the differences in replication and interferon sensitivity for these reovirus parental strains and reassortants. However, these mappings show us that certain genome segments can be responsible for certain broad reovirus properties such as interferon sensitivity. Nonetheless, it is unlikely that these genome segments can totally account for the observed differences and they probably work in concert with other viral proteins in each cell type, and possibly cellular proteins to achieve a certain trait.

7.5 Summary of Conclusions

Our results showed that reassortant and parental Reoviruses behaved differently with respect to growth and IFN response in different cell lines. We demonstrated a complicated interplay between the Reovirus biology and the cellular microenvironment in which the virus grows and replicates. Virus abilities such as interferon induction, interferon sensitivity versus resistance, and protein production versus yield, as well as the presence or absence of certain gene segments (and therefore the multiple combinations of possible gene interactions) are all factors that affect the overall virus growth and protein production. Conversely, through the cellular point of view, factors such as fibroblast or epithelial morphology, tumour cell or normal cell, interferon producing or interferon deficient properties also play key roles in the final effect achieved.

From our data and analyses, it appears that improved oncolysis is not entirely associated with interferon sensitivity, suggesting that there may be more to the oncolysis picture than the current Reovirus-*Ras* model. The mapping of certain properties, like interferon sensitivity and yield, to specific genome segments sheds light on Reovirus protein functions and how these proteins are responsible for large scale phenotype of the viruses. Furthermore, since aspects of Reovirus biology could not be owed to a single gene segment (that is applicable in all cell lines), our results indicate a strong interplay among more than one genome segment and gene product that causes these Reoviruses and the reassortants to behave differently in different cell lines.

Our data also demonstrates that recombinant manipulations can generate reassortants with novel properties, such as improved oncolysis, and support the idea that novel Reoviruses may be generated for the future treatment of current reovirus-resistant cancers.

REFERENCES

1. **Alain, T., K. Hirasawa, K. J. Pon, S. G. Nishikawa, S. J. Urbanski, Y. Auer, J. Luider, A. Martin, R. N. Johnston, A. Janowska-Wieczorek, P. W. Lee, and A. E. Kossakowska.** 2002. Reovirus therapy of lymphoid malignancies. Blood **100:**4146-53.

2. **Alarcon-Riquelme, M. E.** 2006. Nucleic acid by-products and chronic inflammation. Nat Genet **38:**866-7.

3. **Au, W. C., W. S. Yeow, and P. M. Pitha.** 2001. Analysis of functional domains of interferon regulatory factor 7 and its association with IRF-3. Virology **280:**273-82.

4. **Barton, E. S., J. D. Chappell, J. L. Connolly, J. C. Forrest, and T. S. Dermody.** 2001. Reovirus receptors and apoptosis. Virology **290:**173-80.

5. **Bell, J. C., K. A. Garson, B. D. Lichty, and D. F. Stojdl.** 2002. Oncolytic viruses: programmable tumour hunters. Curr Gene Ther **2:**243-54.

6. **Bergeron, J., T. Mabrouk, S. Garzon, and G. Lemay.** 1998. Characterization of the thermosensitive ts453 reovirus mutant: increased dsRNA binding of sigma 3 protein correlates with interferon resistance. Virology **246:**199-210.

7. **Boehme, K. W., K. M. Guglielmi, and T. S. Dermody.** 2009. Reovirus nonstructural protein sigma1s is required for establishment of viremia and systemic dissemination. Proc Natl Acad Sci U S A **106:**19986-91.

8. **Brown, E. G.** 1998. Reovirus M1 gene expression. Curr Top Microbiol Immunol **233:**197-213.

9. **Chandran, K., and M. L. Nibert.** 2003. Animal cell invasion by a large nonenveloped virus: reovirus delivers the goods. Trends Microbiol **11:**374-82.

10. **Chappell, J. D., J. L. Duong, B. W. Wright, and T. S. Dermody.** 2000. Identification of carbohydrate-binding domains in the attachment proteins of type 1 and type 3 reoviruses. J Virol **74:**8472-9.

11. **Chappell, J. D., V. L. Gunn, J. D. Wetzel, G. S. Baer, and T. S. Dermody.** 1997. Mutations in type 3 reovirus that determine binding to sialic acid are contained in the fibrous tail domain of viral attachment protein sigma1. J Virol **71:**1834-41.

12. **Coffey, M. C., J. E. Strong, P. A. Forsyth, and P. W. Lee.** 1998. Reovirus therapy of tumors with activated Ras pathway. Science **282:**1332-4.

13. **Connolly, J. L., E. S. Barton, and T. S. Dermody.** 2001. Reovirus binding to cell surface sialic acid potentiates virus-induced apoptosis. J Virol **75:**4029-39.

14. **Danthi, P., M. W. Hansberger, J. A. Campbell, J. C. Forrest, and T. S. Dermody.** 2006. JAM-A-independent, antibody-mediated uptake of reovirus into cells leads to apoptosis. J Virol **80:**1261-70.

15. **Danthi, P., T. Kobayashi, G. H. Holm, M. W. Hansberger, T. W. Abel, and T. S. Dermody.** 2008. Reovirus apoptosis and virulence are regulated by host cell membrane penetration efficiency. J Virol **82:**161-72.

16. **De Benedetti, A., G. J. Williams, L. Comeau, and C. Baglioni.** 1985. Inhibition of viral mRNA translation in interferon-treated L cells infected with reovirus. J Virol **55:**588-93.

17. **Desmyter, J., J. L. Melnick, and W. E. Rawls.** 1968. Defectiveness of interferon production and of rubella virus interference in a line of African green monkey kidney cells (Vero). J Virol **2:**955-61.

18. **Douville, R. N., R. C. Su, K. M. Coombs, F. E. Simons, and K. T. Hayglass.** 2008. Reovirus serotypes elicit distinctive patterns of recall immunity in humans. J Virol **82:**7515-23.

19. **Duncan, M. R., S. M. Stanish, and D. C. Cox.** 1978. Differential sensitivity of normal and transformed human cells to reovirus infection. J Virol **28:**444-9.

20. **Emeny, J. M., and M. J. Morgan.** 1979. Regulation of the interferon system: evidence that Vero cells have a genetic defect in interferon production. J Gen Virol **43:**247-52.

21. **Fields, B. N., D. M. Knipe, P. M. Howley, and D. E. Griffin** 2001, posting date. Fields' virology. Lippincott Williams & Wilkins 4th. [Online.]

22. **Forrest, J. C., and T. S. Dermody.** 2003. Reovirus receptors and pathogenesis. J Virol **77:**9109-15.

23. **Furlong, D. B., M. L. Nibert, and B. N. Fields.** 1988. Sigma 1 protein of mammalian reoviruses extends from the surfaces of viral particles. J Virol **62:**246-56.

24. **Gaillard, R. K., and W. K. Joklik.** 1980. The antigenic determinants of most of the proteins coded by the three serotypes of reovirus are highly conserved during evolution. Virology **107:**533-6.

25. **Garcia-Sastre, A., and C. A. Biron.** 2006. Type 1 interferons and the virus-host relationship: a lesson in detente. Science **312:**879-82.

26. **Garcia, M. A., J. Gil, I. Ventoso, S. Guerra, E. Domingo, C. Rivas, and M. Esteban.** 2006. Impact of protein kinase PKR in cell biology: from antiviral to antiproliferative action. Microbiol Mol Biol Rev **70:**1032-60.

27. **Gauntt, C. J.** 1973. Induction of interferon in L cells by reoviruses. Infect Immun **7:**711-7.

28. **Gonzalez-Lopez, C., J. Martinez-Costas, M. Esteban, and J. Benavente.** 2003. Evidence that avian reovirus sigmaA protein is an inhibitor of the double-stranded RNA-dependent protein kinase. J Gen Virol **84:**1629-39.

29. **Guo, Z. S., S. H. Thorne, and D. L. Bartlett.** 2008. Oncolytic virotherapy: molecular targets in tumor-selective replication and carrier cell-mediated delivery of oncolytic viruses. Biochim Biophys Acta **1785:**217-31.

30. **Hashiro, G., P. C. Loh, and J. T. Yau.** 1977. The preferential cytotoxicity of reovirus for certain transformed cell lines. Arch Virol **54:**307-15.

31. **Henry, G. L., S. J. McCormack, D. C. Thomis, and C. E. Samuel.** 1994. Mechanism of interferon action. Translational control and the RNA-dependent protein kinase (PKR): antagonists of PKR enhance the translational activity of mRNAs that include a 161 nucleotide region from reovirus S1 mRNA. J Biol Regul Homeost Agents **8:**15-24.

32. **Hirasawa, K., S. G. Nishikawa, K. L. Norman, T. Alain, A. Kossakowska, and P. W. Lee.** 2002. Oncolytic reovirus against ovarian and colon cancer. Cancer Res **62:**1696-701.

33. **Hiscott, J.** 2007. Triggering the innate antiviral response through IRF-3 activation. J Biol Chem **282:**15325-9.

34. **Holm, G. H., J. Zurney, V. Tumilasci, S. Leveille, P. Danthi, J. Hiscott, B. Sherry, and T. S. Dermody.** 2007. Retinoic acid-inducible gene-I and interferon-beta promoter stimulator-1 augment proapoptotic responses following mammalian reovirus infection via interferon regulatory factor-3. J Biol Chem **282:**21953-61.

35. **Hoyt, C. C., S. M. Richardson-Burns, R. J. Goody, B. A. Robinson, R. L. Debiasi, and K. L. Tyler.** 2005. Nonstructural protein sigma1s is a determinant of reovirus virulence and influences the kinetics and severity of apoptosis induction in the heart and central nervous system. J Virol **79:**2743-53.

36. **Huismans, H., and W. K. Joklik.** 1976. Reovirus-coded polypeptides in infected cells: isolation of two native monomeric polypeptides with affinity for single-stranded and double-stranded RNA, respectively. Virology **70:**411-24.

37. **Iwatsuki, M., K. Mimori, T. Yokobori, H. Ishi, T. Beppu, S. Nakamori, H. Baba, and M. Mori.** Epithelial-mesenchymal transition in cancer development and its clinical significance. Cancer Sci **101:**293-9.

38. **Jacobs, B. L., and R. E. Ferguson.** 1991. The Lang strain of reovirus serotype 1 and the Dearing strain of reovirus serotype 3 differ in their sensitivities to beta interferon. J Virol **65:**5102-4.

39. **Kalluri, R., and R. A. Weinberg.** 2009. The basics of epithelial-mesenchymal transition. J Clin Invest **119:**1420-8.

40. **Kaufman, R. J.** 2002. The Double-Stranded RNA-Activated protein Kinase PKR. CRC Press LLC.

41. **Kelly, K., S. Nawrocki, A. Mita, M. Coffey, F. J. Giles, and M. Mita.** 2009. Reovirus-based therapy for cancer. Expert Opin Biol Ther **9:**817-30.

42. **Kim, M., Y. H. Chung, and R. N. Johnston.** 2007. Reovirus and tumor oncolysis. J Microbiol **45:**187-92.

43. **Klymkowsky, M. W., and P. Savagner.** 2009. Epithelial-mesenchymal transition: a cancer researcher's conceptual friend and foe. Am J Pathol **174:**1588-93.

44. **Marcato, P., M. Shmulevitz, D. Pan, D. Stoltz, and P. W. Lee.** 2007. Ras transformation mediates reovirus oncolysis by enhancing virus uncoating, particle infectivity, and apoptosis-dependent release. Mol Ther **15:**1522-30.

45. **Mbisa, J. L., M. M. Becker, S. Zou, T. S. Dermody, and E. G. Brown.** 2000. Reovirus mu2 protein determines strain-specific differences in the rate of viral inclusion formation in L929 cells. Virology **272:**16-26.

46. **Minuk, G. Y., R. W. Paul, and P. W. Lee.** 1985. The prevalence of antibodies to reovirus type 3 in adults with idiopathic cholestatic liver disease. J Med Virol **16:**55-60.

47. **Morin, M. J., A. Warner, and B. N. Fields.** 1996. Reovirus infection in rat lungs as a model to study the pathogenesis of viral pneumonia. J Virol **70:**541-8.

48. **Nibert, M. L., R. L. Margraf, and K. M. Coombs.** 1996. Nonrandom segregation of parental alleles in reovirus reassortants. J Virol **70:**7295-300.

49. **Norman, K. L., M. C. Coffey, K. Hirasawa, D. J. Demetrick, S. G. Nishikawa, L. M. DiFrancesco, J. E. Strong, and P. W. Lee.** 2002. Reovirus oncolysis of human breast cancer. Hum Gene Ther **13:**641-52.

50. **Norman, K. L., K. Hirasawa, A. D. Yang, M. A. Shields, and P. W. Lee.** 2004. Reovirus oncolysis: the Ras/RalGEF/p38 pathway dictates host cell permissiveness to reovirus infection. Proc Natl Acad Sci U S A **101:**11099-104.

51. **Norman, K. L., and P. W. Lee.** 2005. Not all viruses are bad guys: the case for reovirus in cancer therapy. Drug Discov Today **10:**847-55.

52. **Parker, J. S., T. J. Broering, J. Kim, D. E. Higgins, and M. L. Nibert.** 2002. Reovirus core protein mu2 determines the filamentous morphology of viral inclusion bodies by interacting with and stabilizing microtubules. J Virol **76:**4483-96.

53. **Poggioli, G. J., T. S. Dermody, and K. L. Tyler.** 2001. Reovirus-induced sigma1s-dependent G(2)/M phase cell cycle arrest is associated with inhibition of p34(cdc2). J Virol **75:**7429-34.

54. **Poggioli, G. J., C. Keefer, J. L. Connolly, T. S. Dermody, and K. L. Tyler.** 2000. Reovirus-induced G(2)/M cell cycle arrest requires sigma1s and occurs in the absence of apoptosis. J Virol **74:**9562-70.

55. **Rodgers, S. E., J. L. Connolly, J. D. Chappell, and T. S. Dermody.** 1998. Reovirus growth in cell culture does not require the full complement of viral proteins: identification of a sigma1s-null mutant. J Virol **72:**8597-604.

56. **Rudd, P., and G. Lemay.** 2005. Correlation between interferon sensitivity of reovirus isolates and ability to discriminate between normal and Ras-transformed cells. J Gen Virol **86:**1489-97.

57. **Samuel, C. E.** 1998. Reoviruses and the interferon system. Curr Top Microbiol Immunol **233:**125-45.

58. **Samuel, C. E., R. Duncan, G. S. Knutson, and J. W. Hershey.** 1984. Mechanism of interferon action. Increased phosphorylation of protein synthesis initiation factor eIF-2 alpha in interferon-treated, reovirus-infected mouse L929 fibroblasts in vitro and in vivo. J Biol Chem **259:**13451-7.

59. **Samuel, C. E., D. A. Farris, and D. A. Eppstein.** 1977. Mechanism of interferon action. Kinetics of interferon action in mouse L929 cells: translation inhibition, protein phosphorylation, and messenger RNA methylation and degradation. Virology **83:**56-71.

60. **Sarkar, G., J. Pelletier, R. Bassel-Duby, A. Jayasuriya, B. N. Fields, and N. Sonenberg.** 1985. Identification of a new polypeptide coded by reovirus gene S1. J Virol **54:**720-5.

61. **Sharpe, A. H. a. B. N. F.** 1983. Pathogenesis of reovirus infection. Plenum Press, New York.

62. **Sherry, B.** 2002. The role of interferon regulatory factors in the cardiac response to viral infection. Viral Immunol **15:**17-28.

63. **Sherry, B.** 2009. Rotavirus and reovirus modulation of the interferon response. J Interferon Cytokine Res **29:**559-67.

64. **Sherry, B., J. Torres, and M. A. Blum.** 1998. Reovirus induction of and sensitivity to beta interferon in cardiac myocyte cultures correlate with induction of myocarditis and are determined by viral core proteins. J Virol **72:**1314-23.

65. **Shmulevitz, M., P. Marcato, and P. W. Lee.** Activated Ras signaling significantly enhances reovirus replication and spread. Cancer Gene Ther **17:**69-70.

66. **Shmulevitz, M., P. Marcato, and P. W. Lee.** 2005. Unshackling the links between reovirus oncolysis, Ras signaling, translational control and cancer. Oncogene **24:**7720-8.

67. **Shmulevitz, M., L. Z. Pan, K. Garant, D. Pan, and P. W. Lee.** Oncogenic Ras promotes reovirus spread by suppressing IFN-beta production through negative regulation of RIG-I signaling. Cancer Res **70:**4912-21.

68. **Silverstein, S. C., J. K. Christman, and G. Acs.** 1976. The reovirus replicative cycle. Annu Rev Biochem **45:**375-408.

69. **Silverstein, S. C., M. Schonberg, D. H. Levin, and G. Acs.** 1970. The reovirus replicative cycle: conservation of parental RNA and protein. Proc Natl Acad Sci U S A **67:**275-81.

70. **Smith, J. A., S. C. Schmechel, A. Raghavan, M. Abelson, C. Reilly, M. G. Katze, R. J. Kaufman, P. R. Bohjanen, and L. A. Schiff.** 2006. Reovirus induces and benefits from an integrated cellular stress response. J Virol **80:**2019-33.

71. **Smith, J. A., S. C. Schmechel, B. R. Williams, R. H. Silverman, and L. A. Schiff.** 2005. Involvement of the interferon-regulated antiviral proteins PKR and RNase L in reovirus-induced shutoff of cellular translation. J Virol **79:**2240-50.

72. **Song, L., Y. Zhou, J. He, H. Zhu, R. Huang, P. Mao, and Q. Duan.** 2008. Comparative sequence analyses of a new mammalian reovirus genome and the mammalian reovirus S1 genes from six new serotype 2 human isolates. Virus Genes **37:**392-9.

73. **Stewart, M. J., K. Smoak, M. A. Blum, and B. Sherry.** 2005. Basal and reovirus-induced beta interferon (IFN-beta) and IFN-beta-stimulated gene expression are cell type specific in the cardiac protective response. J Virol **79:**2979-87.

74. **Strong, J. E., M. C. Coffey, D. Tang, P. Sabinin, and P. W. Lee.** 1998. The molecular basis of viral oncolysis: usurpation of the Ras signaling pathway by reovirus. Embo J **17:**3351-62.

75. **Strong, J. E., and P. W. Lee.** 1996. The v-erbB oncogene confers enhanced cellular susceptibility to reovirus infection. J Virol **70:**612-6.

76. **Strong, J. E., D. Tang, and P. W. Lee.** 1993. Evidence that the epidermal growth factor receptor on host cells confers reovirus infection efficiency. Virology **197:**405-11.

77. **Tai, J. H., J. V. Williams, K. M. Edwards, P. F. Wright, J. E. Crowe, Jr., and T. S. Dermody.** 2005. Prevalence of reovirus-specific antibodies in young children in Nashville, Tennessee. J Infect Dis **191:**1221-4.

78. **Tyler, K. a. O., MBA.** 1998. Reoviruses. Springer-Verlag Berlin Heidelberg, New York.

79. **Tyler, K. L., P. Clarke, R. L. DeBiasi, D. Kominsky, and G. J. Poggioli.** 2001. Reoviruses and the host cell. Trends Microbiol **9:**560-4.

80. **Vorburger, S. A., A. Pataer, S. G. Swisher, and K. K. Hunt.** 2004. Genetically targeted cancer therapy: tumor destruction by PKR activation. Am J Pharmacogenomics **4:**189-98.

81. **Weiner, H. L., D. Drayna, D. R. Averill, Jr., and B. N. Fields.** 1977. Molecular basis of reovirus virulence: role of the S1 gene. Proc Natl Acad Sci U S A **74:**5744-8.

82. **Wenske, E. A., S. J. Chanock, L. Krata, and B. N. Fields.** 1985. Genetic reassortment of mammalian reoviruses in mice. J Virol **56:**613-6.

83. **Wiebe, M. E., and T. W. Joklik.** 1975. The mechanism of inhibition of reovirus replication by interferon. Virology **66:**229-40.

84. **Wilcox, M. E., W. Yang, D. Senger, N. B. Rewcastle, D. G. Morris, P. M. Brasher, Z. Q. Shi, R. N. Johnston, S. Nishikawa, P. W. Lee, and P. A. Forsyth.** 2001. Reovirus as an oncolytic agent against experimental human malignant gliomas. J Natl Cancer Inst **93:**903-12.

85. **Yang, W. Q., D. Senger, H. Muzik, Z. Q. Shi, D. Johnson, P. M. Brasher, N. B. Rewcastle, M. Hamilton, J. Rutka, J. Wolff, C. Wetmore, T. Curran, P. W. Lee, and P. A. Forsyth.** 2003. Reovirus prolongs survival and reduces the frequency of spinal and leptomeningeal metastases from medulloblastoma. Cancer Res **63:**3162-72.

86. **Yap, T. A., A. Brunetto, H. Pandha, K. Harrington, and J. S. Debono.** 2008. Reovirus therapy in cancer: has the orphan virus found a home? Expert Opin Investig Drugs **17:**1925-35.

87. **Yue, Z., and A. J. Shatkin.** 1997. Double-stranded RNA-dependent protein kinase (PKR) is regulated by reovirus structural proteins. Virology **234:**364-71.

88. **Zhang, P., and C. E. Samuel.** 2007. Protein kinase PKR plays a stimulus- and virus-dependent role in apoptotic death and virus multiplication in human cells. J Virol **81:**8192-200.

89. **Zurney, J., T. Kobayashi, G. H. Holm, T. S. Dermody, and B. Sherry.** 2009. Reovirus mu2 protein inhibits interferon signaling through a novel mechanism involving nuclear accumulation of interferon regulatory factor 9. J Virol **83:**2178-87.